STRUCTURAL AND FUNCTIONAL CHARACTERIZATION OF TlyA HEMOLYSIN FROM *Helicobacter pylori*

NITCHAKAN SAMAINUKUL

A THESIS SUBMITTED IN PARTIAL FULFILLMENT
OF THE REQUIREMENTS FOR THE DEGREE OF
DOCTOR OF PHILOSOPHY (IMMUNOLOGY)
FACULTY OF GRADUATE STUDIES
MAHIDOL UNIVERSITY
2019

Copyright by Mahidol University

COPYRIGHT OF MAHIDOL UNIVERSITY

Thesis
entitled

STRUCTURAL AND FUNCTIONAL CHARACTERIZATION OF TlyA HEMOLYSIN FROM *Helicobacter pylori*

.....
Ms. Nitchakan Samainukul
Candidate

.....
Gerd Katzenmeier,
Ph.D. (Molecular Biology)
Major advisor

.....
Prof. Wanpen Chaicumpa,
D.V.M. (Hons.), Ph.D. (Microbiology)
Co-advisor

.....
Somphob Leetachewa,
Ph.D. (Molecular Genetics and Genetic Engineering)
Co-advisor

.....
Asst. Prof. Chalermpol Kanchanawarin,
Ph.D. (Physics)
Co-advisor

.....
Suparerk Borwornpinyo,
Ph.D. (Physiology)
Co-advisor

.....
Prof. Patcharee Lertrit,
M.D., Ph.D. (Biochemistry)
Dean
Faculty of Graduate Studies
Mahidol University

.....
Prof. Sunee Korbsrisate,
Ph.D. (Microbiology)
Program Director
Doctor of Philosophy Program in Immunology
Faculty of Medicine Siriraj Hospital
Mahidol University

Copyright by Mahidol University

Thesis
entitled

STRUCTURAL AND FUNCTIONAL CHARACTERIZATION OF TlyA HEMOLYSIN FROM *Helicobacter pylori*

was submitted to the Faculty of Graduate Studies, Mahidol University
for the degree of Doctor of Philosophy (Immunology)
on
February 20, 2019

.....
Ms. Nitchakan Samainukul
Candidate

.....
Asst. Prof. Busaba Powthongchin,
Ph.D. (Molecular Genetics and Genetic Engineering)
Chair

.....
Gerd Katzenmeier,
Ph.D. (Molecular Biology)
Member

.....
Prof. Wanpen Chaicumpa,
D.V.M. (Hons.), Ph.D. (Microbiology)
Member

.....
Suparerk Borwornpinyo,
Ph.D. (Physiology)
Member

.....
Prof. Chanan Angsuthanasombat,
Ph.D. (Biochemistry)
Member

.....
Prof. Patcharee Lertrit,
M.D., Ph.D. (Biochemistry)
Dean
Faculty of Graduate Studies
Mahidol University

.....
Prof. Prasit Watanapa,
M.D., FSCS, FRCS, Ph.D. (Surgery)
Dean
Faculty of Medicine Siriraj Hospital
Mahidol University

Copyright by Mahidol University

ACKNOWLEDGEMENTS

I would like to express my sincere appreciation to my advisor Lect. Gerd Katzenmeier for the continuous support of my Ph.D. study. His guidance helped me in all the time of research and writing of this thesis.

My sincere gratitude is extended to my co-advisors Prof. Wanpen Chaicumpa, Asst. Prof. Chalermpol Kanchanawarin, Lect., Suparerk Borwornpinyo and Lect. Somphob Leetacheewa for the encouragement, insightful comments, and immense knowledge. And I would like to thank Asst. Prof. Busaba Powthongchin who was the chair and external examiner of the thesis defense.

I would like to express my greatest gratitude to Prof. Chanan Angsuthanasombat, for his invaluable insights for my research, and invigorating inspiring discussions and suggestions. I could not have imagined having better mentors for my Ph.D study.

My sincere thanks also go to Mr. Aung Khine Linn for the stimulating discussions and encouraging me throughout my study. I would like to thank our lab manager, Mrs. Somsri Sakdee, for her kind help and friendship during my stay in the lab.

I would also like to express my appreciation for my family, for their moral support throughout this challenging time. And finally, last but by no means least, also to everyone in the BRIC lab, it was great research environment with all of you during last 3 years. Thank you for your friendship and support.

Nitchakan Samainukul

Copyright by Mahidol University

STRUCTURAL AND FUNCTIONAL CHARACTERIZATION OF TlyA HEMOLYSIN FROM *Helicobacter pylori*

NITCHAKAN SAMAINUKUL 5838607 SIIM/D

Ph.D. (IMMUNOLOGY)

THESIS ADVISORY COMMITTEE: GERD KATZENMEIER, Ph.D., WANPEN CHAICUMPA, D.V.M. (HONS.), Ph.D., SOMPHOB LEETACHEWA, Ph.D., SUPARERK BORWORNPINYO, Ph.D., CHALERMPOL KANCHANAWARIN, Ph.D.

ABSTRACT

Helicobacter pylori gene product HP1086, designated as 'non-conventional' hemolysin named TlyA, is a virulence factor which plays an important role in persistent colonization and disease progression. In this study, 27-kDa TlyA from *H. pylori* was produced as a soluble recombinant protein in *E. coli* and purified to near homogeneity by cation exchange chromatography. Purified TlyA was biologically active as proven by membrane-perturbating activity against liposomes *in vitro*. Quaternary structural assembly and membrane-perturbing activity of TlyA negatively influenced by the addition of reducing agent DTT, thus suggesting a possible function of disulfide bonds for protein activity. Structural model suggests the potential formation of inter-molecular disulfide bridges between Cys^{124} and Cys^{128} residues located in the interface within the dimeric assembly. In addition, *in silico* modeling suggests S-adenosyl methionine (SAM) binding to TlyA could be inhibited by sinefungin which shares the similar binding residues with SAM. Recombinant TlyA causes cytotoxicity in human gastric cells and induces production of cytokine IL-8. Overall, this study disclosed an important role of intermolecular disulfide bonds structural assembly and membrane-perturbing activity of *H. pylori* TlyA.

KEY WORDS: *Helicobacter pylori* / TlyA HEMOLYSIN / IMMUNE RESPONSE / DISULFIDE BONDS

Copyright by Mahidol University

115 pages

CONTENTS

Copyright by Mahidol University

CONTENTS (cont.)

Copyright by Mahidol University

CONTENTS (cont.)

Copyright by Mahidol University

CONTENTS (cont.)

Copyright by Mahidol University

LIST OF TABLES

Copyright by Mahidol University

LIST OF FIGRURES

Copyright by Mahidol University

LIST OF FIGRURES (cont.)

Copyright by Mahidol University

CHAPTER I
INTRODUCTION

Helicobacter pylori infects approximately half of the world's population and it is estimated that 90% of duodenal ulcers and up to 80% of gastric ulcers are caused by *H. pylori*. Infection with *H. pylori* substantially increases the risk of gastric cancer and thus, World Health Organization (WHO) classified it as a class I carcinogen (1, 2). The reported 50% incidence rate makes *H. pylori* one of the most widespread infections so far (2). However, only a tenth of the infected people develop benign gastric diseases such as dyspepsia, gastric ulcer and peptic ulcer, etc., and less than 1% develop malignant gastric cancer (3).

H. pylori produces a wide range of virulence factors which are important for effective colonization, persistent infection and disease development such as urease, catalase, lipopolysaccharides, adhesins, the cytotoxin-associated gene A and vacuolating cytotoxin VacA (4). However, there is a considerable variation of virulence factor production amongst different *H. pylori* strains.

H. pylori strains and such variation could be the underlying reason for different clinical outcomes in infected individuals (5). Most of the well-known virulence factors are characterized on the molecular details for their roles in *H. pylori* pathogenesis. However, comparatively, very little is known regarding the hemolytic activity conferred by *H. pylori*. Earlier research has demonstrated the presence of hemolytic factor in *H. pylori* and the *in vitro* hemolytic activity against erythrocytes was documented before. Bio-informatics analysis of *H. pylori* 26695 genome reveals the presence of putative hemolysin gene, HP1086. This protein displays sequence similarity to those of TlyA proteins from *Mycobacterium tuberculosis* and *Serpulina hyodysenteriae*, hence named as *H. pylori* TlyA (6-9).

Copyright by Mahidol University

TlyA is classified as a virulence factor in several bacteria and is evolutionarily conserved in many Gram-positive bacteria such as *Listeria monocytogenes, Streptococcus thermophilus or Bacillus thuringiensis* (10) and

Gram-negative bacteria such as *H.* pylori and Escherichia *coli.* A TlyA homolog can even be found in *Homo sapiens***.** DNA sequence encoding TlyA can be found in all sequenced *H. pylori* strains, but its role and function are underreported. While the majority of the research on the subject of *H. pylori* focuses on VacA and CagA, only limited studies can be found on the topic of TlyA, a potential multifunctional protein which could play a crucial role in *H. pylori* survival and pathogenesis. Prior reports of hemolysis activity in *H. pylori* culture or supernatant dates back to late 80s and early 90s, a few years after the initial discovery of *H. pylori*. These reports have suggested either incubation with *H. pylori* culture or concentrated supernatant induced hemolysis in erythrocytes from pig, sheep and humans. The hemolysis activity was growth phase and concentration dependent, heat-labile and strain dependent (6, 9, 11). Analysis of putative hemolysin genes within *H. pylori* 26695 genome reveals 6 separate gene loci each conferring certain degree of hemolysis in various red blood cells (RBCs) (12). Two proteins, HP1086 and HP1490, were identified by sequence homology to cytolysins of several pathogenic bacteria and the HP1086 gene product was later named as TlyA for its sequence similarity to TlyA hemolysin from other organisms such as *M. tuberculosis* and *S. hyodysenteriae* (7).

TlyA could play a role in persistent *H. pylori* infection as *H. pylori* with mutant TlyA gene showed reduction in hemolytic activity and reduced colonization in mouse models and introduction of TlyA gene confers hemolytic activity in previously non-hemolytic *E. coli* strain. The production of TlyA gene is also higher under iron limiting conditions which might suggest the possible role of TlyA in nutrient acquisition and metabolism (7).

TlyA can bind to both RBCs and AGS cells (a human gastric adenocarcinoma cell line) and induces cytotoxicity and reduced viability (13). Lata *et. al* reported the production of recombinant TlyA in *E. coli* and however, it should be noted that the expressed protein is mostly in insoluble form and the purified TlyA induces hemolysis of RBCs in high concentrations (20 μM) and under prolonged incubation (13). Follow up paper from Lata *et.al* also showed that TlyA binds to the liposomes and causes agglutination and membrane fusion in time and concentration-dependent manner (13). However, neither the mechanism of TlyA binding to the lipid membranes nor the structural basis leading to cell lysis is yet to be investigated.

Copyright by Mahidol University

TlyA has a molecular mass of 27-kDa and by far-UV CD, the secondary structure content was estimated to be 15% α-helical and 34% β-sheet (13). *H. pylori* TlyA possesses genetic similarity with orthologues from *M. tuberculosis, S. thermophilus, E. coli,* or *Bacillus subtilis*. Many of such TlyA homologs also possesses ribosomal methyltransferase activity which catalyze the transfer of a methyl group from S-adenosyl-L-methionine (SAM) to a nucleoside residue in an rRNA molecule and thus modulate their activity, function and folding.

TlyA could also modulate host immune response as *M. tuberculosis* mutants lacking TlyA gene induce increased production of pro-inflammatory cytokine interleukin-12 (IL-12) and reduced anti-inflammatory cytokine IL-10 cytokine production, which sharply contrasts with the immune responses induced by wild-type *M. tuberculosis*. Mutants are also more vulnerable to autophagy by macrophages and animals infected with the TlyA-deficient mutant show improved host-protective immune responses, reduced bacillary load, and increased survival compared with animals infected with wild-type *M. tuberculosis* (14). Disruption of this gene leads to capreomycin resistance phenotype in *M. tuberculosis* (15). No literature is available on host immune response and *H. pylori* TlyA so far.

M. tuberculosis TlyA can reach bacterial surface and extracellular milieu even though it does not seems to depend on either twin-arginine translocation pathway (Tat-pathway) or secretion pathway (Sec-pathway) dependent pathways for transport (16). On the cell surface, TlyA co-localizes with the heparin-binding hemagglutinin (HBHA) protein which is a known component of outer cell membrane although TlyA can be detected in smaller quantities in soluble fraction also. TlyA homologs possess the ability to be the multi-functional protein which is responsible for several roles in bacteria pathogenesis. Unlike VacA and CagA which mainly targets the host cells, intracellular TlyA could function as an enzyme during bacterial life cycle whereas secreted TlyA could play a role in nutrient acquisition thereby promoting *H. pylori* survival. However, only *in vitro* hemolytic activity of *H. pylori* is reported with no explanation regarding the underlying mechanism or the structural requirements.

Copyright by Mahidol University

Expression of recombinant *H. pylori* TlyA in *E. coli* has been shown to produce a soluble protein which was able to bind to human red blood cells (hRBCs) and to cause hemolysis in a concentration-dependent manner (13, 17). Hemolysis

induced by TlyA was reduced in the presence of saccharides such as raffinose and dextran-40 thereby suggesting the formation of pores in the cell membrane. Changes in cell morphology and increased cytotoxicity were also observed upon exposure of AGS cells to recombinant TlyA. The protein induced the agglutination of hRBCs and liposomes whereby for the latter a concentration-dependent release of fluorophores from dye-entrapped liposomes was observed (13). Exposure of TlyA to temperatures ≥37°C leads to the formation of amyloid-like aggregates which still retain cytotoxicity to human gastric cells (18). Thus, TlyA could be acting as a bi or multifunctional protein which facilitates *H. pylori* infection whilst playing a critical role as methyltransferase enzyme in metabolic pathway within *H. pylori*.

The structure-function relationship characterization of the TlyA could elucidate the role of this unique protein in *H. pylori* pathogenesis. Furthermore, the understanding of the TlyA structure in relation to its biological activity would provide insights into molecular environment where the virulence factors from pathogenic bacteria exert their intrinsic and extrinsic activities.

Copyright by Mahidol University

CHAPTER II
LITERATURE REVIEW

2.1 Brief history

Helicobacter pylori is a Gram-negative, helical or spiral shape and has flagella at one end. Average size of the organism measures about 2-4 µm×0.5-1.0 µm. *H. pylori* is a microaerophilic organism and can be found in extremely acidic environments such as human stomach. It is commonly found in the pyloric part of the stomach inside the lining of the epithelium (19). The co-existence of *H. pylori* and human can be dated back to thousands of years ago as *H. pylori* DNA was detected in ancient human remains recovered in Canadian Glacier (20).

H. pylori was first observed since 19th century where curved bacteria were found in the stomach but the organism was not isolated until 1980s. In 1982, .R. Warren, a pathologist together with B.J. Marshall, a physician, noticed the presence of microorganism in gastric mucosa from patients with gastritis. And they assumed that living organism do exist in acidic environment, however, they weren't able to prove the direct association until Warren did a daring and audacious experiment. He drank a culture containing *H. pylori* and underwent endoscopy when symptoms of gastritis start to develop. The endoscopic results showed inflammation of gastric mucosa and the bacteria which later to be known as *H. pylori* is cultured from his stomach (21).

Discovery of living bacteria in acidic environment dramatically shifted the pathological view of gastric related diseases and treatment of such illnesses. Previously, antibiotics were not administered in gastric diseases such as peptic ulcer or gastric ulcer as assumption of stomach as germ free environment (22). However, the evidence of *H. pylori* in human stomach protract previous claims and antibiotics were used for gastric diseases. For their discovery, Warren and Marshall received a Nobel prize in Physiology or Medicine in 2005

Copyright by Mahidol University

2.2 Prevalence of *H. pylori* infection

H. pylori is one of the most common bacterial infection across the world with World Health Organization (WHO) estimating 50% infection rate within world's population (23) (Figure 2.1). However, only a tenth of the infected people develop benign gastric diseases such as dyspepsia, gastric ulcer and peptic ulcer, etc., and less than 1% develop malignant gastric cancer (24). *H. pylori* is related to the mild gastric diseases such as gastritis to severe diseases such as gastric cancer and in 1994, WHO classified *H. pylori* as a etiological agent for gastric cancer and class I carcinogen (25).

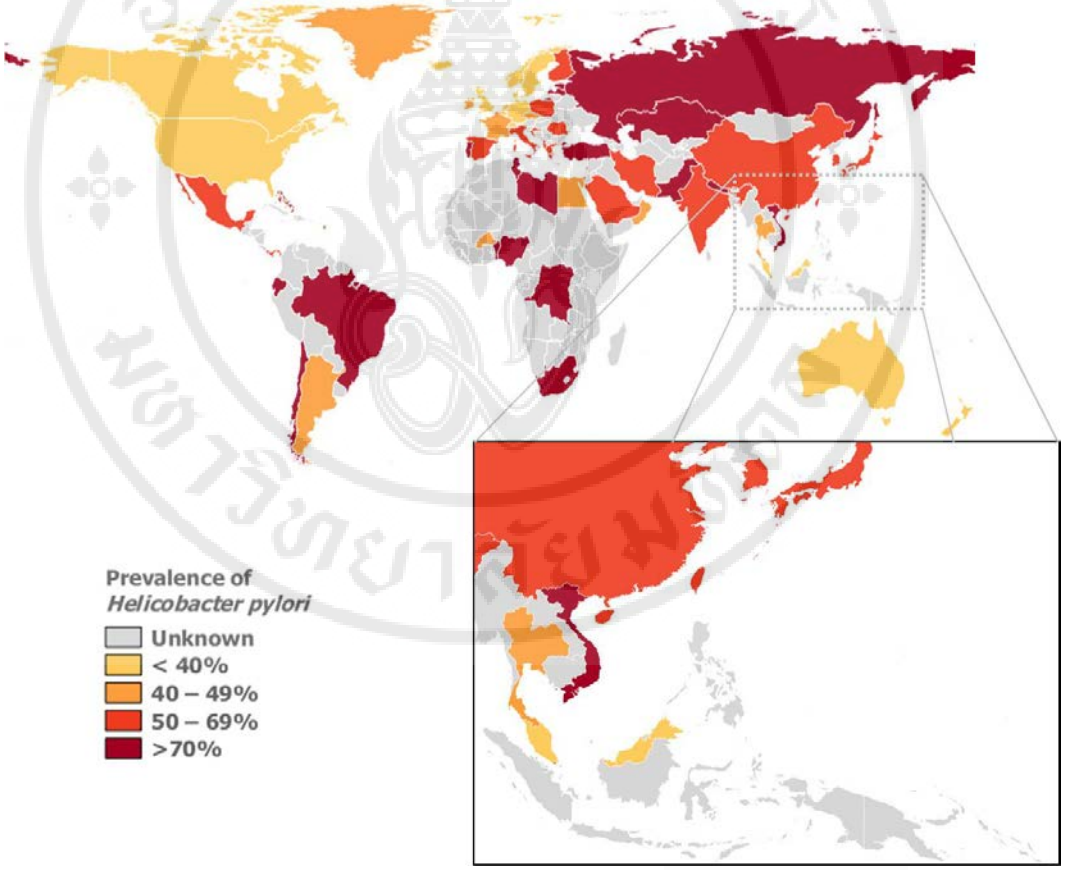

Copyright ® 2017 Elsevier B.V.

Figure 2.1 Prevalence of *H. pylori* infection.

The overall prevalence of *H. pylori* infection is strongly correlated with socioeconomic conditions. The prevalence among middle-aged adults is over 80 percent in many developing countries, as compared with 20 to 50 percent in industrialized countries (23).

Copyright by Mahidol University

Mode of transmission for *H. pylori* is unclear, with several suggested transmission routes such as oral-oral route, oral-fecal route (26) and contact spread route (27). Some studies also suggested the *H. pylori* transmission *via* contaminated food or water source (28). *H. pylori* can also survives in common household foods such as non-pasteurized or pasteurized milk (29), vegetables such as carrots, lettuce (30), cabbage, spinach (31), etc., and packaged food products such as ground beef (32), apple juice or orange juices (30). The reports of *H. pylori* in sterilized products is more alarming as it seems that *H. pylori* can survive in standardized industrial sterilization processes. Previous studies reported the possible mode direct contact between subjects or familial clustering as strong correlation between a family history of *H. pylori* infection and incidence of *H. pylori* in the offspring (33). Furthermore, *H. pylori* prevalence is increased in families with sero-positive members compared to families with sero-negative members (34, 35).

The acquisition rate of *H. pylori* suggests the presence of risk factors or pre-disposing conditions. The prevalence could be related to socio-economic or environmental conditions as *H. pylori* prevalence in developed countries is reported to be much lower than that of developing countries (2, 36). In East Asia, the reported sero-prevalence rates were 58.07% in China (37), 80% in India (38), 39.3% in Japan (39), 59.6% in South Korea (40), 57% in Thailand (41). Moreover, infection during childhood in developed countries is much lower (<5% in USA (42)) whilst that of developing countries is more than 50% (43) and infection rate could be up to 90% (44). Overall, *H. pylori* prevalence rate across the world is ~50%, and with 7 billion inhabitants, up to ~3.5 billion peoples could be infected by *H. pylori* by 2019.

Furthermore, clarithromycin-resistant *H. pylori* is classified by WHO in 2018 as high priority pathogen for research and development of new antibiotics (45). And among the WHO list of priority pathogens, *H. pylori* is by far the widest spread infection in the world, highlighting the importance of research and attention on such common pathogen.

Copyright by Mahidol University

2.3 Virulence factors from *H. pylori*

Whole genome sequence is available for 4 different *H. pylori* strains, each of which shows an average 1.6 million base pairs of DNAs, coding for ~1500 genes (46-48). Among them, several genes were coded for virulence factors which diverse from component of bacterial cell membrane such as lipopolysaccharides which induces immune response in host to secreted factors which modulate host function, immune response and promote bacteria survival (4) (Figure 2.2). The virulence factor production varies from one genotype to another and could be the underlying reason why certain infected people develop gastric diseases eventually leading to malignancy (49). Most of these virulence factors have been known soon after the initial discovery of the bacterium itself, however, TlyA appears to be underreported when compared to the literature available for vacuolating cytotoxin A (VacA) or Cytotoxin-associated gene A (CagA) or urease (Figure 2.3).

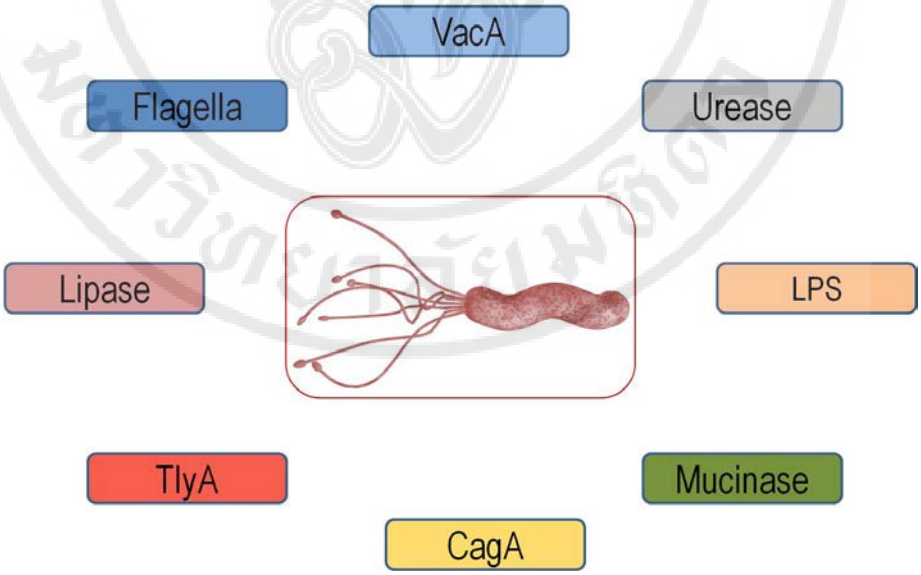

Figure 2.2 Virulence factors produced by *H. pylori*.

CagA, VacA, lipopolysaccharide (LPS). *H. pylori* uses flagella for movement, urease for neutralization of acidic pH in the stomach, LPS for adhesion and immune response. VacA and CagA for host cell remodeling and modulation of immune response and mucinase and lipase and secretory enzymes. TlyA could induce apoptosis and hemolysis in host erythrocytes leading to increase iron availability.

Copyright by Mahidol University

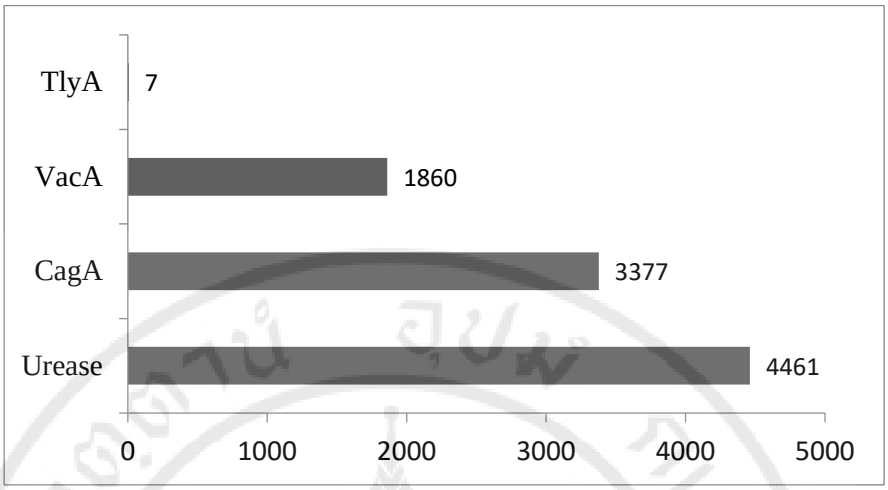

Copyright ® 2019 NCBI

Figure 2.3 Publications related to *H. pylori* virulence factors in NCBI.

Total publications for CagA, VacA, urease and TlyA from 1960s to 2019 are counted. Source: NCBI.

2.4 Urease, VacA and CagA

Urease neutralizes the highly acidic environment in stomach by converting urea to ammonia and carbon dioxide. Urea is taken up by *H. pylori* via a proton-gated channel (50) and hydrolyzed by urease to produce ammonia creating a relatively neutral pH environment. The secreted ammonia can also modulate morphology and transport machinery of the host cells and play a role in gastric ulceration (51, 52). CagA employs the type IV secretion system to be delivered to the host cells (53). Upon entering the host cells, CagA disrupt the regulatory function of actin cytoskeleton system changing the cell morphology and playing a role as an immune-modulator to the host cells (54). VacA can cause intracellular vacuoles in cultured mammalian cell lines or *H. pylori* infected human gastric mucosa (55, 56). VacA can also cause various effects upon the host cells such as vacuolation in the intracellular organelles (57), apoptosis induction *via* activation of caspase 3 and modulation of host immune system by interfering in the proliferation of T cells (58).

Copyright by Mahidol University

2.5 *H. pylori* and host immune response

H. pylori uses multiple strategies to penetrate the host immune system and manipulate the subsequent immune response to ensure its persistence in the gut. Foremost, the overlying mucous layer on the stomach epithelial cell is penetrated by skew-wise motion *via* flagella, and meanwhile the encoded urease enzyme neutralizes the gastric acid by converting urea into ammonia and carbamate leading to increase in alkalinity around *H. pylori* (59). Whereas adhesion to mucin layer of the stomach and binding especially to gastric epithelial cell is achieved by LPS and adhesion molecules (19). Following *H. pylori* colonization, the typical response of the host would be to respond with innate and adaptive immune response which are aimed to remove the infection. And as a Gram-negative bacteria, the encoded LPS would trigger the host immune response by acting as pathogen associated molecular patterns (PAMPs) *via* binding to toll like receptor 4 (TLR4) among the pattern recognition receptors (PRRs) (60). However, LPS from *H. pylori* is proven to be ~1000 fold less active than LPS from *Escherichia coli* which results from the removal of phosphate groups from the lipid A backbone (61). In contrast to other Gram-negative bacteria, *H. pylori* does not release flagellin and recombinant flagellin from *H. pylori* displays significant reduction in TLR5 recognition when compared to flagellin from *Salmonella typhimurium* due to modification in its N-terminal domain (62). Endosomal localized TLR9, however can recognize *H. pylori* DNA, but the response is anti-inflammatory rather than pro-inflammatory (63). DC-SIGN (dendritic cell specific intercellular adhesion molecule-3-grabbing non-integrin) is a C-type lectin receptor (CLR) which recognizes and binds to mannose type carbohydrates (PAMPs) leading to immune system activation and assisting in pathogen clearance (64, 65). *H. pylori* contains fucosylated DC-SIGN ligands which dissociate the signaling complex downstream of DC-SIGN, thereby suppressing the pro-inflammatory signaling response (64). *H. pylori* modulation of host immune responses and overall subversion strategy can be seen in Figure 2.4. Virulence factors produced from *H. pylori* are also implicated in the manipulation of host immune response. VacA produced by *H. pylori* can inhibit T cell proliferation by manipulation of signaling cascades downstream of TCR/IL-2 complex. VacA is also reported to inhibit the translocation of T cell transcription factor NF-AT (nuclear factor of activated T-cells) into nucleus and prevents further

Copyright by Mahidol University

activation of T cell specific immunologically important genes (66). Another virulence factor produced by *H. pylori* and implicated to function in T cell pathway is γ-gluytamyl-transpeptidase (GGT), which blocks the activation of T cells by inducing the arrest of T cells in G-1 phase by interfering with the expression of crucial cell-cycle regulatory proteins such as p27 (67, 68). Both VacA and GGT can also manipulate the T cell differentiation pathway by promoting the differentiation of naïve T cells into regulatory T cells (Tregs). Dendritic cells (DCs) are antigen presenting cells (APCs) which can process antigen, secrete cytokines and induce differentiation of naïve $CD4^+$ T cells into helper and effector T cells (69). However, DCs which are exposed to *H. pylori* preferentially induce the differentiation of naïve T cells into Tregs rather than effector T cells *via* the expression of Treg specific transcription factor Foxp3 and anti-inflammatory cytokine interleukin-10 (IL-10) in naïve T cells (70). This notion is supported by several reports that *H. pylori* infected patients (asymptomatic, duodenal ulcer and gastric cancer) displays accumulation of Tregs in gastric mucosa, especially higher in cancer-affected tissues of gastric cancer patients (71-73). Another cytokine which is reported to be overexpressed in in gastric mucosa exposed to *H. pylori* is multifunctional IL-8. The expression of IL-8 directly correlates with a poor prognosis in gastric cancer.

Overall, *H. pylori* employs several approaches to evade the host immune system and several *H. pylori*-produced factors are involved in host immune system modulation and persistence infection. *H. pylori* and its virulence factors induces several genes in host cells which are potential determinants of inflammation, angiogenesis, and metastasis including IL-8 (74), cyclooxygenase-2 (COX-2) (75), monocyte chemoattractant protein-1(MCP-1) (76) and vascular endothelial growth factor (VEGF) (77). However, limited information is available regarding activation and manipulation of innate and adaptive immune response by *H. pylori* and molecular basic of gastric cancer development in regards to host–pathogen interaction *via* virulence factor production is also in question.

Copyright by Mahidol University

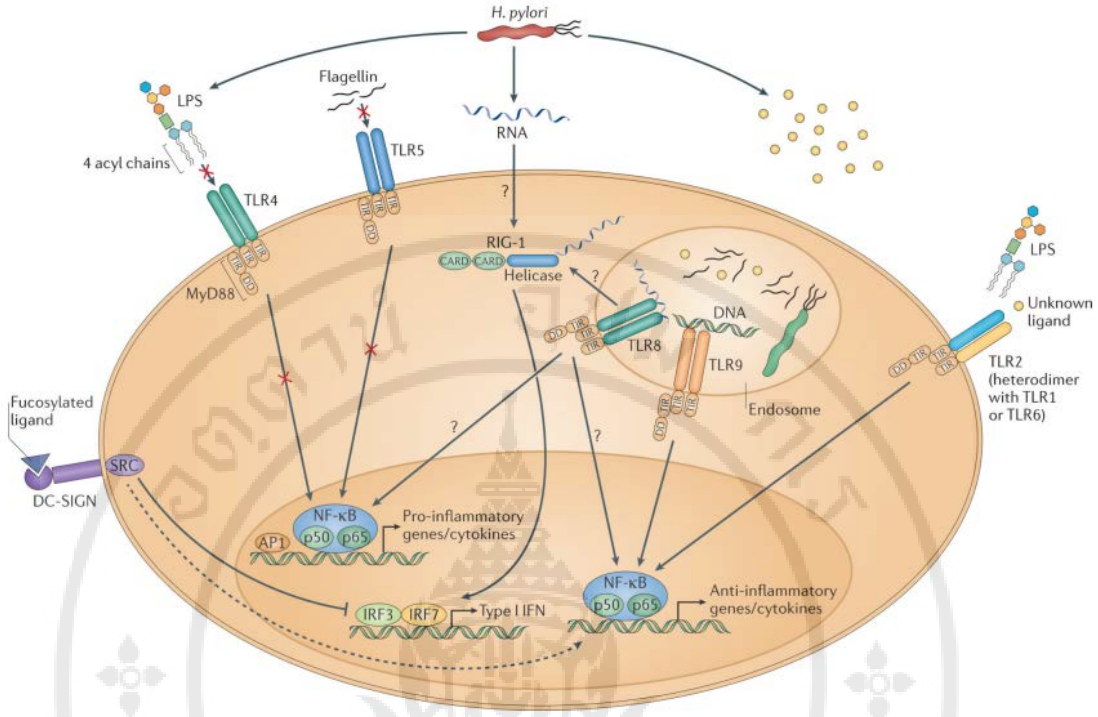

Copyright ® 2013 Springer Nature

Figure 2.4 *H. pylori* subversion of innate immune recognition.

H. pylori harbors PAMPs evolved to evade detection by pro-inflammatory TLRs. *H. pylori* expresses tetra-acylated LPS, which is less bioactive and prevent detection by TLR4. *H. pylori* flagella are not detected by TLR5 due to mutations in the TLR5 binding site of flagellin. *H. pylori* DNA, as well as an as yet uncharacterized PAMP are detected by TLRs 9 and 2, respectively; which activate anti-inflammatory signaling pathways and anti-inflammatory IL-10 expression. 5'triphosphorylated RNA is detected by the RLR RIG-I, which activates the transcription factors IRF3 and IRF7 to induce type I IFN expression, and is potentially detected also by TLR8 in endosomes. *H. pylori*'s fucosylated DC-SIGN ligands suppress activation of the signaling pathways downstream of CLR and activate anti-inflammatory genes (78). DD, death domain; TIR, Toll/Interleukin-1 receptor domain; CARD, caspase activation and recruitment domain; MyD88, myeloid differentiation primary response gene 88; DC-SIGN, dendritic cell-specific intercellular adhesion molecule-3 grabbing non-integrin; SRC, steroid receptor coactivator.

Copyright by Mahidol University

2.6 TlyA

TlyA is a virulence protein which is evolutionarily conserved in both Gram-positive bacteria such as *Listeria monocytogenes*, *Streptococcus thermophilus* and *Bacillus thuringiensis* (10) and Gram-negative bacteria such as *H. pylori* or *E. coli*. TlyA can be found in all sequenced *H. pylori* strains, but its role and function are underreported. Sequence analysis and alignment of TlyA gene within published *H. pylori* genomes reveals strictly conserved nature of TlyA protein (Figure 2.5). The list of *H. pylori* strains and their corresponding TlyA gene with their NCBI accession numbers are listed in Table 2.1. While most of the research on the topic of *H. pylori* focuses on VacA and CagA, few works have been done to study the multifunctional protein which may possibly play an essential role in *H. pylori* survival and pathogenesis. Discovery of hemolytic activity in *H. pylori* culture and supernatant dates back to late 80s and early 90s, a few years after the initial discovery of *H. pylori*. Earlier reports have suggested either incubation with *H. pylori* culture or concentrated supernatant induced hemolysis in erythrocytes from pig, sheep and humans. The hemolysis activity was growth phase and concentration dependent, heat-labile and strain dependent (6,9,11). The presence of putative hemolysin genes within *H. pylori* 26695 genome reveals 6 separate gene loci within the chromosome each conferring certain degree of hemolysis in various red blood cells (RBCs) (12). Two proteins, HP1086 and HP1490, were identified by sequence homology to cytolysins of several pathogenic bacteria and the HP1086 gene product was later named as TlyA for its sequence similarity to TlyA hemolysin from other organisms such as *Mycobacterium tuberculosis* and *Serpulina hyodysenteriae* which function as both methyltransferases and hemolysins (7).

Copyright by Mahidol University

Table 2.1 List of *H. pylori* genomes and corresponding *tly*A gene

***H. pylori* strain and Genebank ID**	**TlyA Genebank ID**	**Country of origin**	**Reference**
Strain 7C CP012905.1	ALM80461.1	Mexico	(79)
Strain LS483488.1	SQJ10127.1	UK	http://www.sanger.ac.uk
Strain SS1 CP009259.1	AQM65389.1	USA	(80)
Strain oki154 CP006823.1	AHN38727.1	Japan	(81)
Strain oki102 CP006820.1	AHN34411.1	Japan	(81)
Strain oki673 CP006825.1	AHN41634.1	Japan	(81)
Strain Rif1 CP003905.1	AFV43893.1	Russia	(82)
Strain B38 FM991728.1	CAX28910.1	France	(83)
Strain 26695 AE000511.1	AAD08129.1	USA	(46)
Strain 26695-1MET CP010436.1	AJF10859.1	Japan	(84)
Strain B8 FN598874.1	CBI66762.1	Germany	(85)
Strain J99 AE001439.1	AAD05917.1	USA	(48)

Copyright by Mahidol University

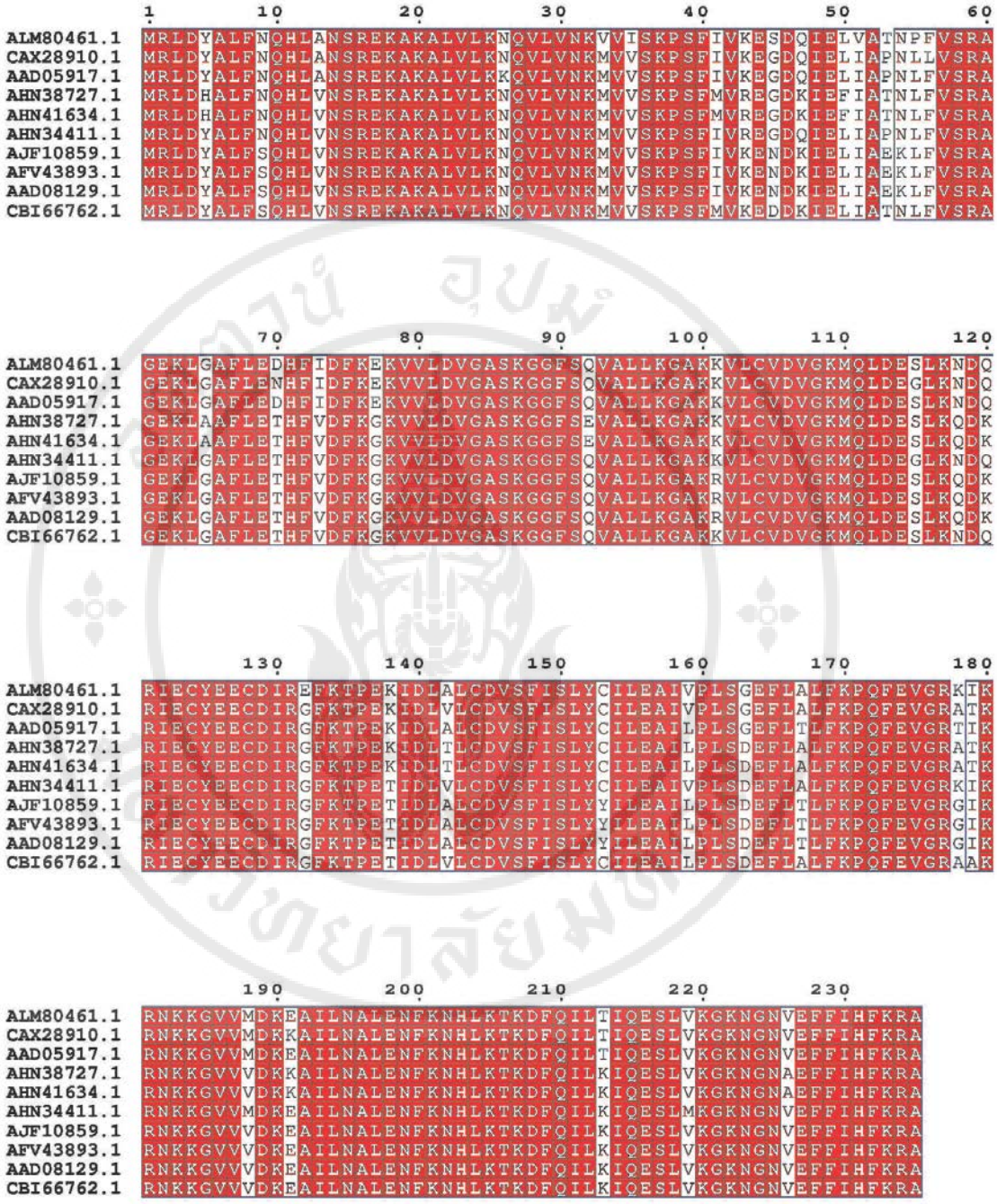

Figure 2.5 Sequence alignment between TlyA from different *H. pylori* genomes.

Multiple sequence alignments of the *tly*A gene from sequenced strains of *H. pylori*. Amino acid sequences encoding *tly*A gene were retrieved from available *H. pylori* genomic database and alignment was performed using ClustalW.

Copyright by Mahidol University

2.6.1 TlyA transcription, translation, regulation, and secretion

Currently no information regarding *H. pylori tly*A transcriptional start site or the regulation of gene expression is available. Gene synteny analysis of its homolog from *M. tuberculosis* reveals that all genes within the TlyA operon are involved in cell metabolism, cell wall biosynthesis and cell signaling rather than bacterial virulence mechanism suggesting the role of TlyA in metabolic pathway (Figure 2.6). TlyA is translated into a 27-kDa protein, with no typical secretion signal sequence (13). Its homolog from *M. tuberculosis* displayed secretion onto cell membrane when expressed as recombinant protein in *E. coli* suggesting the presence of secreted TlyA on the *E. coli* outer membrane (16).

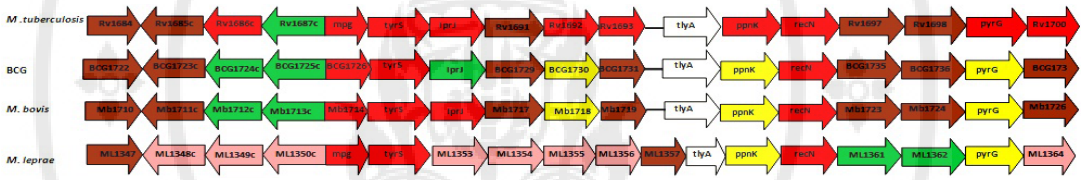

Copyright ® 2011 Springer Nature

Figure 2.6 *tly*A transcriptional unit gene syntheny.

Genes are represented as arrows and are draw according to transcriptional orientation and genome functional annotation. Arrow color representation for gene function annotation is as follows: green for cell wall synthesis, red for signal transduction, brown for evolutionarily conserved, yellow for intermediary metabolism, white for *tly*A, pink for pseudogenes, (86).

2.6.2 Membrane-pore formation by TlyA

Bacterial virulence factors or toxins affect the host cells by binding/targeting the host cells and induces changes by exerting enzymatic activity in intracellular targets or by forming pores in the plasma membranes of the cells (87). *H. pylori* TlyA binds to the erythrocytes and epithelial cells but no subsequent intracellular enzymatic activity is reported (7). However, TlyA mediated hemolysis of erythrocytes can be inhibited in the presence of osmoprotective saccharides suggesting the potential formation of transmembrane pores (7,13). However, recent report also

Copyright by Mahidol University

suggested TlyA causes the agglutination of erythrocytes and liposome thereby leading to membrane permeabilization (13).

2.6.3 TlyA structure

Far-UV CD spectra of the 27-kDa TlyA estimated 15% α-helix, and 34% β-secondary structures in the protein (13). Exposures to temperatures above 37°C resulted in a considerable change in the far-UV CD profile of the protein and in binding of extrinsic fluorescence dye 8-anilino-1-naphthalene sulfonate to TlyA suggesting the presence of temperature dependent conformational states of TlyA. Furthermore, the exposure to elevated temperatures results in gross secondary and tertiary structural changes in the protein leading to formation of amyloid-like aggregated assemblies (18). This property could be due to the presence of specific region ($F^{148}ISLYYILEAIL^{159}$) which is the typical sequence for amyloidogenic proteins and such region could be responsible for aggregation-prone property of *H. pylori* TlyA (18).

2.6.4 TlyA activities in *in vitro* assay systems

2.6.4.1 Effects on epithelial cells

One of the reported activities of TlyA is its ability to cause cytotoxicity of cultured cells. Cytotoxicity can be observed 24 hours after addition of TlyA to cells and is concentration dependent. Flow cytometry studies suggested the binding of TlyA to epithelial cells and both cell morphology and integrity were affected by TlyA treatment (13). Currently, the mechanism for TlyA-induced cytotoxicity is not known.

2.6.4.2 Effects on erythrocytes

When added to human erythrocytes, TlyA induce cell aggregation and hemolysis, the latter can be blocked by saccharides bigger than 1 nm suggesting the formation of pores in erythrocyte membranes (13). TlyA is necessary and sufficient for *H. pylori*-induced hemolysis as *H. pylori* TlyA negative mutants showed reduction in hemolytic activity compared to wild type (WT) *H. pylori* expressing TlyA (7). Although the mechanisms by which TlyA induces hemolysis are not fully understood, TlyA-induced hemolysis has been shown to depend on

Copyright by Mahidol University

incubation time and required high concentration of toxin (up to 20 μM) suggesting a slow mechanism of action (13).

2.6.4.3 Effects on artificial lipid vesicles

Liposomes are lipid bilayer vesicles which can be used as a model to study the binding of target protein to lipid membranes and lytic mechanism. TlyA binds to the liposomes and induces agglutination and membrane permeabilization (13). It should be noted that the reported studies indicated the requirement of high concentration of TlyA for binding and lysis of lipid membrane is similar in both erythrocytes and artificial lipid vesicles suggesting a similar mechanism of action (13). And since artificial lipid vesicles lacks membrane proteins and receptors, the mechanism of TlyA induced membrane perturbation could be by pore formation *via* binding to lipids rather than specific receptor.

2.6.4.4 Effects on immune cells and system

Effect of *H. pylori* TlyA on immune system is yet to be investigated, however, its homolog from *M. tuberculosis* displays immunomodulation properties both *in vitro* and *in vivo*. *M. tuberculosis* strain lacking TlyA mutant induces increased production of pro-inflammatory cytokine and reduced production of anti-inflammatory cytokines such as IL-1β and IL-10 which is sharply different from that of wild type *M. tuberculosis*. TlyA mutant *M. tuberculosis* also more susceptible to autophagy by macrophages and animals infected with the TlyA mutant *M. tuberculosis* exhibited increased host-protective immune responses, reduced bacillary load, and increased survival compared with animals infected with wild type *M. tuberculosis*. (14).

2.6.5 Activity of TlyA in animal models

Animal models have been utilized to investigate a potential role of TlyA in promoting *H. pylori* colonization of the mammalian stomach. TlyA mutant strains of *H. pylori* showed substantially reduced ability to colonize stomach of mice which indicates that TlyA is essential for gastric colonization (7).

Copyright by Mahidol University

2.6.6 Comparisons of TlyA activities *in vitro* and *in vivo*

TlyA binds to and induces cytotoxicity against human gastric epithelial cells *in vitro* (7,13,18). Although unproven as yet, TlyA homologs displayed S-adenosyl-L-methionine (SAM) dependent *in vitro* methyltransferase activity of *E. coli* ribosomes which suggests possible critical function of TlyA in *H. pylori in vivo* (88, 89). Moreover, TlyA displays genetic similarity toward homologs from *M. tuberculosis*, *S. hydrodystentriae* and *Camphylobacter jejuni* suggesting the conserved nature of the TlyA across several bacterial strains (88). Studies performed using the homologs of the *tly*A gene showed that the mutation of *tly*A gene affects colonizing abilities of other pathogenic bacteria such as *Brachyspira hyodysenteriae* and *C. jejuni* indicating that TlyA protein might play important role during bacterial invasion into host cells (90, 91). Major TlyA activity observed *in vitro* is hemolysis of erythrocytes, however, the *in vivo* significance of such activity in *H. pylori* pathogenesis is unclear. The probable *in vivo* impact of TlyA could be to increase the availability of nutrients or essential metals which are scarce in stomach environment. The availability of metal such as iron is reported to influence the expression of major virulence factors in *H. pylori* such as VacA or the secretion of outer membrane vesicles (92). Furthermore, *H. pylori* infection is proposed to be the causative for iron deficiency anaemia (93, 94). However, currently available information on *H. pylori* TlyA is very limited as few studies are available regarding the *in vitro* activities and their respective underlying mechanisms and regarding the sequence-structure-function relationship of TlyA. Therefore, there is substantial interest in defining *in vitro* TlyA activities that could be relevant *in vivo* for promoting *H. pylori* pathogenesis or the development of *H. pylori* related gastric diseases.

In summary, TlyA is a bacterial toxin that displays sequence and structural similarity with other known bacterial proteins in amino acid sequence, protein structure, biological activity and virulence mechanism. Both epithelial cells and erythrocytes are sensitive to TlyA mediated cytotoxicity and membrane perturbation, respectively. *In vivo*, TlyA enhances the capacity of *H. pylori* to colonize the stomach and contributes to the pathogenesis of *H. pylori* persistence infection. It will be imperative to characterize the mechanism by which TlyA causes membrane

Copyright by Mahidol University

perturbation in host cells, to identify the activity of TlyA that are most significant *in vivo* and to exemplify the structural and functional relationships of TlyA.

Copyright by Mahidol University

CHAPTER III
OBJECTIVES

3.1 Ultimate objective

To evaluate structure-function relationships of the TlyA protein from *H. pylori*

3.2 Objectives

1. To clone and express recombinant TlyA from *H. pylori* and, subsequently purify

2. To establish a biological assay for TlyA activity *in vitro*

3. To analyze TlyA binding and effect to AGS cells and lipid membranes

4. To construct a 3D model of TlyA and structurally analyze *via* multiple sequence alignment and homology-based modeling

5. To identify and evaluate putative residue/s responsible for TlyA binding and/or activity by *in silico* analysis and *in vitro* assays

Copyright by Mahidol University

CHAPTER IV
MATERIALS AND METHODS

4.1 Materials

4.1.1 Chemicals

• Acetic acid (Glacial)	Lab-Scan
• Acrylamide (30%)	AppliChem
• Ammonium persulfate	Sigma
• Ampicillin	Sigma
• Bacteriological agar	Conda
• Bacteriological peptone	Conda
• Bovine serum albumin	Promega
• Bradford protein assay reagent	Biorad
• Bromophenol blue	Sigma
• 5-Bromo-4-chloro-3-indolyl phosphate	Sigma
• Nitro blue tetrazolium	Sigma
• Coomassie brilliant blue R-250	Sigma
• Calcium chloride	Sigma
• Chloroform	BDH
• Cholesterol	Avanti
• 1,4-Dithiothreitol (DTT)	Sigma
• Deoxynucleotide triphosphates	Pharmacia Biotech
• 3, 3′-Diaminobenzidine (DAB)	Vector
• Ethanol (absolute)	VWR
• 4-(2-Hydroxyethyl)-1-piperazineethanesulfonicacid (HEPES)	Merck

Copyright by Mahidol University

• Phosphatidylcholine	Avanti
• Phosphatidylethanolamine	Avanti
• Glycerol	Merck
• Isopropyl-β-D-thiogalactopyranoside	Sigma
• λ*Hin*dIII digested DNA marker	Gibco BRL
• Nitroblue tetrazolium	Sigma
• Phenylmethylsulfonyl fluoride (PMSF)	Thermo Fisher
• Protein standards marker	Biorad
• Sodium carbonate	Fluka
• Sodium chloride	Vetec
• TEMED	Biorad
• Triton X-100	Sigma
• Tween-20	Sigma
• Yeast extract	Conda

4.1.2 Enzymes

• KOD Plus Neo DNA polymerase	TOYOBO
• T4 DNA ligase	Fermentas
• Lysozyme (EC 3.2.1.17, L-6876)	Sigma
• Ribonuclease A (RNase A, EC 3.1.27.5)	Sigma
• Trypsin Type XIII (TPCK treated)	Sigma
• *Ava*I	NEB
• *Hin*dIII	Thermo Fisher
• *Nde*I	Thermo Fisher

Copyright by Mahidol University

4.1.3 Recombinant plasmids

4.1.3.1 pD441-TlyA

The recombinant plasmid containing the *tly*A gene encoding the 27-kDa toxin and this was used as template for construction of pET17-b-TlyA plasmid (Figure 4.1).

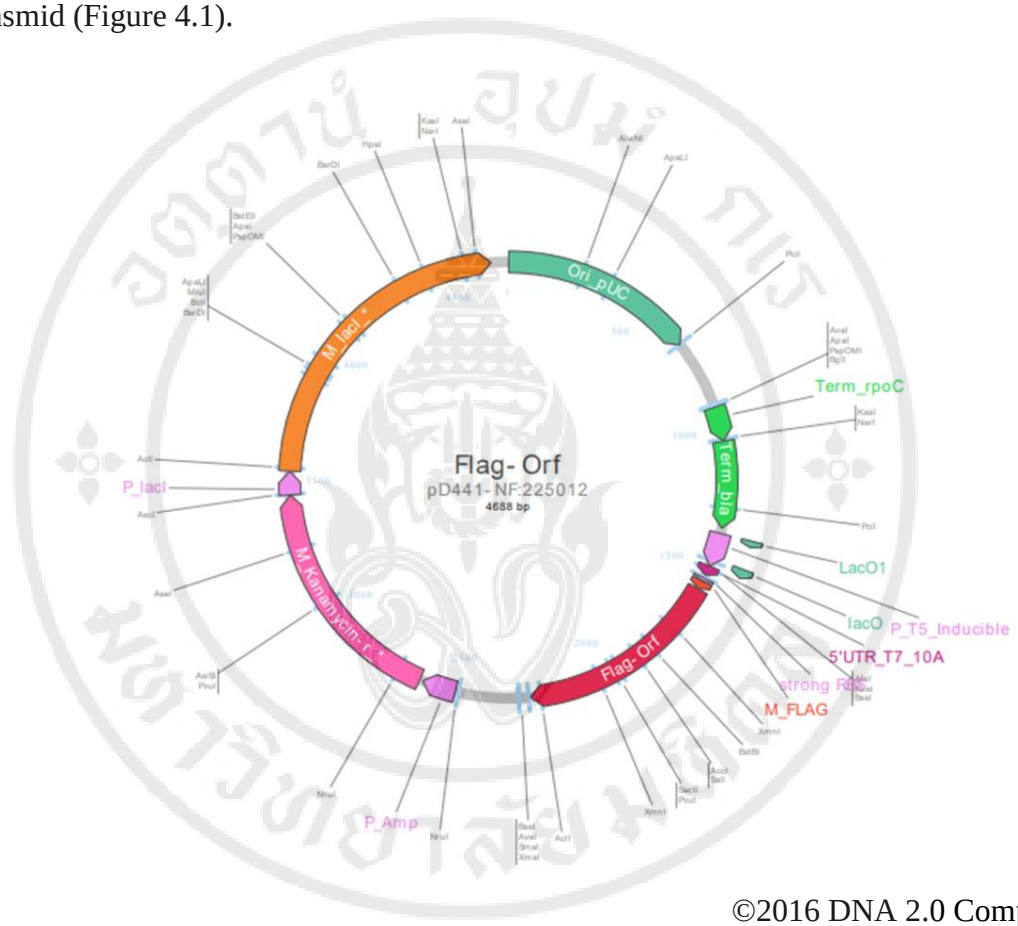

©2016 DNA 2.0 Company

Figure 4.1 Physical map of pD441 plasmid.

The Figure shows the recombinant pD441 plasmid containing the *tly*A gene (red arrow). Green arrow represents origin of replication and magenta arrow represent kanamycin resistant gene.

Copyright by Mahidol University

4.1.3.2 pET-17b-TlyA

The recombinant plasmid containing the *tly*A gene encoding the 27-kDa toxin (figure 4.2).

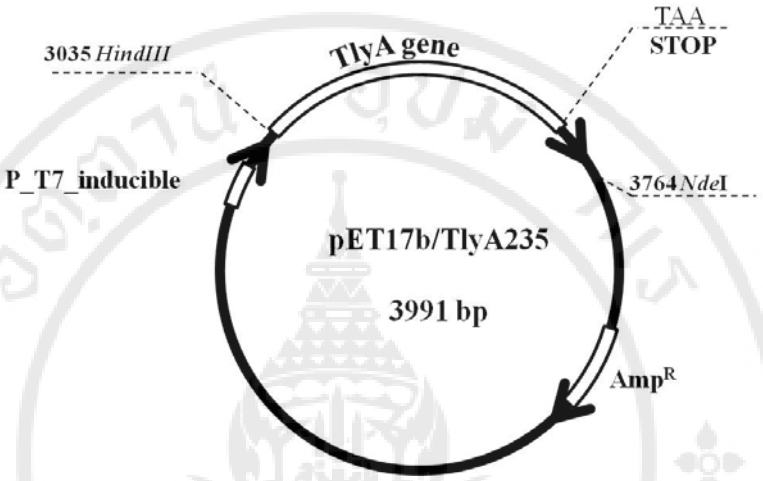

Figure 4.2 Physical map pET17b/TlyA235 plasmid.

The figure shows the recombinant pET-17b plasmid containing the *tly*A gene (white box), flanked by *Hin*dIII and *Nde*I restriction sites.

4.1.4 Antibodies

- Mouse anti-FLAG Sigma
- Rabbit anti-mouse-ALP conjugated Sigma
- Goat Anti-mouse-AF488 Thermo Fisher

4.1.5 DNA sequencing primers

The primers for sequencing TlyA-encoding plasmids T7

Forward: 5'- TAATACGACTCACTATAGGG-3'

T7 Reverse: 5'-TAGTTATTGCTCAGCGGTGG-3'

Copyright by Mahidol University

4.1.6 Primers to subclone *tly*A from FLAG/TlyA235 into pET-17b

Following sequences were used as forward and reverse primers for sub-cloning of *tly*A into pET-7b vector.

Forward primer: 5'ATTCATATGCATCATCATCATCATCATCGTCTG GATTATGCGCTGTTTAG -3'

Reverse primer: 5'-GCGCAAGCTTTTATGCACGCTTAAAGTGGATG AA-3'

4.1.7 Bacterial strains

- *Escherichia coli* BL21(DE3)

[B F– ompT gal dcm lon hsdSB(rB–mB–) λ(DE3 [lacI lacUV5-T7p07 ind1 sam7nin5]) [malB+]K-12(λS)] (Invitrogen)

- *Escherichia coli* JM109

[endA1 glnV44 thi-1 relA1 gyrA96 recA1 mcrB+ Δ(lac-proAB) e14- [F' traD36 proAB+ lacIq lacZΔM15] hsdR17(rK-mK+)] (NEB).

4.1.8 Instruments

- Geneamp PCR system 2400 Perkin-Elmer
- Gel electrophoresis units Biorad
- FPLC Spectrosystem, p2000, Thermo Scientific
- TE 70, ECL semidry transfer unit Amersham
- Mini Extruder Avanti
- Spectrophotometer U2000 Hitachi
- Spectrofluorometer Jasco
- Sonicator XL2020 Misonix

4.1.9 Miscellaneous

- HiTrapTM SP HP column (5 ml) GE
- PD-10 desalting columns GE
- Membrane filter, 0.2 µm pore size (47 mm diameter) Merck
- 10-kDa MWCO columns Merck
- Multianalyte ELISA kit Qiagen

Copyright© by Mahidol University

4.2 Methods

4.2.1 Plasmid extraction by alkaline lysis method

A single colony was inoculated in 3 ml LB broth containing 100 µg/ml ampicillin and grown at 37°C with 220 rpm shaking for 12-16 hours. The cells were pelleted by centrifugation at 8,000 × g for 5 minutes and re-suspended in 200 µl of solution I (50 mM glucose, 10 mM EDTA, 25 mM Tris-HCl, pH 8.0). RNase A was added to final concentration of 100 µg/ml and incubated for 2-3 minutes at room temperature. 200 µl of solution II (0.2 M NaOH, 0.1% SDS) was added and immediately mixed by gentle inversion. 300 µl of solution III (3 M sodium acetate) was added and mixed by gentle inversion. The mixture was centrifuged at 20,000 × g for 5 minutes and the supernatant was transferred to a new tube. DNA was precipitated by addition of sodium acetate to the final concentration of 0.3 M and 3 volumes of ice cold 95% ethanol followed by centrifugation at 20,000 × *g* for 10 minutes. The supernatant was discarded the DNA precipitate was re-suspended in 20 µl of MilliQ water (95).

4.2.2 Agarose gel electrophoresis of DNA

Agarose powder (0.8-1.2% w/v) was dissolved in TAE buffer (40 mM Tris-HCl, 40 mM acetic acid, 25 mM EDTA, pH 8.0) and the gel mixture was cooled down to about 55°C and poured into the mould to solidify at room temperature. DNA sample was mixed with 6× DNA loading dye (Thermo Science) at ratio 1:5 (v/v) and the mixture was loaded into the wells of the agarose gel submerged in TAE buffer. Electrophoresis was performed at constant voltage (100 V) until the dye reached the bottom of the gel. After electrophoresis, the gel was washed with distilled water and stained by DNA staining solution (Hydragreen^{TM}) for 30 minutes followed by de-staining in distilled water for another 30 minutes. The gel was visualized under UV light and scanned by the Geldoc® XR documentation system (Biorad). The amount of DNA was estimated by comparison with standard DNA markers of known concentration.

Copyright by Mahidol University

4.2.3 PCR

The primer pairs (Material 4.1.6) were designed and synthesized (IDT, USA) in order to subclone *tly*A gene into pET-17b plasmid. PCR reaction was prepared in a 0.25 ml PCR tube containing 20 µl of a reaction mixture.

DNA template	20	ng
dNTPs	0.2	mM each
Forward primer	10	pmol
Reverse primer	10	pmol
10x buffer for KOD Plus Neo	10	µl
KOD Plus Neo DNA polymerase	1	U

Sterilized MilliQ water was added to a final volume of 20 µl.

The temperature cycling parameters are shown in Figure. 4.3, and PCR products were examined on 1.2% agarose gels.

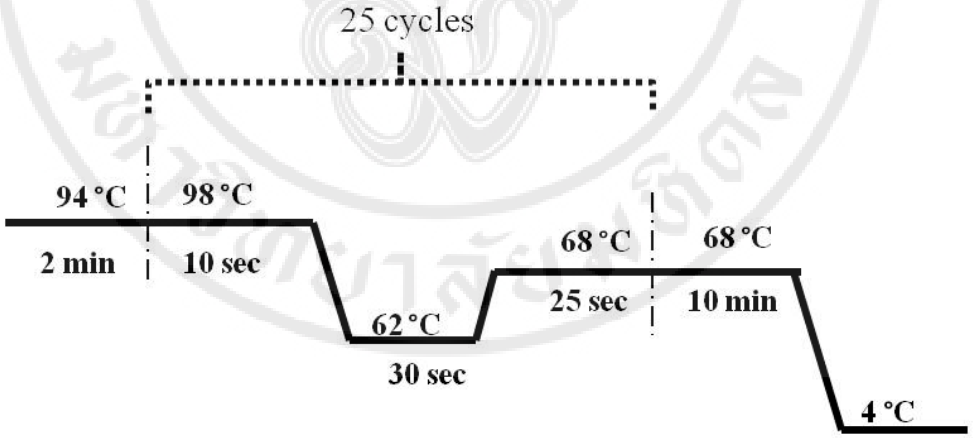

Figure 4.3 Temperature parameters for PCR reaction.

4.2.4 Digestion of PCR products and pET-17b vector

The PCR amplification products and pET-17b vector were incubated with *Hin*dIII and *Nde*I restriction endonucleases at 37°C for 1 hour to digest the backbone vector and insert (PCR product). The digestion reaction parameters are shown in Table 4.1 and 4.2.

Copyright by Mahidol University

Table 4.1 Reaction parameters for digestion of PCR product.

Components	Final concentration
PCR product	1 µg
10 x fast digest buffer	1 x
*Hin*dIII	1 U
*Nde*I	1 U

Table 4.2 Reaction parameters for digestion of vector backbone (pET-17b).

Components	Final concentration
pET-17b	1 µg
10 x fast digest buffer	1 x
*Hin*dIII	1 U
*Nde*I	1 U

4.2.5 Preparation of competent *E. coli* cells by calcium chloride method

A single colony of *E. coli* strain JM 109 or BL21 (DE3) was inoculated into 5 ml of LB broth and incubated at 37°C with 220 rpm shaking for 12-16 hours. The overnight culture was inoculated into fresh LB broth final concentration of 0.01 OD (optical density) and then incubated at 37°C until the OD_{600} reached 0.3-0.4. The cells were chilled on ice for 5-10 minutes followed by centrifugation at 5,000 × *g* for 5 minutes. The pellet was resuspended in 10-15 ml of ice-cold 0.1 M $CaCl_2$ and centrifuged as previously. After washing, the cells were resuspended in 2 ml of ice-cold 0.1 M $CaCl_2$ supplemented with glycerol (25% v/v) and the 100 µl of cells were aliquoted into 1.5 ml microcentrifuge tubes and kept at -80 °C until usage (96).

4.2.6 Ligation and transformation

The digested DNA fragments (PCR products and pET-17b) were ligated at vector: insert ratio of 1:3 using T4 DNA ligase at 16°C for 12-16 hours. The ligation products were transformed into JM 109 *E. coli* using heat shock method. One vial of *E. coli* was used for transformation; 10 ng of ligated products were added and the mixture was heated at 42°C for 60 seconds followed by placing on ice for 10 minutes.

Copyright by Mahidol University

900 µl of sterile LB media was added and incubated at 37°C for 45 minutes. Cells were plated on LB agar plates supplemented with 100 µg/ml ampicillin and incubated at 37°C for 12-16 hours.

4.2.7 Protein expression

The recombinant clones were inoculated in 5 ml of LB broth supplemented with 25 µg/ml kanamycin or 100 µg/ml ampicillin and incubated at 25 °C, 30 °C or 37°C, 220 rpm for 12-16 hours. The overnight culture was used to inoculate LB media to the final concentration of 0.01 OD and incubation was continued at 25 °C, 30 °C or 37°C, 220 rpm until OD_{600} reached 0.5-0.6. Protein expression was induced by addition of IPTG to the final concentration of 0.1 mM and expression was continued for 4-6 hours. Protein expression was analyzed on SDS-PAGE.

4.2.8 SDS-polyacrylamide gel electrophoresis (SDS-PAGE)

Protein sample was prepared by mixing the sample with loading buffer (8% SDS, 40% glycerol, 0.4% bromophenol blue, 200 mM Tris-HCl, pH 6.8) at a ratio of 3:1 (v/v) and DTT was added to a final concentration of 100 mM followed by heating at 95°C for 10 minutes. The samples were centrifuged at 10,000 × *g* for 1 minute and the supernatant was loaded on each well of SDS-polyacrylamide gel. For semi-native gels, protein samples were mixed with sample buffer lacking SDS and DTT and loaded onto SDS-PAGE gels.

SDS-PAGE gel was prepared using mini-Protean™ II electrophoresis system (BIORAD). Stacking gel contains 5% gel, 0.125 M Tris-HCl (pH 6.8) and 0.1% SDS, whereas separating gel contains 12% gel, 0.375 M Tris-HCl (pH 8.8) and 0.1% SDS. The gel was run in Tris-glycine buffer (19.2 mM glycine, 0.01% SDS, 25 mM Tris-HCl, pH 8.3) at constant voltage until the dye reached the bottom. Following electrophoresis, gel was washed by distilled water followed by staining with staining solution (50% ethanol, 10% glacial acetic acid, 0.1% Coomassie brilliant blue R250 in distilled water) for 1 hour and de-stained with de-staining solution (10% ethanol, 10% acetic acid in distilled water) until the background was clear.

Copyright by Mahidol University

4.2.9 Purification of TlyA by cation exchange chromatography

Protein purification was achieved by using a Spectra SYSTEM™ (Thermosci) FPLC. Cell lysate containing the TlyA protein was re-suspended in buffer A (50 mM HEPES, pH 8.2) and lysozyme was added to a final concentration of 0.1 mg/ml. PMSF was added to a concentration of 1 mM before sonication and sonicated for 10 minutes at 4°C using Misonix XL2020 Sonicator (Hofstra, USA). The sonicated mixture was centrifuged at 8000 × *g* for 5 minutes to separate soluble and insoluble proteins. The soluble fraction (5-10 ml) was injected into HiTrap SP HP cation exchange chromatography column (GE) equilibrated with buffer A. The column was washed with buffer A (1 ml/minute) and proteins were eluted by stepwise elution from 20% to 100% of buffer B (50 mM HEPES, 1 M NaCl, pH 8.2) at a flow rate of 1 ml/minute and 1 ml fractions were collected. 20 µl of each fraction were analyzed on SDS-PAGE (15% gel). Fractions containing TlyA were pooled and dialyzed against the 1000-fold volume of hemolysis assay buffer (20 mM Tris-HCl pH 7.4, 150 mM NaCl) for 2 hours and then overnight against the same volume.

4.2.10 Western blot analysis of TlyA

TlyA fractions (total, soluble and insoluble) were run on SDS-PAGE (15% gel) and the proteins were transferred onto nitrocellulose membrane by semidry transfer at 100 V for 1 hour. The membrane was blocked with 5% BSA in PBS buffer (137 mM NaCl, 27 mM KCl, 10 mM Na_2HPO_4, 1.8 mM KH_2PO_4, pH 7.4) for 1 hour at room temperature followed by addition of monoclonal anti-FLAG antibody (Sigma, USA) at 1: 3000 ratio and incubated for 1 hour. The membrane was washed by PBS buffer supplemented with 0.1% tween 20 for 3 times, 5 minutes each. The membrane was incubated with secondary antibody, anti-mouse IgG conjugated with alkaline phosphatase (Sigma, USA) at a dilution of 1:5000. The membrane was washed as previously and the signal was developed by addition of nitro-blue tetrazolium and 5-bromo-4-chloro-3'-indolyphosphate to visualize the signal. Blots were routinely incubated for 1-3 minutes.

Copyright by Mahidol University

4.2.11 Determination of protein concentration

Protein concentrations were determined by Bradford protein assay (97). Bovine serum albumin (BSA) standards were prepared as final concentrations of 1, 2, 3, 4 and 5 mg/ml of BSA in PBS respectively. Undiluted or 10-fold diluted samples in 50 µl volume are mixed with 200 µl of Bradford assay reagent (Bio-rad) in 96 well flat bottom plates (Sterilin) and absorbance was measures spectrophotometrically at 595 nm (SpectraMax 250, Molecular Devices, USA). Concentrations of the samples were calculated from the standard curve.

4.2.12 Membrane Perturbing assays

4.2.12.1 Preparation of entrapped-sulforhodamine B liposomes

A lipid mixture composed of phosphatidylethanolamine (PE) and phosphatidylcholine (PC) was prepared at a ratio of 1:1 (w/w) in a glass vials (Wheaton) and the mixture was slowly dried under a gentle breeze of nitrogen. The dried lipid mixture was re-suspended in 200 µl of assay buffer (20 mM HEPES pH 7.4, 150 mM NaCl) containing 100 mM sulforhodamine B (Sigma) and the mixture was subjected to several freeze-thaw cycles. Large unilamellar vesicles (LUVs) were prepared by passing the mixture through mini-extruder assembled with 0.1 µm polycarbonate membrane (Avanti polar lipids, USA) for 21 times. Untrapped dyes were removed by PD-10 columns (GE) and the fractions were analyzed by phosphorous content analysis.

4.2.12.2 Fluorescence dye release assay

The membrane perturbing activity of TlyA was assayed by the release of entrapped sulforhodamine B. The assays were performed in a final volume of 100 µl dye entrapped liposomes (10 µM) at E_x-565 nm, E_m-586 nm followed by addition of various concentrations of TlyA. The fluorescence intensity was measured for 15-30 minutes and Triton-X was added to final concentration of 0.1% to achieve the maximum lysis of LUVs. Following formula was used to calculate the percentage of fluorescence recovery.

Copyright by Mahidol University

$$\mathbf{F}t = \frac{(\mathbf{I}f - \mathbf{I}o)}{(\mathbf{I}max - \mathbf{I}o)} \times 100$$

$\mathbf{F}_t$ =% of fluorescence recovery

$\mathbf{I}_o$=Initial fluorescence

$\mathbf{I}_f$= fluorescence observed after adding toxin

$\mathbf{I}_{max}$= total fluorescence observed after adding Triton-X

4.2.12.3 Fluorescence dye release assay

TlyA at 16 µM was incubated with 10 µM liposomes for 15 minutes at 25°C in a final volume of 100 µl assay buffer (20 mM HEPES pH 7.4, 150 mM NaCl). After incubation, the mixture was centrifuged at 10,000 × *g* for 5 minutes supernatant was discarded. The pellets were washed for 3 times with assay buffer to remove unbound proteins followed by resuspension with 30 µl of assay buffer. SDS loading dye was added to the mixture and heated at 95°C for 10 minutes prior to loading onto SDS-PAGE gels. Liposomes without TlyA were used as a negative control.

4.2.13 Cell culture assays

4.2.13.1 Culture of a human gastric adenocarcinoma cell line

AGS cells (ATCC) were cultured in T-25 flask (Costar) at a density of 0.25 × 10^6 cells/25 cm^2 in Ham's F12 medium supplemented with 1% glutamax (Thermo Fisher), 1% penicillin/streptomycin and 10% fetal bovine serum (FBS, EmbryoMax®, Merck) in a 5% CO_2 atmosphere at 37°C.

4.2.13.2 Cell viability assay

AGS cells were seeded in 96 well plates (Corning) at a density of 1.25 × 10^4 cells/well prior to addition of TlyA protein. Purified TlyA protein at varying concentrations (1-20 µM) was added to the culture medium overlying the adherent cells and incubated for 24 hours at 37°C/5% CO_2. TlyA-induced reduction in cell viability was quantitated by Prestoblue™ cell viability assay (Thermo Fisher) according to manufacturer's instructions. Prestoblue™ is a resazurin-based solution which utilizes the reducing ability of living cells to quantitatively measure cell viability. Resazurin (7-hydroxy-3H-phenoxazin-3-one 10-oxide) is a blue dye which can permeate the cells and is weakly fluorescent, but when taken up by the living cells,

Copyright by Mahidol University

it is reduced to red fluorescent resorufin which can be measured fluorometrically at 590 nm (98). The amount of resorufin can therefore be correlated to the viable cell population. Briefly, Prestoblue® reagent was added to cell culture medium (10% v/v) and incubated for 1 hour at 37°C/5% CO_2 prior to reading out fluorescence. The top fluorescence was measured by Multimode Detector (DTX 880, Beckman Coulter) at E_x-565 nm, E_m-586 nm. Ethanol at 20% (v/v) was used as a positive control to induce 100 % cell death as described before (99).

4.2.13.3 Profiling of TlyA induced cytokine production

AGS cells were grown in 24 well plates (Costar) and treated with 10 µM TlyA per well for 24 hours at 37°C/5% CO_2. After incubation, medium overlaying the cells were collected and briefly centrifuged at 1000 × g for 10 minutes to remove cellular debris. TlyA-induced cytokine production was measured by human inflammatory cytokines multi-analyte ELISA array™ kit (Qiagen) according to manufacturer's protocol. Briefly, 50 µl of cell culture supernatants were mixed with same volume of sample buffer and added to each well of 96-well plate pre-coated with antibodies against human cytokines and incubated at room temperature for 2 hours. After incubation, unbound antigens were washed by wash buffer and detection antibodies were added to each well and incubated at room temperature for 1 hour. Following incubation with detection antibodies, avidin-HRP conjugate was added to each well and incubated for 30 minutes in the dark. 100 µl of development solution was added to each well and incubated for 15 minutes in the dark. 100 µl of stop solution was added to each well and the signal was quantitated by measuring absorbance at 450 nm. Untreated cells were used as negative control and the antigen cocktail supplied in the commercial kit was used a positive control.

4.2.14 Immunocytochemical staining

AGS cells were grown on coverslips and treated with 10 µM TlyA for 24 hours at 37°C/5% CO_2. After incubation, coverslips were washed with PBS prior to fixation with 4% formaldehyde and/or permeabilization with 0.1% Triton X-100 (v/v). Coverslips were washed with PBS for 3 times prior to incubation with blocking buffer (1%BSA in PBS) for 1 hour at 37°C followed by incubation with primary antibody (Mouse anti-FLAG (Sigma) in a ratio of 1:500 and incubated as before. Coverslips

Copyright by Mahidol University

were washed with PBS for 3 times followed by incubation with secondary antibody (goat anti-mouse, Alexa Fluor 488) at 1 µg/ml for 1 hour at 37°C. Coverslips were washed again with PBS for 4 times prior to mounting on glass slides. Mounted slides were observed by confocal microscopy (Zeiss, LSM 880) at 80 magnification.

4.2.15 *In silico* characterization of TlyA structure and function

4.2.15.1 Multiple sequence alignment

Amino acid sequence encoding TlyA were retrieved from Uniprot (id: O25718) and submitted to HHpred server (version 3.0.0 beta, PDB_mmCIF70 database) (100) for sequence and structural similarity analysis. Results were analyzed based on sequence similarity score, e-value and sequences for alignments were selected based on Smith-Waterman score (101). Alignment was analyzed and images were prepared by Jalview (102).

4.2.15.2 Secondary structure prediction

TlyA secondary structure assembly was predicted by alignment of TlyA and its homologs with known structural data. Prediction was performed by I-TASSER server (103), and the secondary structure and topology analysis was attained by European Bioinformatics Institute (EMBL-EBI) protein analysis web-based server (104).

4.2.15.3 Homology modelling and analysis of TlyA structure

Amino acid sequence of TlyA was retrieved from Uniprot (id: O25718) and secondary structure composition was predicted by Phyre 2 server (105). The amino acid sequence of TlyA was submitted to HHpred server (version 3.0.0 beta, PDB_mmCIF70 database) (100), and templates are selected based on Smith-Waterman score (101). TlyA model was constructed by MODELLER (106) and energy minimized using YASARA (http://www.yasara.org/). Structure accuracy was evaluated by Molprobity (107) and Ramachandran plot using RAMPAGE server (108). The measurements of distances between indicated residues were calculated by PYMOL (109) and images were prepared by Molscript (110).

Copyright by Mahidol University

4.2.15.4 Prediction of TlyA quaternary structural assembly

Previously constructed TlyA monomer was submitted to oligomer prediction by GalaxyWEB (111). Amino acid residues lining protein-protein interfaces were assigned based on aligned structures. Structure accuracy was evaluated by as before. The measurements of distances between indicated residues were calculated by PYMOL (109) and images were prepared by Molscript (110).

4.2.15.5 Prediction of protein-protein interface for dimerization

Dimeric assembly of TlyA was analyzed for protein-protein interaction European Bioinformatics Institute (EMBL-EBI) protein analysis web-based server (104). Disulfide bonds, salt bridges and hydrogen bond formation between adjacent monomeric TlyA were evaluated and depicted as schematic diagram.

4.2.15.6 Prediction of TlyA function by conserved domain analysis

Amino acid sequence encoding TlyA was submitted to Pfam web server for conserved domain analysis and function prediction (112). Identified domains were analyzed and conserved sequences are aligned to TlyA sequence for visualization of evolutionarily conserved and functionally relevant residue/regions.

4.2.15.7 Prediction of TlyA sub cellular localization

TlyA's subcellular localization was analyzed by consensus prediction among LocTree3 (113), CELLO (114), LipoP 1.0 (115), PSLpred (116) and SLP-Local (117). The overall consensus predicted localization was assigned for TlyA localization within *H. pylori*.

4.2.15.8 Prediction of TlyA binding to S-adenosyl methionine

Binding site between TlyA and S-adenosyl methionine (SAM**)** was predicted by docking of two molecules using Autodock Vina (118). Search space was confined to the previously predicted RNA binding s4domain as in method 4.2.15.6. Both target protein (TlyA) and ligand (SAM) were converted to PDBQT file type which contains Gasteiger partial equalization of orbital electronegativities (PEOE) partial charges and united-atom representation prior to docking by Autodock. Docked model was analyzed by PYMOL program (109) and pictures were generated by Molscript program (110).

Copyright by Mahidol University

4.2.15.9 Construction of phylogenetic tree of TlyA

The phylogenetic tree for TlyA was built with Neighbor Joining method (NJ), using p-distance as substitution model MEGA Version X (119). Bootstrap number was set manually to 5000 iterations. Phylogenetic tree construction included the sequences for *H. pylori* TlyA proteins and sequence homologs as analyzed by NCBI blast (120) using *H. pylori tly*A gene as query. Sequences and gene accession ID can be seen in supplements.

4.2.15.10 TlyA transcriptional unit assembly prediction

Amino acid sequence encoding TlyA was used to visualize the transcriptional unit gene synteny in selected *H. pylori* strains with different bacterial virulence and disease association using prokaryotic synteny & taxonomy explorer (121). The resulting gene synteny was analyzed and genes were classified and colored according to respective functions.

4.2.15.11 Calculation of evolutionary conservation rate to identify conserved positions in TlyA

Evolutionarily conserved of amino acid positions in TlyA was calculated using an empirical Bayesian inference, starting from protein structure and sequence, respectively by evolutionary trace analysis (122) and results were mapped onto TlyA sequence.

4.2.15.12 Prediction of *in vivo* function and ligand binding sites via MSA and clustering algorithm

Amino acid sequence encoding TlyA was analyzed for biological function annotation and ligand binding sites by sequence, structure and protein-protein interaction based method using Cofactor web-based server for structure-based multiple-level predictions (123). All predicted ligand binding models were analyzed and compared against previously constructed TlyA-SAM docking model by PYMOL (109).

Copyright by Mahidol University

CHAPTER V
RESULT I
PURIFICATION AND FUNCTIONAL CHARACTERIZATION OF TlyA

5.1 Construction of wild type TlyA plasmids

5.1.1 Construction of the FLAG/TlyA235 plasmid

FLAG/TlyA235 plasmid (Figure 5.1a) was constructed by gene synthesis and sub-cloned into pD441 plasmid. Presence of *tly*A gene in the plasmid was confirmed by restriction digestion with *Ava*I (Figure 5.1b) and sequencing analysis. Resulting plasmid, FLAG/TlyA235 was used to transform BL21 (DE3) *E. coli* and expression trials were carried out to optimize production of soluble TlyA.

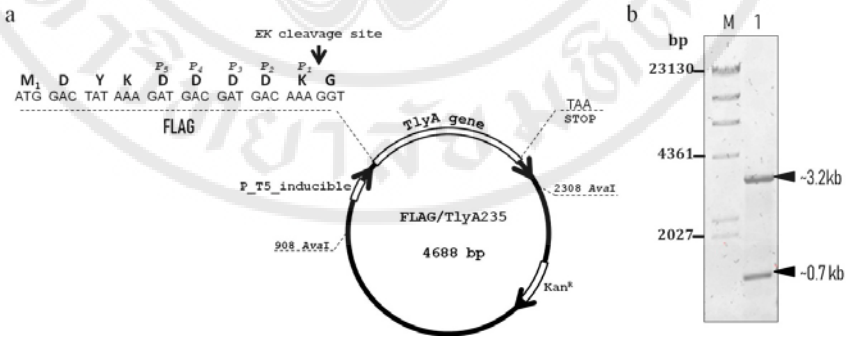

Figure 5.1 FLAG/TlyA plasmid map and restriction analysis

(a) Gene encoding *H. pylori* TlyA was synthesized and sub-cloned into pD441 plasmid, generating a 4688-bp FLAG/TlyA235 plasmid. (b) Agarose gel (Hydra green-stained 1%) analysis for the restriction digestion of FLAG/TlyA235 by restriction enzyme (*Ava*I). FLAG/Tlya235 plasmid has two cleavage sites for *Ava*I. Plasmid digestion shows DNA fragments (3288 and 700 bp, respectively) at predicted sizes. M: *Hin*dIII-digested λ-DNA marker**,** lane 1: the *Ava*I digested FLAG/Tlya235 plasmid.

Copyright by Mahidol University

5.1.2 Constructions of the His/TlyA235 plasmid

5.1.2.1 *tly*A amplification by PCR

Previously constructed FLAG/TlyA235 plasmid was used as a template to amplify *tly*A gene by PCR as described in Methods 4.2.3. Analysis of PCR product (~0.7-kb) by agarose gel electrophoresis showed the presence of PCR product with expected size (Figure 5.2).

5.1.2.2 Digestion, ligation and transformation

Both PCR product (insert) and backbone plasmid (pET-17b) were double digested by restriction digestion prior to ligation (Figure 5.3). Digested DNA fragments were ligated in a vector: insert ratio of 1:3 in the presence of 5 mM ATP and ligation products were transformed into BL-21 (DE3) *E. coli* as described in Method 4.2.6.

5.1.2.3 Screening of transformants

Transformants were screened for correct insert by restriction digestion using *Nde*I and *Hin*dIII. Digestion pattern proved that the recombinant plasmid contains *tly*A gene (Figure 5.4). Clones were further confirmed by sequencing analysis.

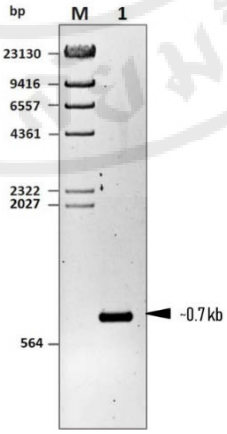

Figure 5.2 PCR amplification of *tly*A.

Agarose gel (Hydra green-stained 1%) analysis of the PCR-amplified *tly*A gene. Previously constructed FLAG/TlyA235 plasmid was used as a template and *tly*A gene was amplified by specific primers as described in Materials 4.1.6. M: λ*Hin*dIII marker, lane 1: PCR product of *tly*A.

Copyright by Mahidol University

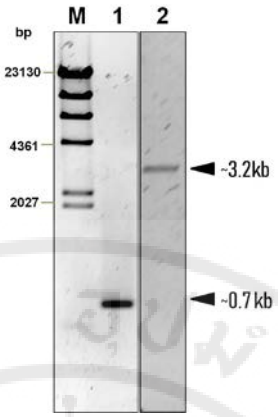

Figure 5.3 Restriction digestion of *tly*A and pET-17 b.

Agarose gel (Hydra green-stained 1 %) analysis of the double digested *tly*A gene (insert) and pET-17b (backbone). Both insert and vector DNA were digested with *Nde*I and *Hin*dIII. M: λ*Hin*dIII marker, lane 1: Digested PCR product of tlyA, lane 2: Digested PCR product of pET-17b

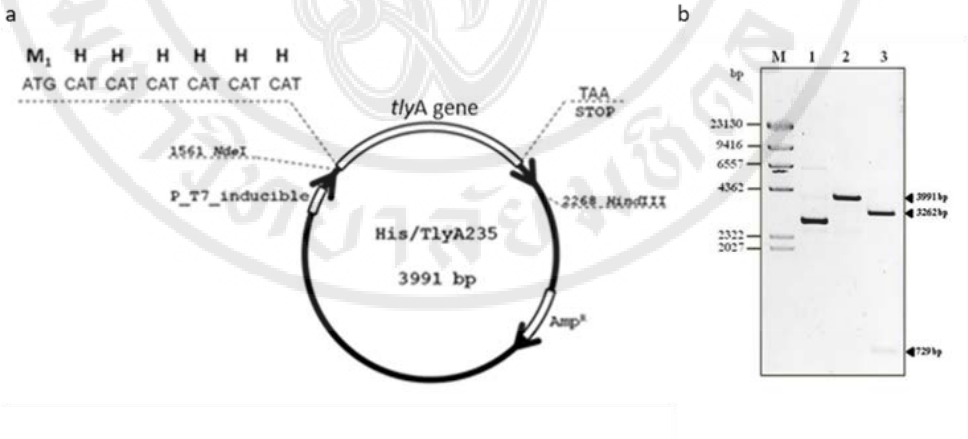

Figure 5.4 His/TlyA plasmid map and restriction analysis

(a) Gene encoding *H. pylori* TlyA was synthesized and sub-cloned into pET-17b plasmid, generating a 3991-bp His/TlyA235 plasmid. N-terminal His tag was included for downstream purposes. (b) Agarose gel (Hydra green-stained 1%) analysis of the single or double digested His/TlyA235 (lanes 2-3) and pET-17b (lane 1). Both were digested with *Nde*I and *Hin*dIII. M: λ*Hin*dIII marker, lane 1: pET-17b digested with *Hin*dIII, lane 2: His/TlyA235 digested with *Hin*dIII, lane 3: His/TlyA235 digested with *Hin*dIII and *Nde*I.

Copyright by Mahidol University

5.1.2.4 Protein expression of His/TlyA235

Recombinant TlyA was overexpressed after IPTG induction. Expression profile showed that TlyA expression as early as 1 hour, and the protein is stable throughout 12 hours (Figure 5.5).

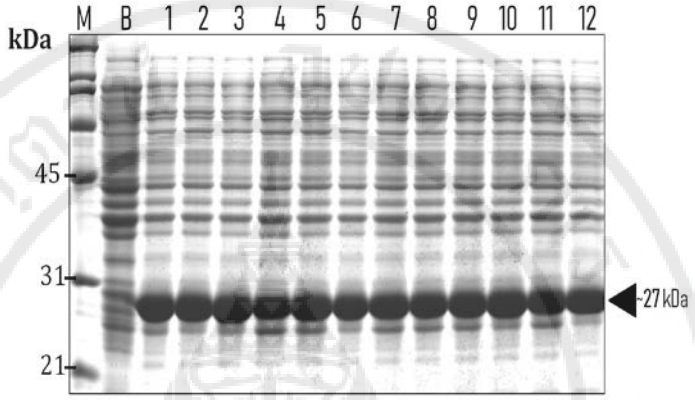

Figure 5.5 Expression profile of His/TlyA235.

Fractions corresponding to each time point were collected and normalized to 1 OD. For each indicated time point, 0.1 OD_{600} was loaded on SDS-PAGE (15% gel) and incubation was continued for up to 12 hours after induction with 0.1 mM IPTG. M: molecular weight marker, B: before induction, lanes 1-12: hours after induction. The band of the 27-kDa TlyA protein is indicated.

5.1.2.5 Expression of the soluble recombinant TlyA from His/TlyA235

TlyA was expressed under control of the T7 promoter in *E. coli* BL-21 (DE3) upon IPTG induction at 25°C, 30°C and 37°C. TlyA was highly expressed (~50 mg/l) at 1-hour post-induction (Figure 5.5). However, the expressed protein at this temperature only yielded insoluble inclusions after sonication (Figure 5.6). Therefore, incubation temperature and/or induction cell density (OD) were varied to optimize the production of soluble TlyA. Expression at lower temperatures (<30°C) enhanced the presence of TlyA in the soluble fraction albeit the total protein expression was lower than that of expression at 37°C (Figure 5.6). Variation of the induction OD did not result in a remarkable increase in the amount of soluble target protein (data not shown).

Copyright by Mahidol University

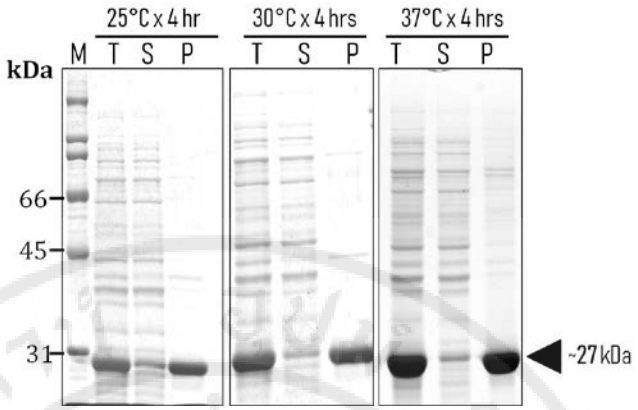

Figure 5.6 Optimization of expression temperature for His/TlyA235.

Cells were grown for 4 hours at 25°C, 30°C and 37°C. Induction was carried out at an OD_{600} of 0.4-0.6 by IPTG (0.1 mM). Samples were separated in to cell lysate (T), soluble fraction (S) and insoluble pellet fraction (P) by centrifugation after sonication. TlyA was expressed as predominant protein in the insoluble fraction at 25°C, 30°C and 37°C.

5.2 Expression of the soluble recombinant TlyA from FLAG/TlyA235

When the TlyA protein was expressed under control of the T5 promoter in *E. coli* BL-21 (DE3) upon IPTG induction at 37°C, TlyA was highly expressed (~20 mg/l) just after 1-hour post-induction (Figure 5.7). However, at this temperature only insoluble inclusions were obtained after sonication (Figure 5.8). Therefore, incubation temperature and/or induction cell density (OD) were varied to optimize production of soluble TlyA. Expression at lower temperatures enhanced the presence of TlyA in the soluble fraction albeit the total protein expression was lesser than that of expression at 37°C (Figure 5.8). Variations of induction OD did not show remarkable increase in soluble expression of target protein (data not shown).

Copyright by Mahidol University

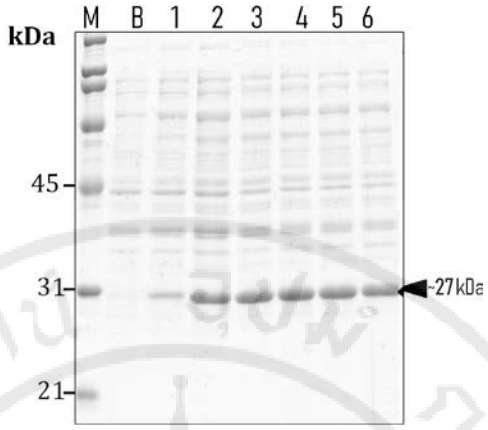

Figure 5.7 Expression profile of FLAG/TlyA235.

Fractions corresponding to each time point were collected and normalized. For each indicated time point 0.1 OD_{600} was loaded on SDS-PAGE (15% gel). Incubation was continued for up to 6 hours after induction with 0.1 mM IPTG at 37°C. M: molecular weight marker, B: before induction, lanes 1-6: 1-6 hours after induction, respectively. The band of the 27-kDa TlyA protein is indicated.

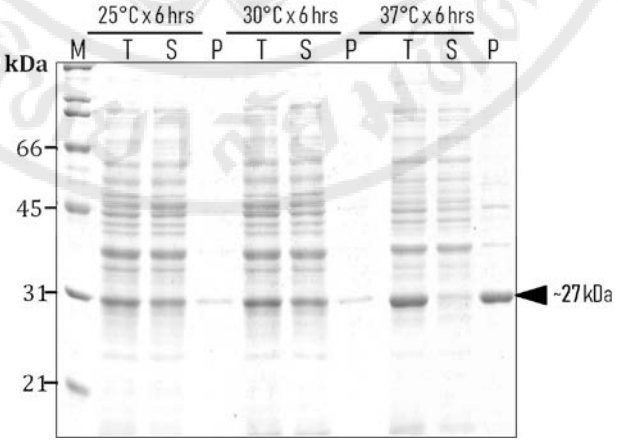

Figure 5.8 Optimization of expression temperature.

Cells were grown for 6 hours at either 25°C or 30°C or 37°C. Induction was carried out at an OD_{600} of 0.4-0.6 by IPTG (0.1 mM). Samples were separated in cell lysate (T), soluble fraction (S) and insoluble pellet fraction (P) by centrifugation after sonication. TlyA was expressed as predominant protein in soluble fraction when expressed at 25°C and 30°C.

Copyright by Mahidol University

5.3 TlyA purification by FPLC *via* ion exchange chromatography

TlyA was purified by FPLC *via* ion exchange chromatography as described in Methods 4.2.9. TlyA in HEPES buffer, pH 8.2 (to maintain the net positive charge on the TlyA molecule) was purified by cation exchange chromatography (Figures 5.9, 5.10). It should be noted that at pH 7.4 numerous bound proteins were co-eluted with TlyA (Figure 5.11) and near homogeneity purification was only achieved when a binding buffer at pH 8.2 was used. TlyA binds to the cation exchange chromatography column (GE) with high specificity since only slight amounts of TlyA are found in the flow-through and wash fractions during purification (Figure 5.10). TlyA was eluted at salt concentrations higher than 0.5 M which validated the overall positive charge as well as the predicted isoelectric point of ~9.27. The protein was purified to near-homogeneity as seen on SDS-PAGE (Figure 5.12). Desalting *via* dialysis against 20 mM Tris-HCl, pH 7.4, at 4°C overnight neither affected protein solubility nor structural integrity since no degradation products were detected following two rounds of dialysis (Figure 5.13). The purification profile and corresponding gel can be seen in Figures 5.9 and 5.10. After the bound fractions were eluted, protein concentrations of the purified protein were determined by using the Bradford protein assay.

Copyright by Mahidol University

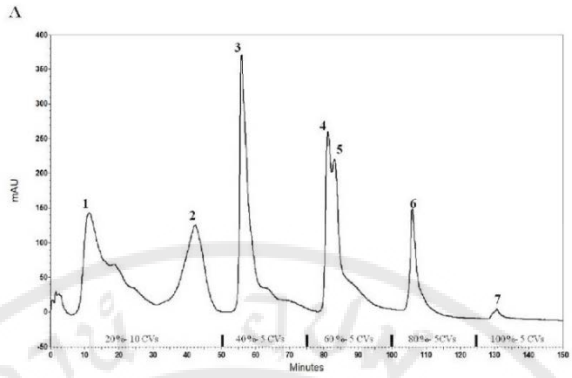

Figure 5.9 Purification of TlyA by cation exchange chromatography (CEC).

The soluble fraction was loaded onto a HiTrap SP HP cation exchange column as described in Methods 4.2.9. Proteins were eluted at a flow rate of 1 ml/minute using 1 M NaCl in50 mM HEPES, pH 8.2 at step gradients from 20% to 100%. For each buffer concentration, 5 column volumes were used for elution except for 20% where 10 column volumes were used. Peak fractions (1 ml) as indicated on the chromatogram were collected and 20 µl of each fraction were analyzed on SDS-PAGE.

Figure 5.10 SDS-PAGE of CEC purified TlyA.

The soluble fraction was loaded onto a cation exchange column as described in Methods 4.2.9. Proteins were eluted at a flow rate of 1 ml/min using 1 M NaCl in 50 mM HEPES, pH 8.2, at step gradients from 20% to 100%. Peak fractions (1 ml) as indicated on the chromatogram were collected and 20 µl of each fraction were analyzed on SDS-PAGE. M: molecular weight marker, B: sample before injection, FT: flow-through fraction, lanes 1-8: peak fractions of the chromatogram. Purified TlyA is contained in peak 7.

Copyright by Mahidol University

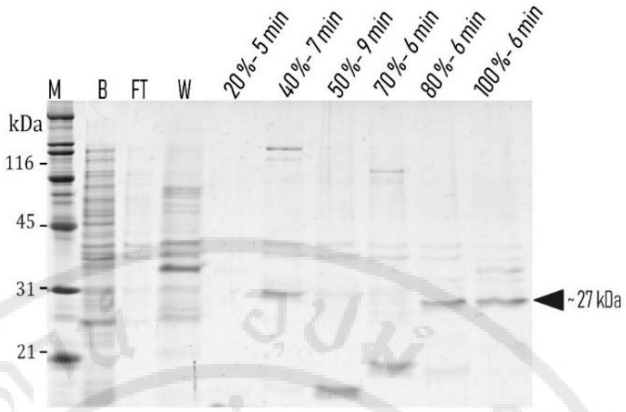

Figure 5.11 SDS-PAGE of TlyA purified by CEC at pH 7.4.

The soluble fraction was loaded onto a cation exchange column as described in Methods 4.2.9. Proteins were eluted at a flow rate of 1 ml/minute using 1 M NaCl in 50 mM HEPES, pH 7.4, at step gradients from 20% to 100%. Peak fractions (1 ml) were collected and 20 µl of each fraction were analyzed on SDS-PAGE. M: molecular weight marker, B: sample before injection, FT: flow-through faction, other lanes are peak fractions of the chromatogram eluted with different percentage of buffer and time. Purified TlyA is contained in 80% and 100% elution fractions, however, several proteins were co-eluted with TlyA.

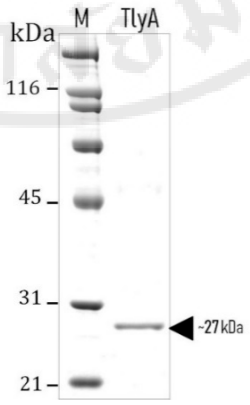

Figure 5.12 SDS-PAGE of purified and concentrated TlyA.

TlyA was purified by cation exchange chromatography and fractions containing TlyA were pooled and concentrated by 10-kDa MWCO columns. Purified protein was analyzed by SDS-PAGE. M: molecular weight marker, TlyA: Purified and concentrated TlyA.

Copyright by Mahidol University

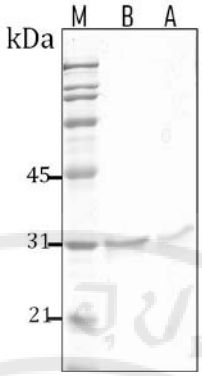

Figure 5.13 SDS-PAGE of TlyA before and after dialysis.

The CEC purified TlyA fractions were pooled and concentrated as described in Methods. The concentrated TlyA was dialyzed against 1000-fold of 20 mM Tris-HCl, pH 7.4, buffer at 4°C to remove NaCl from the sample solution. The structural integrity of the dialyzed sample was analyzed by loading an equal amount of samples on SDS-PAGE. M: molecular weight marker, B: TlyA before dialysis, A: TlyA after dialysis.

5.4 Western blot analysis of TlyA

TlyA fractions (total, soluble, insoluble) were subjected to Western blotting against anti-FLAG antibody as described in Method 4.2.10. The expressed protein was immunoreactive with anti-FLAG antiserum which confirms the presence of the FLAG affinity tag (Figure 5.14).

Copyright by Mahidol University

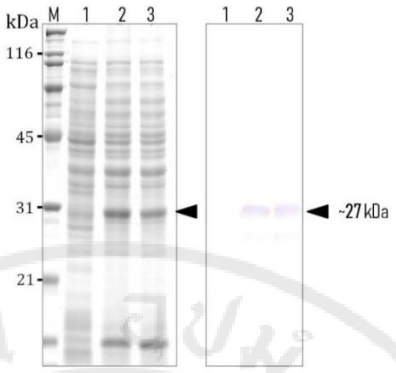

Figure 5.14 Western blot analysis of TlyA

Left panel, SDS-PAGE (Coomassie Brilliant Blue-stained, 12% gel) analysis of *E. coli* extracts expressing TlyA (lane 2) after IPTG induction and soluble fraction (lane 3) after cell lysis and centrifugation. Un-induced *E. coli* cells were used as a negative control (lane 1). Right panel, Western blot analysis of the protein samples corresponding to those in the left panel SDS-PAGE probed with anti-FLAG antibody.

5.5 Membrane-perturbing activity of TlyA against liposomes

Purified fractions of TlyA were tested for their binding and membrane perturbing activity against liposomes (Method 4.2.12). TlyA showed concentration dependent membrane-perturbing activity against liposomes after incubation at 25°C for 10-15 minutes (Figure 5.15). The result showed requirement of high concentrations of toxin for a disruption of the artificial lipid membranes (Figure 5.15).

5.6 Membrane-perturbing activity of TlyA under reducing conditions

Monomeric TlyA has 4 Cys residues which could potentially form disulfide bonds and display sensitivity to reducing agents such as DTT or β-mercaptoethanol. Therefore, membrane perturbation of TlyA was assayed in the presence of 20 mM DTT against liposomes as described before (Method 4.2.12). Purified TlyA displayed markedly reduced membrane-perturbing activity at highest concentration tested (Figure 5.16).

Copyright by Mahidol University

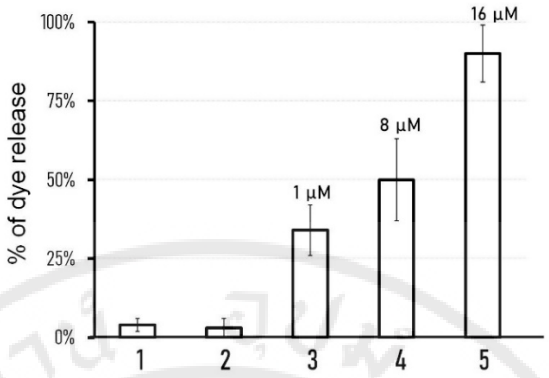

Figure. 5.15 Membrane-perturbing activity of purified TlyA against liposomes.

Liposomes were incubated at the indicated concentrations of purified TlyA at 25°C for 15 minutes. Lysis was measured fluorometrically as amount of dye released at defined wavelengths (λ_{ex}=565nm, λ_{em}=586nm). Lane 1: BSA, lane 2: buffer, lanes 3-5: purified TlyA. Numerical data represent m ± SEM of three independent experiments.

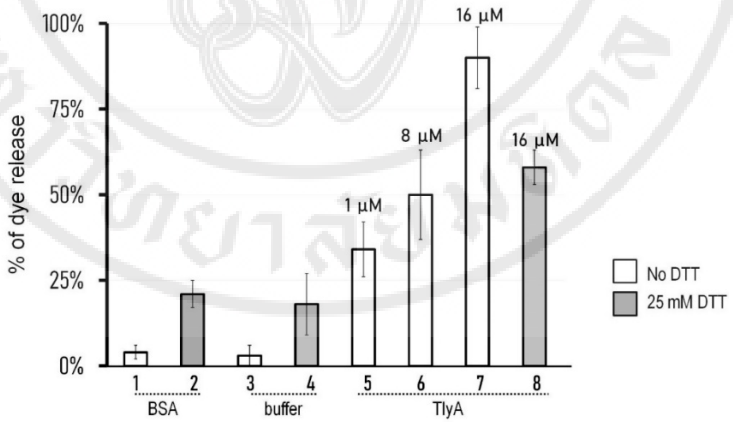

Figure 5.16 Membrane-perturbing activity of purified TlyA against liposomes under reducing and non-reducing conditions.

Liposomes were incubated at the indicated concentrations of purified TlyA at 25°C for 15 minutes with or without 25 mM DTT. Lysis was measured photofluorometrically as amount of dye released at defined wavelengths (λ_{ex}=565nm, λ_{em}=586nm). Lanes 1, 2: BSA, lanes 3, 4: buffer, lanes 4-8: purified TlyA. Grey bars represent the presence of 25 mM DTT in the assay. Numerical data represent mean ± SEM of three independent experiments.

Copyright by Mahidol University

5.7 TlyA quaternary structure under non-reducing conditions

Purified TlyA was analyzed by semi-native gels under reducing or non-reducing conditions to detect a potential formation of quaternary assembly. Under reducing conditions, purified TlyA showed a prominent band of ~27-kDa on SDS-PAGE, however, under non-reducing conditions prominent bands at ~48-kDa and ~38-kDa were observed (Figure 5.17a). The identities of the higher molecular weight bands were confirmed by Western blotting (Figure 5.17b). It should be noted that the quaternary forms of TlyA were also detected by denaturing SDS-PAGE under non-reducing conditions, suggesting a stable interaction among monomeric TlyA subunits as the dissociation of oligomeric forms into monomers is observed only in the presence of reducing agent (Figure 5.18).

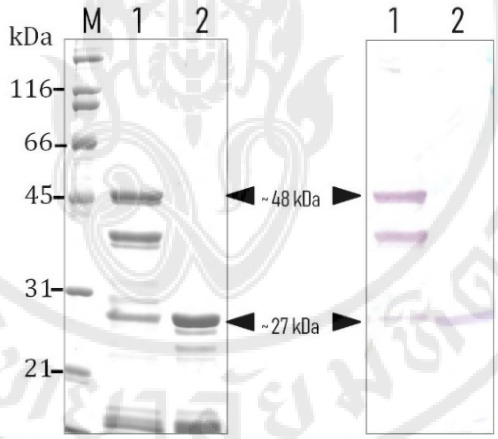

Figure 5.17 TlyA oligomers analyzed by seminative gel.

Left, semi-native PAGE (Coomassie Brilliant Blue-stained 12% gel) of the 27-kDa purified TlyA toxin under reducing (lane 2) or non-reducing conditions (lane 1). Right, Western blot analysis of the protein samples corresponding to those in left panel probed with anti-FLAG antibody. The reactive bands with the sizes of ~27-kDa and apparent oligomers (~38 and ~48-kDa, respectively) were detected by ALP-conjugated secondary antibody.

Copyright by Mahidol University

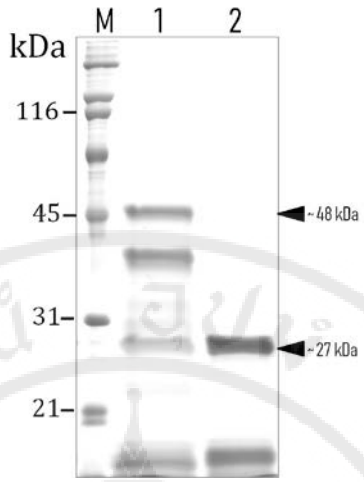

Figure 5.18 TlyA under SDS-PAGE gel.

SDS-PAGE (Coomassie Brilliant Blue-stained, 12 % gel) of the 27-kDa purified TlyA toxin under reducing (lane 2) or non-reducing conditions (lane 1).

5.8 TlyA binding to liposome under reducing conditions

Purified TlyA incubated with liposomes as described in Methods 4.2.12.2 displayed prominent binding to liposomes as can be seen by pull-down assay. However, when tested under identical conditions, TlyA under reducing conditions failed to show similar binding to liposomes implying the putative importance of quaternary conformations in TlyA binding to the lipid membrane (Figure 5.19).

Copyright by Mahidol University

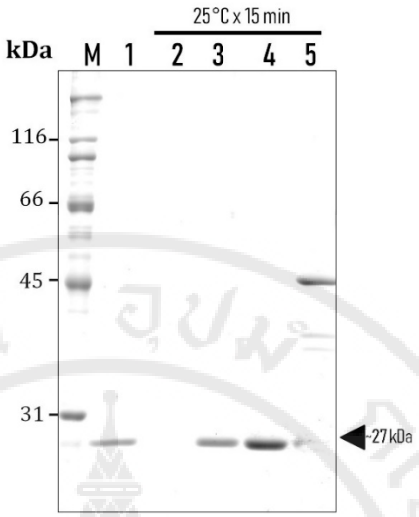

Figure 5.19 Binding of TlyA to liposomes.

SDS-PAGE (Coomassie Brilliant Blue-stained, 12 % gel) of the 27-kDa purified TlyA toxin binding to liposomes under reducing (lane 3) or non-reducing conditions (lane 2, 4, 5). Liposomes were incubated with (lanes 3-5) or without (lane 2) at 25°C for 15 minutes followed by centrifugation and the pellet fraction was re-suspended and loaded onto SDS-PAGE gel. M: molecular weight marker, lane 1: purified TlyA, lane 2: liposomes incubated without TlyA, lane 3: Liposome incubated with TlyA for 15 minutes in the presence of 25 mM DTT, lane 4: Liposome incubated with TlyA for 15 minutes, lane 5: As in lane 4 under semi-native conditions.

5.9 TlyA effect on AGS cell viability

Viability of AGS cells upon treatment of various concentrations of TlyA was evaluated by Presto blue cell viability assay. The Presto blue assay is based on the conversion of resazurin (a blue non-fluorescence compound) into a red-fluorescent dye upon entering viable cells by reducing environment in cytoplasm (98). Results suggested that TlyA displayed concentration-dependent reduction in cell viability in AGS cells (Figure 5.20). TlyA at concentrations higher than 10 µM causes more than 50% reduction in cell viability.

Copyright by Mahidol University

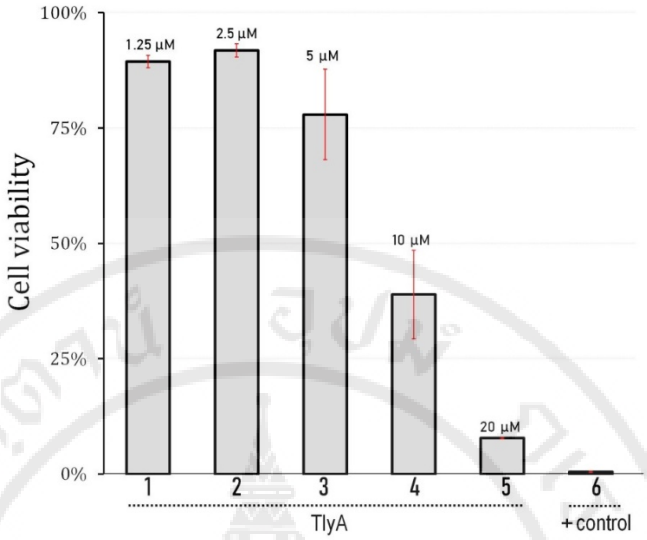

Figure 5.20 Reduction of cell viability by TlyA.

AGS cells were seeded in 96 well plates and purified TlyA at indicated concentrations were added to each well. Cell viability was measured after 24-hour incubation using Prestoblue assay as described in Methods 4.2.13.2. Fluorescence readings of untreated cells are taken as 100% viability. Cells treated with 20% EtOH are used as a positive control. Numerical data represent mean ± SEM of three independent experiments.

5.10 TlyA interaction with AGS cells

After incubation of TlyA with AGS cells at 37 °C for 12 hours, TlyA was clearly seen on the plasma membrane by immunocytochemistry. (Figure 5.21). Furthermore, TlyA did not display significant cytotoxic activity when assayed at less than 20 hours pre-incubation (data not shown).

Copyright by Mahidol University

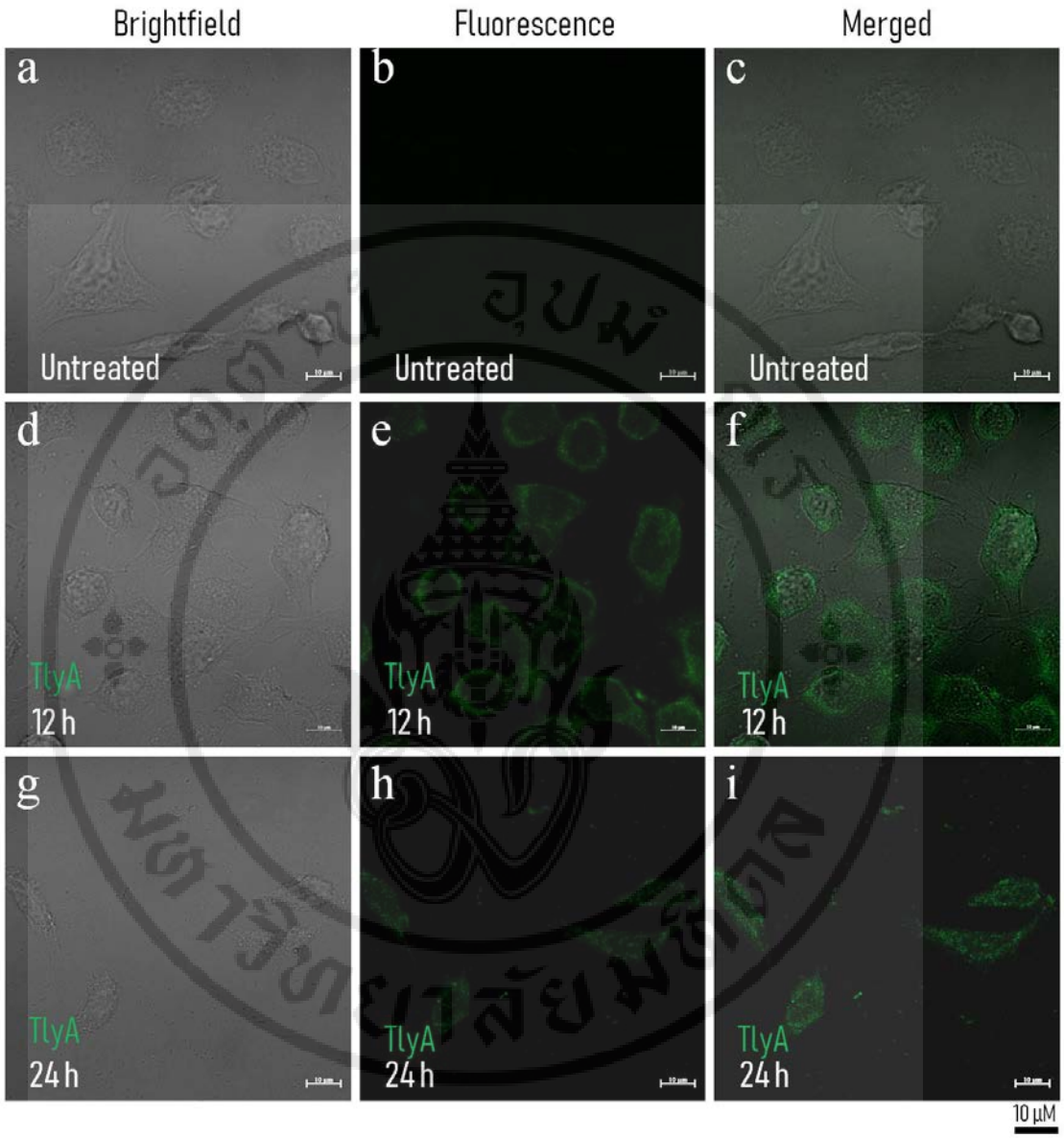

Figure 5.21 Binding and of TlyA by AGS cells.

AGS cells were incubated with (d-i) or without (a-c) with 10 µM TlyA at 37°C for indicated times, and then probed with anti-FLAG antibody to detect TlyA and subsequently with AF-488 (Alexa fluor) labelled secondary antibody. A significant fraction of TlyA was bound by cells at 12 hours. Untreated cells were used as a control (a-c).

Copyright by Mahidol University

5.11 TlyA mediated cytokine production in AGS cells

AGS cells were incubated with TlyA as described before (Method 4.2.13.3). Supernatants of the untreated or TlyA/VacA treated cells were used to measure the TlyA induced production of cytokines. Treatment with TlyA results in reduced production of all cytokines (IL-1α, IL-1β, IL-2, IL-4, IL-6, IL-8, IL-10, IL-12, IL-17A, IFN-γ, TNF-α, and GM-CSF) except IL-8. However, pre-treatment of cells with TlyA prior to VacA treatment neutralized the VacA-mediated production of Il-1β, IL-2 and IL-4 but had no significant effect on other cytokine productions (Figure 5.22).

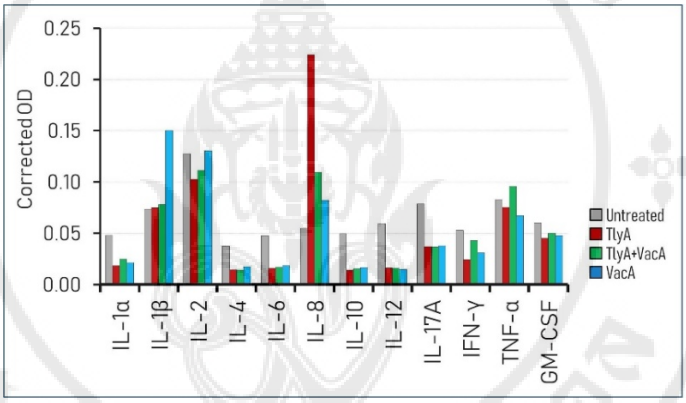

Figure 5.22 TlyA mediated production of cytokines from AGS cells.

AGS cells were incubated with TlyA and/or VacA for 24 hours and cytokines produced in the culture supernatant were measured by ELISA array. Untreated cells were used as control. For single protein assays, AGS cells were treated with 10 µM TlyA (red) or 250 nM VacA (blue) for 24 hours incubation at 37°C under 5% CO_2. For combination assay, AGS cells were incubated with 10 µM TlyA for 12 hours incubation at 37°C under 5% CO_2 and the media overlying cells were replaced by fresh media containing 250 nM VacA and continued incubation for 12 more hours. Media overlying TlyA or VacA or TlyA/VacA treated cells were collected and cytokine content was analyzed by ELISA according to manufacturer's instructions (Add method number). The amount of cytokine was quantitated by measuring absorbance at 450 nm by spectrophotometer. Grey column: untreated cells, red column: cells treated with TlyA only, blue column: cells treated with VacA only, green column: cells treated with both TlyA and VacA.

Copyright by Mahidol University

5.12 Intrinsic fluorescence spectra analysis of TlyA

To compare the structural changes induced by reducing conditions, TlyA in native (non-reduced) and reduced forms were analyzed by intrinsic fluorescence analysis. The fluorescence profiles were measured by emission scanning of purified TlyA using a spectrofluorometer. No spectra shift was observed among two conditions tested as lack of Trp residues in TlyA leads to no visible changes in intrinsic fluorescence.

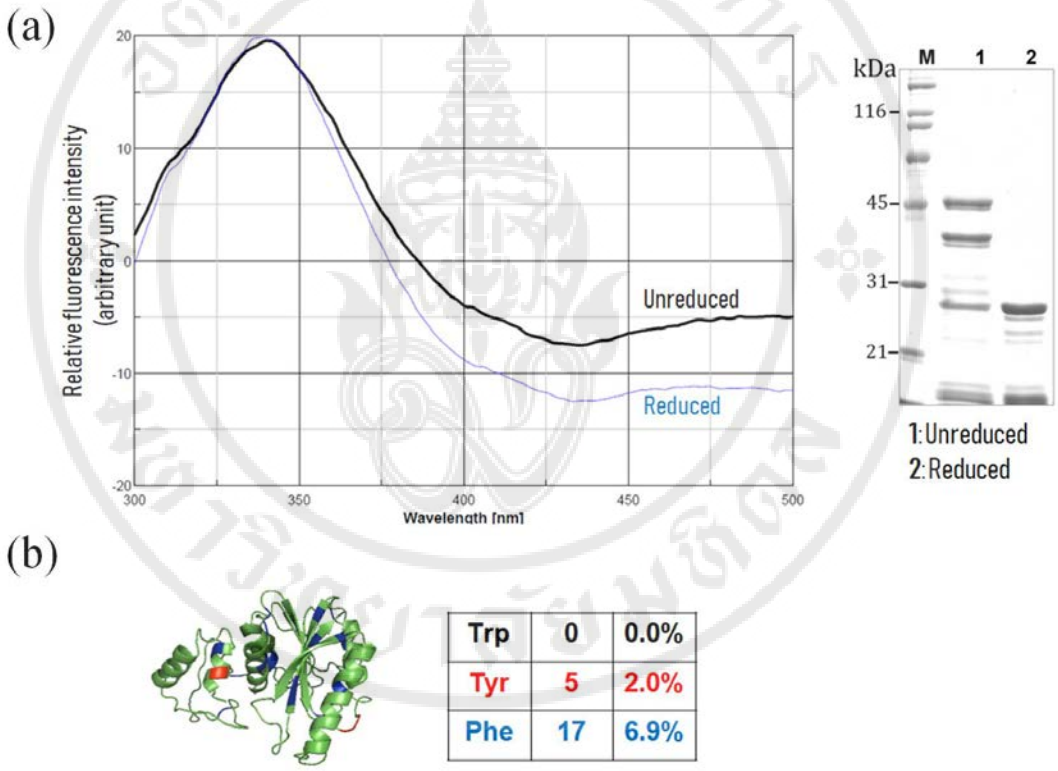

Figure 5.23 Fluorescence emission spectra of purified TlyA.

TlyA under reducing and non-reducing conditions was used to analyzed the intrinsic fluorescence properties. (a) Left, fluorescence spectra analysis of reduced and non-reduced TlyA. Right, Coomassie blue- stained SDS-PAGE (15% gel) analysis of TlyA under reducing (lane 1) and non-reducing conditions (lane 2). (b) Ribbon representation of TlyA model structure highlighting aromatic residues in corresponding colors. TlyA contains Tyr and Phe residues but no Trp.

Copyright by Mahidol University

CHAPTER VI
RESULT II
IN SILICO MODELING AND
TlyA STRUCTURE-FUNCTION ANALYSIS

6.1 TlyA homologs

Amino acid sequence encoding *Helicobacter pylori* TlyA was analyzed for sequence homology by sequence and structure alignment using HHpred (100). Sequence alignment suggests the presence of TlyA homologs across the bacterial kingdom (Gram negative and Gram positive), yeast and even mammals (Figure 6.1). TlyA homologs have diverse functions ranging from enzymatic activity in case of methyltransferase to virulence factor in case of hemolytic activity. TlyA gene is present in archaea (*Methanosarcina mazei*), primitive bacteria such as *Aquifex aeolicus* which can be found in volcanos or hot springs, Gram negative and Gram positive bacteria (*Mycobacterium tuberculosis*, *Streptococcus thermophilus*, *Escherichia coli* and *H. pylori*, *Burkholderia thailandensis*), fungi (*Aspergillus fumigatus*), yeast (*Saccharomyces cerevisiae*) and even advanced mammalian cell systems such as *Mus musculus* or *Homo sapiens* suggesting an evolutionarily conserved functionally important role of TlyA for all life forms.

6.2 TlyA secondary structure prediction

TlyA secondary structure was predicted by comparison with homologs of known structures (103). Structure analysis suggests the presence of anti-parallel beta sheets with alpha helices in between and the presence of a putative hairpin between anti-parallel beta-strands near the amino terminal region of TlyA (Figure 6.2).

Copyright by Mahidol University

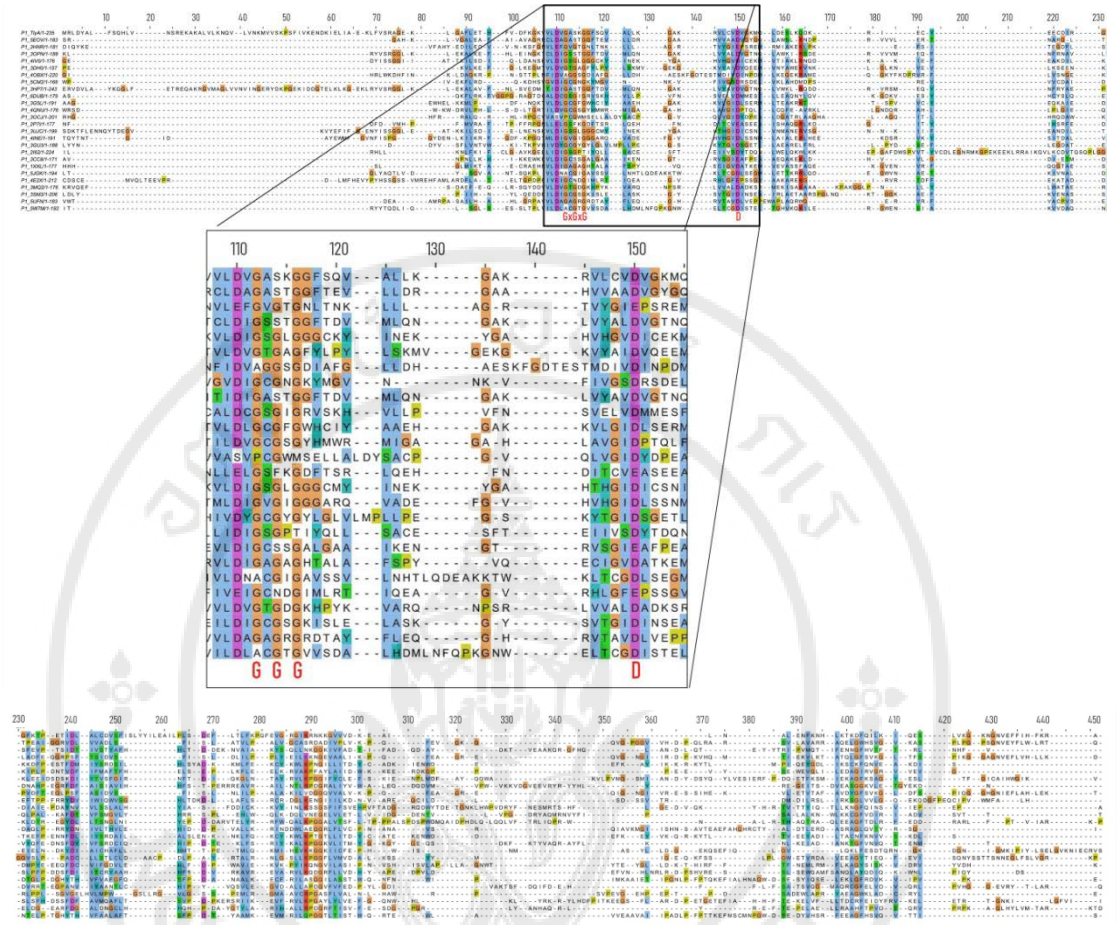

Figure 6.1 Sequence alignment between TlyA from *H. pylori* and its homologs.

Multiple sequence alignments of the TlyA from *H. pylori (*TlyA) with the corresponding region of other related cytolysins and methyltransferases, including SAM-dependent methyltransferase from *Methanosarcina mazei* (3SM3), SAM-dependent methyltransferase from *Aquifex aeolicus* (3DH0), methyltransferase from *Penicillin rubens* (5W7M), rRNA-methyltransferase from *Mycobacterium tuberculosis* **(**5EOV**),** methyltransferase (E.C.2.1.1) from *Bacillus thuringiensis* **(**3HNR), putative hemolysin from *Lactococcus lactis* (3OPN), hemolysin from *Streptococcus thermophilus* (3HP7), SAM dependent methyltransferase from *Listeria monocytogenes* (3G5L), methyltransferase from *Bacillus cereus* (3GU3, 3CC8), methyltransferase from *Bacillus subtilis* (1XXL), methyltransferase from *E. coli* (4QNU), protein from *Bordetella parapertussis* (3OCJ), protein from *Pectobacterium atrosepticum* (3UJC), tetronitrose from *Micromonospora chalcea* (4E2X), 16sRNA

Copyright by Mahidol University

methyltransferase from *Streptomyces* sp. DSM 40477 (3MQ2), phosphoethanolamine N-methyltransferase from *Plasmodium vivax* (4IV0), tRNA methyltransferase from *Yarrowia lipolytica* (5CM2), methyltransferase from *Aspergillus fumigates* (5JGK), SAM dependent methyltransferase from *Burkholderia thailandensis* (5UFN), methylase from *Saccharomyces cerevisiae (*4OBX), methyl transferase from *Caenorhabditis elegans* (4INE), nicotinamide N-methyltransferase from *Mus musculus* (2I62), methyltransferase from *Homo sapiens* (6DUB). Sequence homology was constructed by HHpred, alignment was performed by Clustal Omega (124) and images were prepared by Jalview (102). Zoomed region indicates the presence of conserved amino acid residues suggestive of SAM binding activity. Above figure is miniaturised, to see the full alignment, please see appendix C

Copyright by Mahidol University

(a)

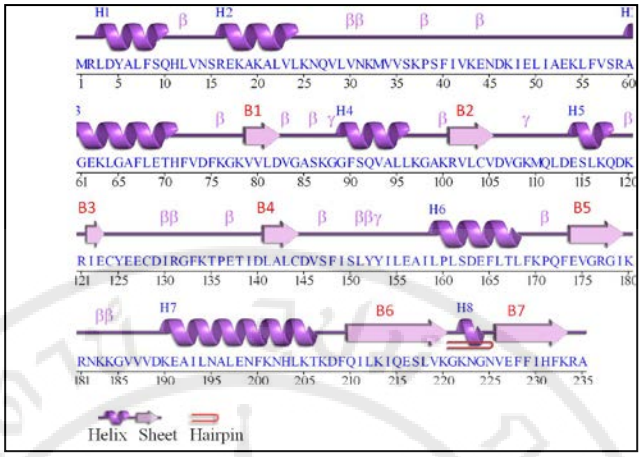

(b)

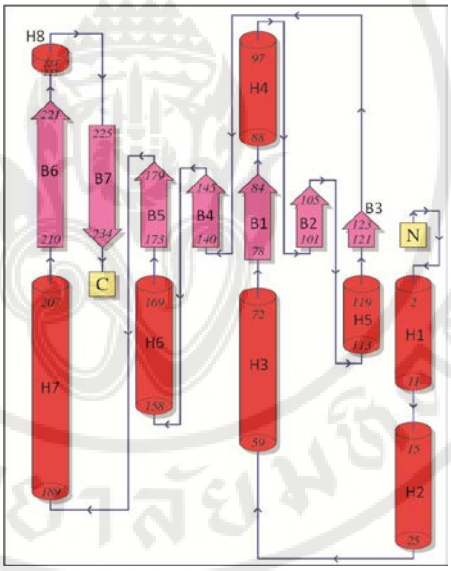

Figure 6.2 TlyA secondary structure composition and topology assignment.

(a) Wiring plot for TlyA. The figure shows the protein sequence place on top with assigned secondary structure for the monomeric TlyA. The β-strands are labelled B1 through B7 and α-helices are labelled H1 through H8. A β-hairpin turn between the two C-terminal β-strands B6 and B7 is also shown. (b) Topology diagram for TlyA. There is a single β-sheet (B1 to B7) and a total of 7-8 helices (H1 to H8). The figure was prepared using the PDBSUM server (104). For (b), helices and strands are colored as red and magenta, respectively.

Copyright by Mahidol University

6.3 Prediction of isoelectric point of TlyA

Isoelectric point represents (pI) the pH at which the protein is neutral and does not migrate in an electric field (point of zero charge) and the zwitterion form is dominant. This property can be utilized as a tool to purify protein based on electrophysical characteristics of individual proteins as proteins with high pI will be positively charged at physiological pH and can bind to cation exchange columns (125). The isoelectric point of TlyA was found to be ~9.27 as a consensus from several web-based algorithms (126) (Figure 6.3).

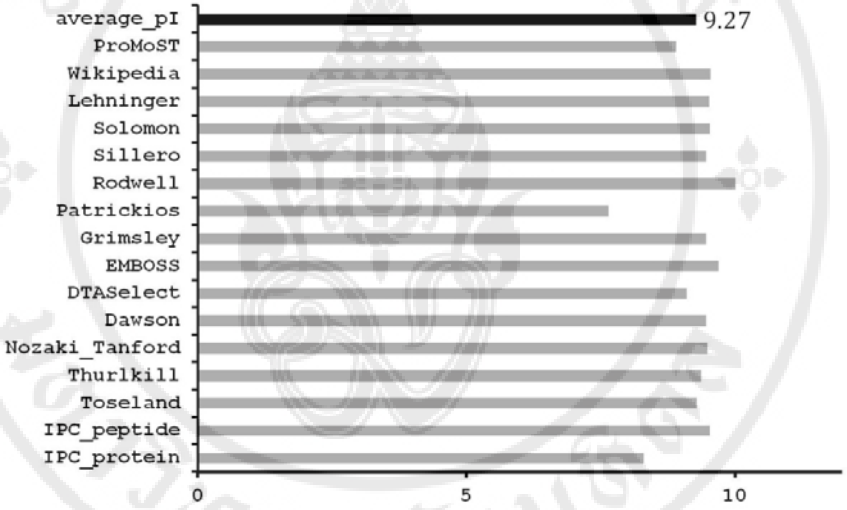

Figure 6.3 Theoretical isoelectric point (pI) based on the amino acid sequence of TlyA from *H. pylori*.

TlyA sequence was analyzed by several algorithms and average isoelectric point (pI) was displayed at the top (black bar).

6.4 Homology modelling of TlyA structure

Homology model of TlyA constructed *via* structure alignment and multiple alignment of TlyA with the best-fit template was used for modelling. The model obtained for TlyA displayed an overall backbone helical fold with β-sheets stacking on top of each other in parallel and anti-parallel orientations resembling a Rossmann fold

Copyright by Mahidol University

forming a three-layered sandwich of α-helix secondary both faces of a β-sheet (αβα) (Figure 6.4). The accuracy of the predicted model was validated by Ramachandran plot analysis using Molprobity (107) which shows that the fraction of residues found in the favored region was 95.7% (220/235), 3.5% (8/235) in allowed regions and 0.9% (2/235) in non-allowed regions (Figure 6.5). Four Cys residues (Cys^{104}, Cys^{124}, Cys^{128}, Cys^{144}) within TlyA could be involved in the formation of intramolecular disulfide bonds. However, distances between Cys residues as predicted by PYMOL program indicated that the Cys residues within monomeric TlyA are too far-off to form intra-molecular disulfide bonds (Figure 6.4). The closest Cys residues (Cys^{104} and Cys^{128}) show a distance of 6.7 Å between their thiol groups, while the typical length of a disulfide bond is approximately ~2 Å (127).

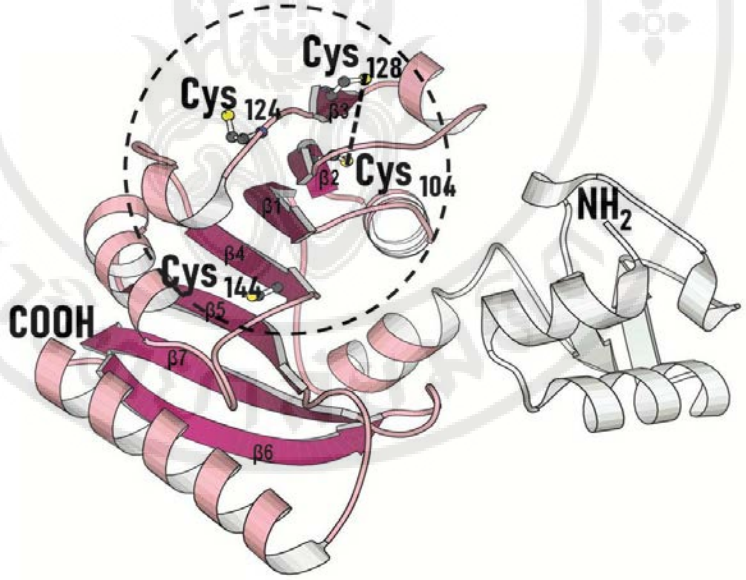

Figure 6.4 Homology-based structure of TlyA

Representative 3D modeled structure of TlyA, showing the presence of overall α-helical fold structure with parallel and antiparallel β -strands in between. β-strands are labelled as β1, β2,. Four Cys residues (Cys^{104}, Cys^{124}, Cys^{128}, Cys^{144}) are depicted as ball and stick model on the cartoon backbone of protein. Carboxy (COOH) and amino terminal (NH_2) are also indicated. Model predicted by Modeller (128) and image prepared by Molscript (110).

Copyright by Mahidol University

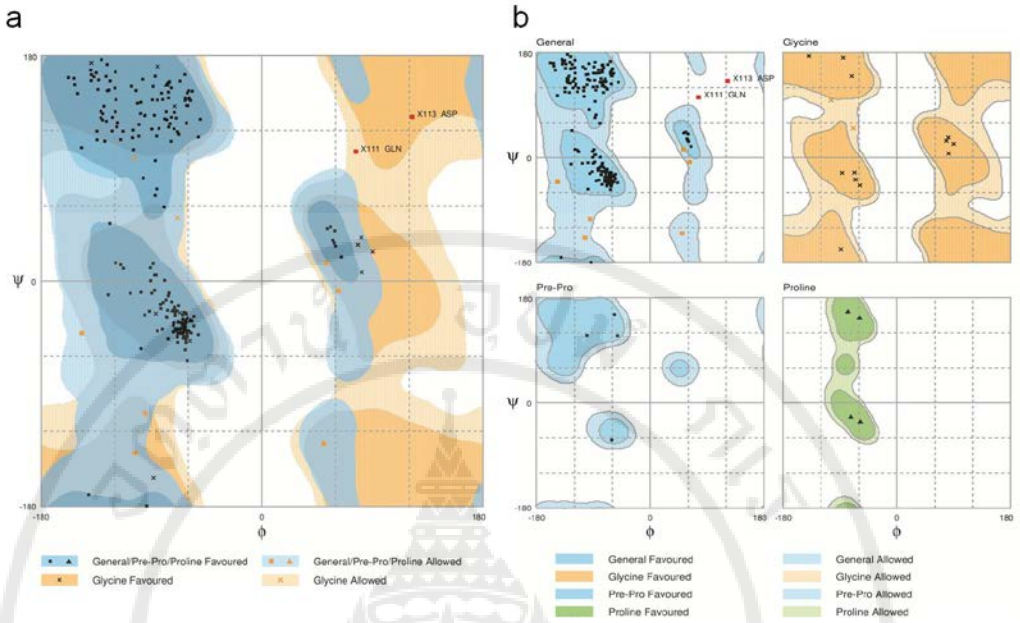

Figure 6.5 Ramachandran plot analysis.

Dark blue and dark orange are favored regions, light blue and light orange are allowed regions. (a) The plot of TlyA model shows the number of residues found in the favored region 95.7% (220/235), allowed region 3.5% (8/235) and outliners 0.9% (2/235) (b) The TlyA model showing general, Gly, pre-Pro, and Pro plots showing the possible ψ and Φ dihedral angles and allowed and disallowed regions for 235 amino acid residues of TlyA.

6.5 Prediction of TlyA quaternary structural assembly

TlyA quaternary structure assembly was predicted by homo-oligomer structure prediction algorithm. The best fit model reveals dimeric assembly of TlyA which suggests the presence of inter-molecular disulfide bonds among monomeric TlyA. However, the observed distance of intermolecular disulfide bonds between monomeric TlyA was ~3.6 Å (Figure 6.6). Although the measured distance exceeds the typical distance between thiol groups for disulfide bond formation (~2 Å), it should be noted that this model represents *in silico* prediction and the actual distance of intermolecular disulfide bonds could only be achieved by crystallographic determination of TlyA structure.

Copyright by Mahidol University

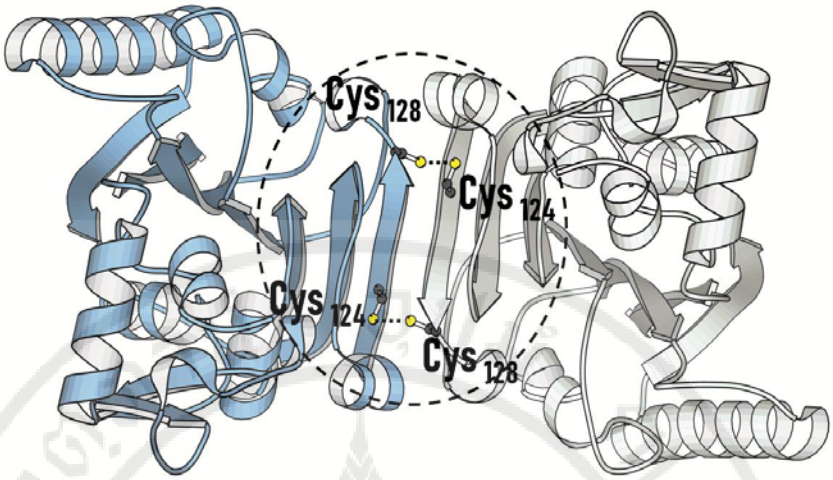

Figure 6.6 Dimeric assembly of TlyA.

Protein dimer model showing the putative disulfide bond forming region between homo-dimeric TlyA. Side chains of Cys^{124} and Cys^{128} in each domain are shown within the dimeric structure. Black dots represent carbon, blue dots represent nitrogen and yellow dots represent thiol groups. Four Cys residues (Cys^{104}, Cys^{124}, Cys^{128}, Cys^{144}) are depicted as ball and stick model on the ribbon backbone of protein. Image prepared by Molscript (110).

6.6 TlyA quaternary assembly

Analysis of interaction between monomeric TlyA in quaternary structure assembly suggested the involvement of salt bridges, disulfide bonds, hydrogen bonds and unbonded residues lining the interface within homo-oligomeric TlyA (Figure 6.7). The residues lining dimer interface and their interactions were calculated as described in Method 4.2.15.4. The list of atom-atom interaction across protein-protein interface can be seen in appendix B.

Copyright by Mahidol University

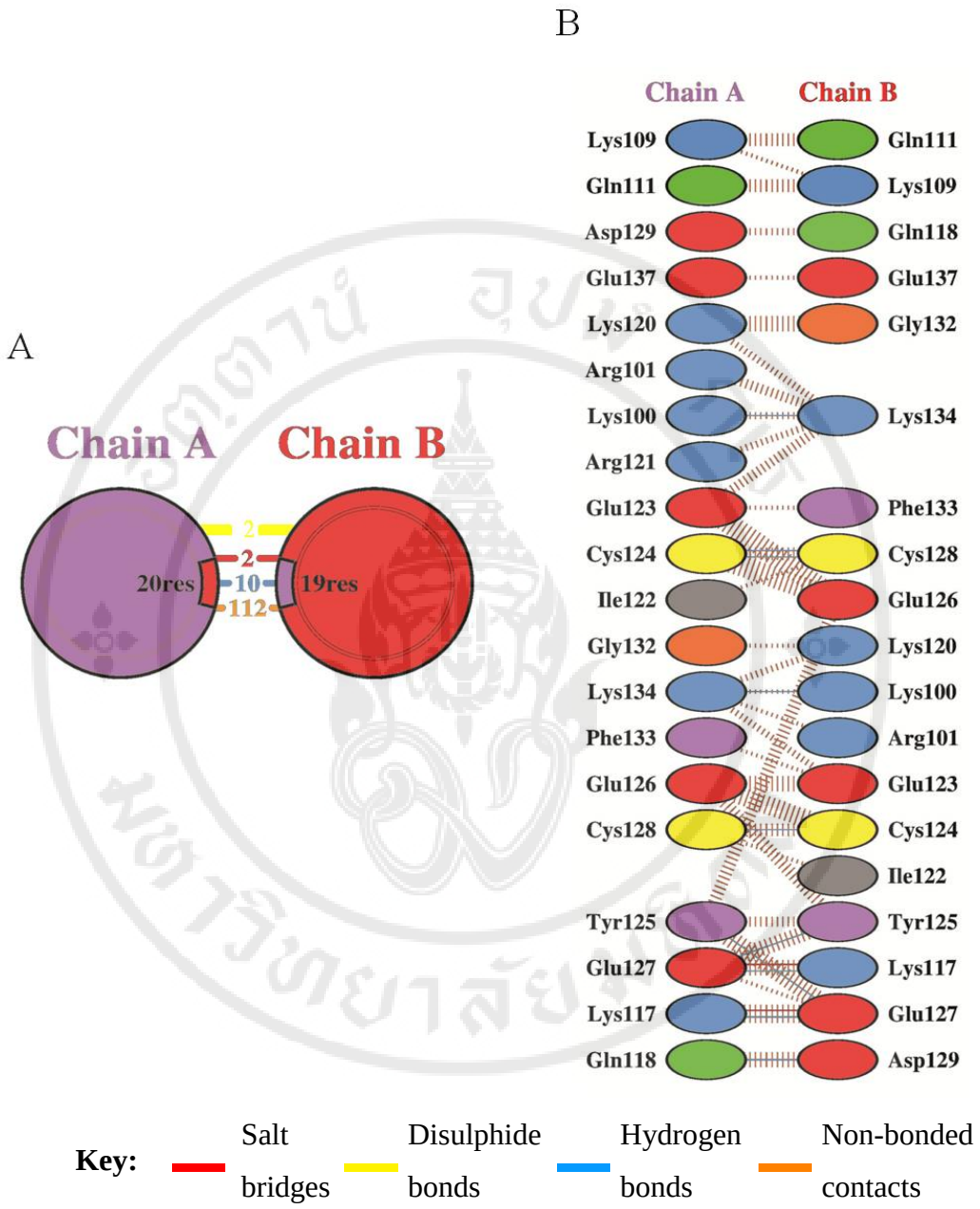

Figure 6.7 Schematic diagram of interactions between protein chains.

Interacting chains are joined by coloured lines, each representing a different type of interaction, as per the key above. The number of H-bond lines between any two residues indicates the number of potential hydrogen bonds between them. For non-bonded contacts, the width of the striped line is proportional to the number of atomic contacts.

Copyright by Mahidol University

6.7 TlyA conserved domain analysis

Sequence analysis suggested the presence of two domains within TlyA sequence; a carboxy terminal nucleic acid binding domain and amino terminal catalytic domain. The C-terminal domain displays sequence similarity to s4 RNA binding domain which is responsible for initiation of rRNA assembly and structural stability (129, 130). The sequence of the TlyA at the N-terminus displays similarity to that of methyltransferase enzymes responsible for methylation of 23 S rRNA at position U2552 of the ribosome (131). The conserved active site of the FtsJ domain which located in catalytic triad consisting of two Lys residues and the negatively charged Asp residue (132) can also be found in TlyA (Figure 6.8)

6.8 Prediction of TlyA subcellular localization

Based on the consensus prediction from different web-based servers, TlyA has been found to display a function in the cytoplasm, possibly play a role in biological processes in the cytoplasmic environment (Table 6.1).

Copyright by Mahidol University

a

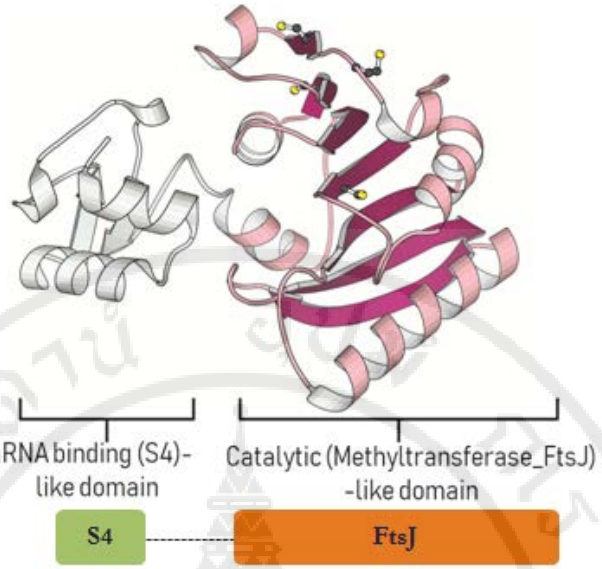

b

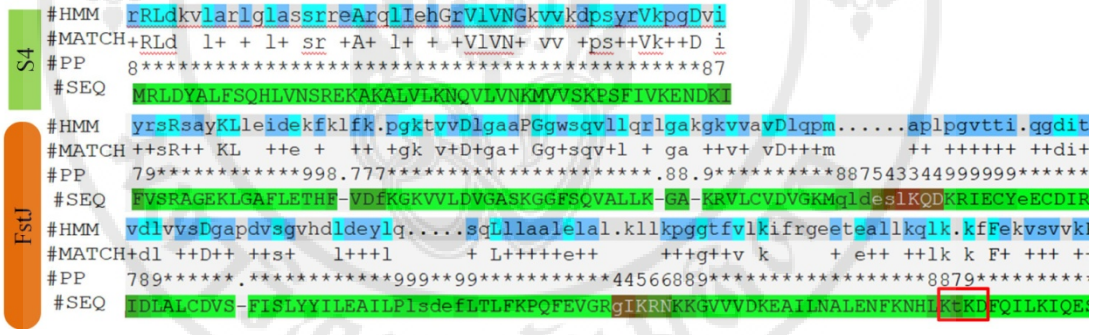

Figure 6.8 TlyA domain prediction and sequence alignment.

(a) TlyA model with two domains; N-terminal methyltransferase FstJ-like domain and C-terminal S4-like RNA binding domain. (b) Sequence alignment between conserved residues in S4 RNA binding domain and FstJ domain against TlyA. Both domain prediction and sequence alignments were performed by Pfam database and prediction server (112).

Copyright by Mahidol University

Table 6.1 TlyA subcellular localization prediction using web-based servers for prokaryotic proteins.

Server	Sub-cellular localization	Reference
LocTree3	cytoplasm	(113)
CELLO	cytoplasm	(114)
LipoP 1.0	cytoplasm	(115)
PSLpred	cytoplasm	(116)
SLP-Local	cytoplasm	(117)

6.9 Prediction of TlyA binding to SAM

Binding between TlyA and SAM was predicted by docking of two molecules using Autodock Vina. Search space was confined to predicted RNA binding s4 domain (Figure 6.8). TlyA structure contains seven β-strands adjoined by α-helices (Figure 6.9 a, b) which moulds a Rossmann fold and a typical of class I methyltransferases (133). Evolutionarily conserved regions of methyltransferase such as GxGxG region at the end of first beta strand and acidic residue at the end of second beta strand can also be seen in TlyA (Figure 6.9 c-f).

Copyright by Mahidol University

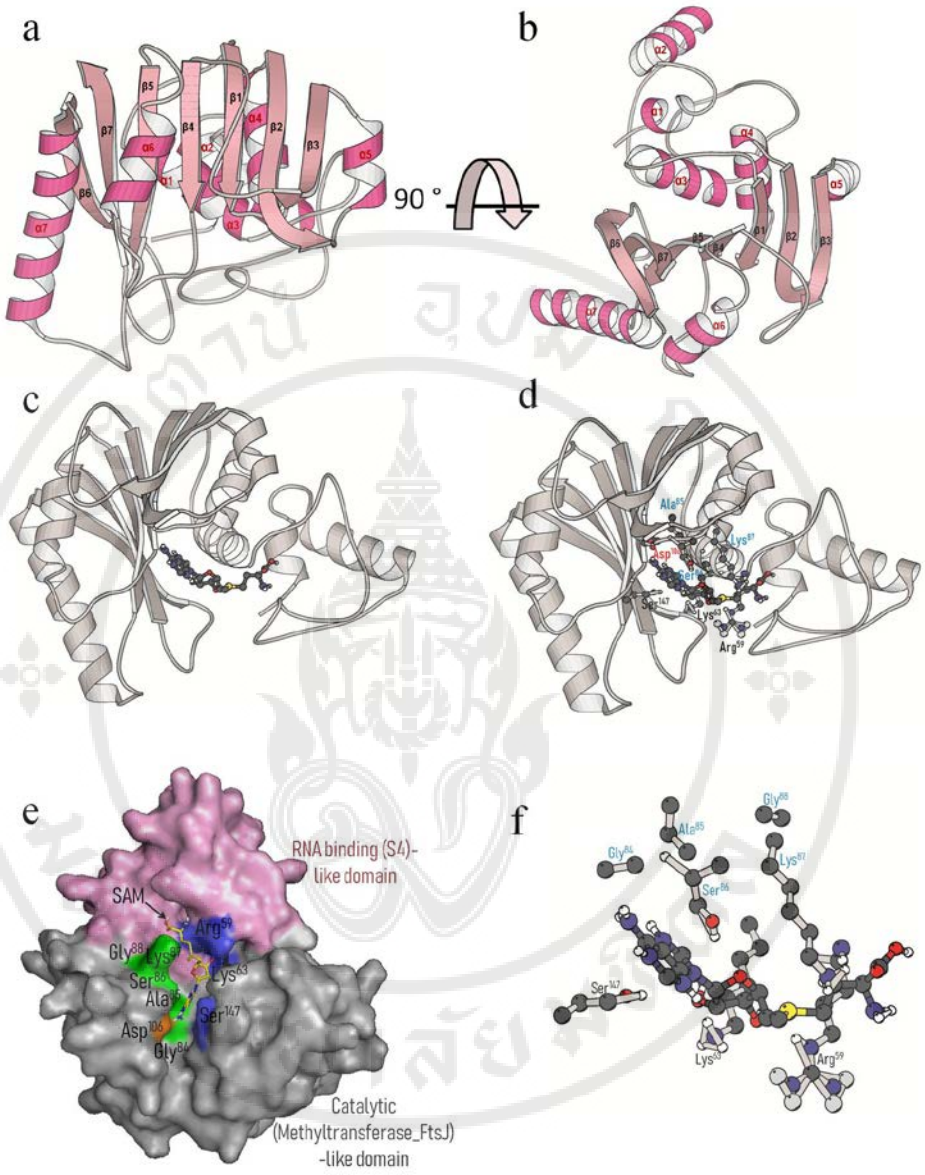

Figure 6.9 Model of TlyA binding to SAM.

(a, b) Orthogonal views of TlyA structure which consists of seven-stranded β-sheets adjoined by α-helices in a Rossmann fold (αβα) which is typical of class I methyltransferases. (c) Model of the TlyA binding to SAM (d) as in (c) with proposed residues for TlyA-SAM interaction. Residues in blue are conserved SAM binding element ($G^{84}ASKG^{88}$) and residue in red is Asp^{106} which is a conserved amino acid involved in forming a hydrogen bond to hydroxyl group of the SAM. (e) TlyA is depicted in surface view and SAM as stick in the binding pocket. (f) Schematic drawing of types residues involved in TlyA binding to SAM.

Copyright by Mahidol University

6.10 Construction of phylogenetic tree of TlyA

TlyA from *H. pylori* and its homologs from other organisms were analyzed for their phylogenetic association using MegaX (119). Evolutionary analysis of *tly*A genes showed similarity by both Neighbor-joining (NJ) methods (Figure 6.10).

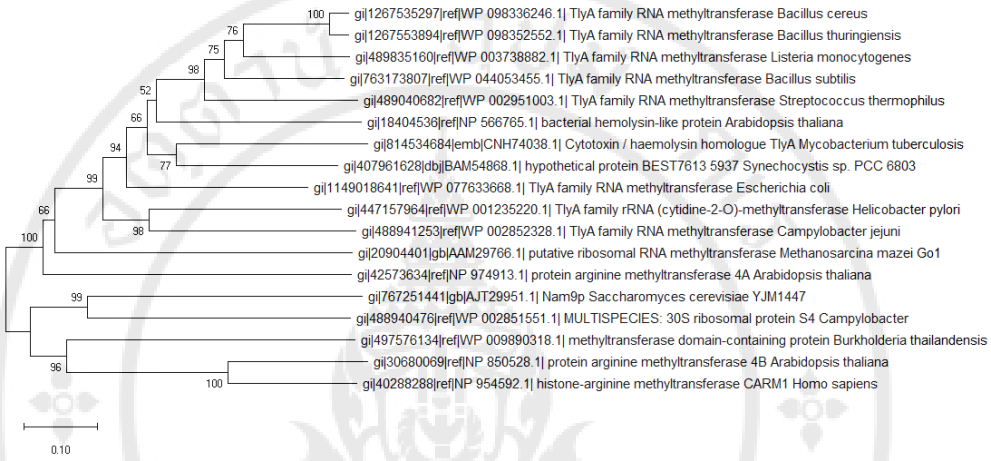

Figure 6.10 Evolutionary relationships of taxa based on the TlyA amino acid sequence.

The bootstrap consensus tree inferred from 5000 replicates is taken to represent the evolutionary history of the taxa analyzed. The percentage of replicate trees in which the associated taxa clustered together in the bootstrap test (5000 replicates) are shown next to the branches. Bootstrap values are shown at each cluster. Evolutionary analyzes were conducted in MEGA X (119).

6.11 TlyA transcriptional unit assembly

TlyA gene locus in different *H. pylori* isolates were compared to observe the *tly*A gene syntheny among *H. pylori* isolates with varying pathogenicity. From the analysis of gene synteny arrangement (Figure 6.11), most of the gene products are involved in metabolic pathways, cell cycle control and signal transduction, however certain genes are involved in cellular adhesion and molecule transport indicating the intertwined role of TlyA in such pathways of *H. pylori in vivo*. No other genes reported to be involved in bacterial virulence were found within this assembly.

Copyright by Mahidol University

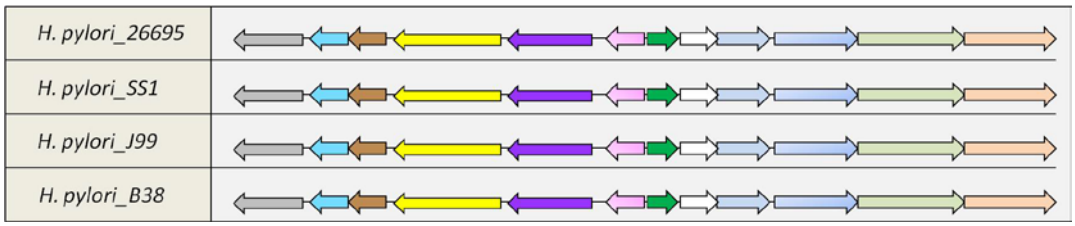

Figure 6.11 *tly*A transcriptional unit gene syntheny.

Genes are represented as arrows and drawn according to transcriptional orientation and function. Color represent gene function: orange-cell cycle control, celadon-DNA replication, light blue-carbohydrate metabolism, white-*tly*A, green-signal peptides, pink-nucleotide biosynthesis, violet-signal transduction, yellow-transport, brown-cell adhesion, cyan-DNA repair and grey-transcription regulation.

6.12 Calculation of evolutionary conservation rate among conserved residues of TlyA

Conserved amino acid in TlyA as calculated by evolutionary trace analysis suggested the presence of several conserved regions within TlyA (Figure 6.12). These conserved regions are in line with previously predicted conserved domains and SAM binding sites suggestive of high accuracy in overall predictions.

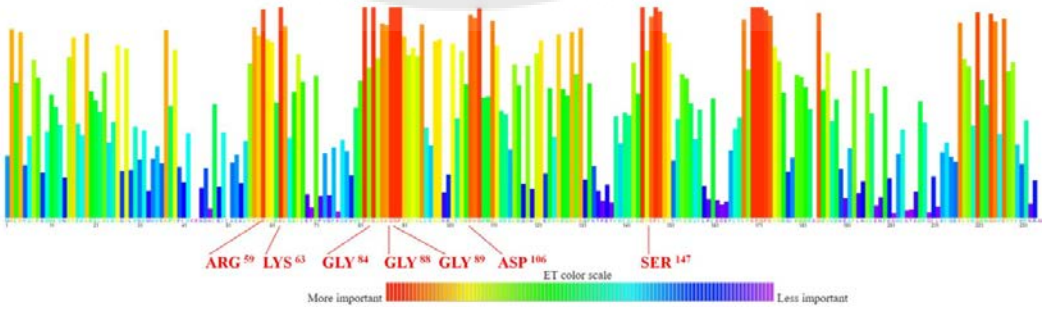

Figure 6.12 Evolutionarily conserved residues of TlyA.

Conserved resides coincides with the SAM binding sites were denoted under the heatmap. Most and least conserved residues are depicted as red and violet, respectively. Conservation heatmap was plotted by ET trace (122).

Copyright by Mahidol University

6.13 Prediction of *in vivo* function of TlyA

In vivo function of proteins can be predicted by sequence and structure-based multiple-level protein-protein interaction-based method (123). Analysis of TlyA sequence suggests the presence of at least two *in vivo* functions, nucleic acid binding and methyltransferase activities (Figure 6.13). The list of predicted functions and corresponding gene ontology are listed in Table 6.2.

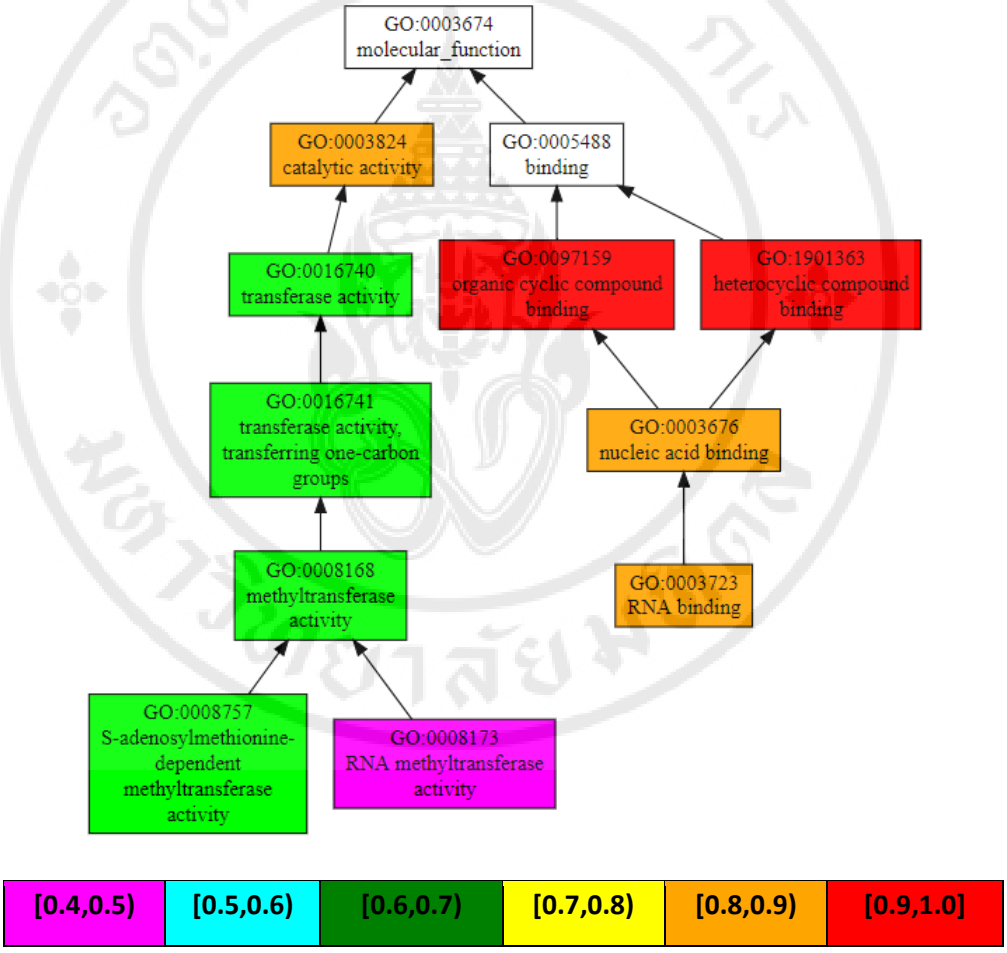

Figure 6.13 Predicted gene ontology hierarchy for TlyA.

The figure shows the predicted terms within the gene ontology hierarchy for molecular function. Confidently predicted terms are color coded by $Cscore^{GO}$. Predicted by Cofactor (123). $Cscore^{GO}$ is the confidence score of predicted GO terms. $Cscore^{GO}$ values range in between [0-1]; where a higher value indicates a better confidence in predicting the function.

Copyright by Mahidol University

Table 6.2 Predicted gene ontology (GO) terms and corresponding functions.

	GO_{term}	$Cscore^{GO}$	GO_{name}
1	GO:1901363 F 0.91	0.91	heterocyclic compound binding
2	GO:0097159 F 0.91	0.91	organic cyclic compound binding
3	GO:0003676 F 0.87	0.87	nucleic acid binding
4	GO:0003824 F 0.85	0.85	catalytic activity
5	GO:0003723 F 0.85	0.85	RNA binding
6	GO:0016740 F 0.69	0.69	transferase activity
7	GO:0016741 F 0.67	0.67	transferase activity transferring one-carbon groups
8	GO:0008168 F 0.66	0.66	methyltransferase activity
9	GO:0008173 F 0.50	0.64	RNA methyltransferase activity
10	GO:0008649 F 0.49	0.50	rRNA methyltransferase activity

$Cscore^{GO}$ is the confidence score of predicted GO terms. $Cscore^{GO}$ values range in between [0-1]; where a higher value indicates a better confidence in predicting the function using the template.

6.14 Prediction of ligand binding sites *via* MSA and clustering algorithm

Analysis of TlyA sequence reveals at least three putative ligand binding sites (Figure 6.14a). Ligands include SAM, Met and sinefungin (SFG) and analysis of binding site between described ligands and TlyA suggests the similarity of binding region between SAM and SFG including the conserved GxGxG region (Figure 6.14b). SFG, an analog of SAM, as a nucleoside analog of SAM in which the $S–CH_3$ (sulfonium moiety) of SAM is replaced by a $C–NH_3$ (amine) and both consist of adenosine linked at the 5' position to the side-chain of an α-amino acid (black arrow, S^{δ} of Met and C^{δ} of ornithine, respectively) (Figure 6.14c).

Copyright by Mahidol University

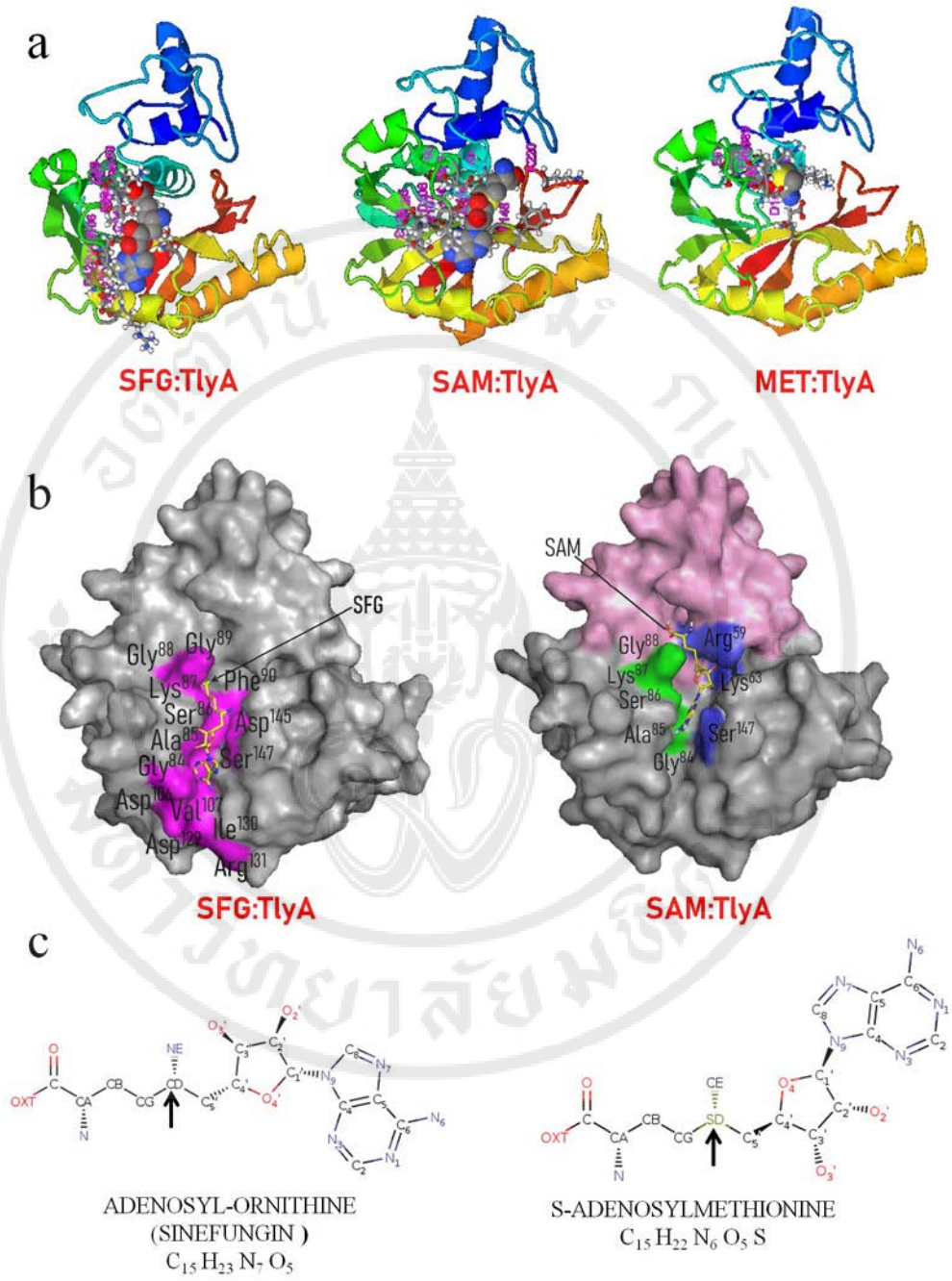

Figure 6.14 TlyA binding to multiple ligands.

(a) model of TlyA structure which is bound with putative ligands. (b) Comparison of binding site and residues involving between SAM and SFG with proposed residues for each ligand interaction with TlyA. (c) Comparison of chemical structure between SAM and SFG.

Copyright by Mahidol University

6.15 Prediction of membrane insertion region of TlyA

TlyA structure contains 8 α-helices, however only the length of helix 7 K^{190}-K^{207} is long enough to span the membrane (~2.7 nm) and therefore modelled as a membrane spanning helix within TlyA quaternary assembly. Modelled assembly consist of four monomeric TlyA which in centre forms a membrane spanning helices and putative pore forming complex (figure 6.15a-e).

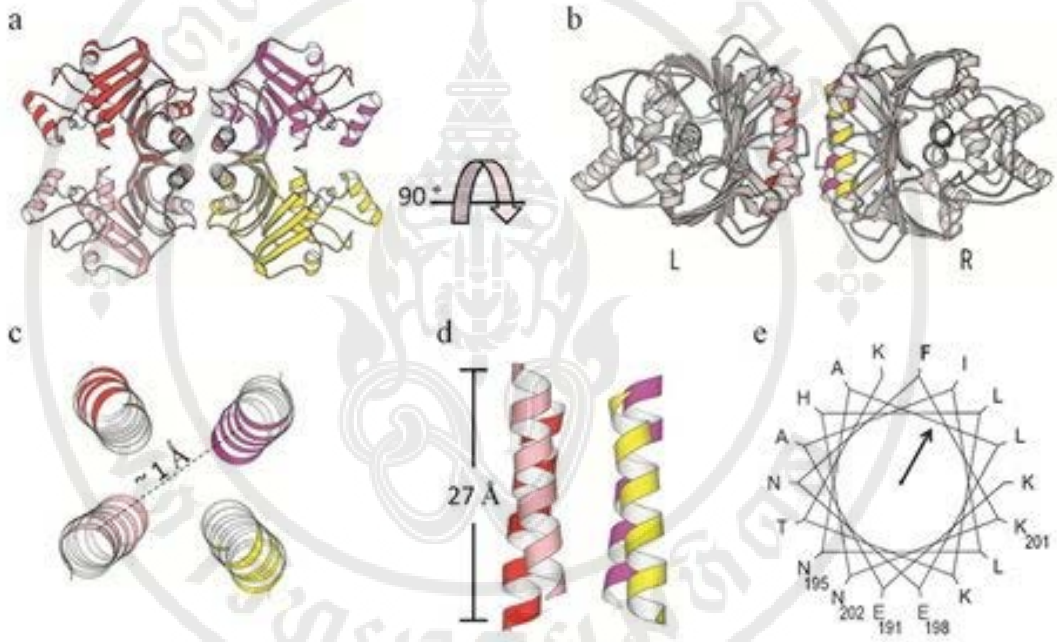

Figure 6.15 Helix 7 mediated membrane insertion model of TlyA tetramer.

(a, b) model of tetrameric TlyA assembly with helix 7 as putative transmembrane region. (c-e) model of helix 7-mediated pore formation. Predicted pore diameter is ~1 Å (c) and length is ~2.7 Å (d). Distances were calculated by Pymol (109), and images were prepared by Molscript (110). (e) Helical wheel projections of helix 7. Clustering of charged and hydrophilic residues on one face of the helix suggests an amphipathic configuration. The arrow in helical wheels corresponds to the hydrophobic moment.

Copyright by Mahidol University

CHAPTER VII
DISCUSSION

Across major kingdoms of life, proteins play significant roles as “working molecules” which are critical to metabolic, structural and signal transduction pathways (134). Depending on the type of organisms, their microenvironment and functional role, proteins evolved to be tailor-made to fit the specific needs of specific organisms in specific environments (135). Best example is thermostable *Taq* polymerases produced from thermophile *Thermus aquaticus* which contains more hydrogen bonds/salt bridges/non-covalent interactions compared to Escherichia *coli* DNA polymerase and is utilized as an enzyme able to withstand the protein-denaturing conditions (high temperature) and thus widely used in polymerase chain reaction (136). Certain proteins, however can be seen in different kingdoms of life for their indispensable roles in survival of each species, and are known as evolutionarily conserved proteins. Roles of these conserved proteins can range from key enzymes in metabolic pathways to structural proteins which play critical roles in structural assembly and signal transduction (137).

Methyltransferase proteins are such proteins which are indispensable due to their roles in transfer of one or more methyl groups to substrates including protein, DNA and RNA resulting transcriptional regulation and post-translational modifications (138). Due to the evolutionary selection, certain proteins can perform more than a single function in a given organism at a given time. Such proteins are known as multi-functional proteins, which could possess ability to catalyze a primary substrate specific function and to account for different secondary reaction (139). These proteins could have evolved by fusion of single domain single function proteins into multi domain multi-function units or by gain of function mutation to single function proteins whilst maintaining their primary roles. This purpose could be to facilitate the interaction between functional units and/or to reduce the energy expenditure of produce proteins through transcription-translation processes (139).

Copyright by Mahidol University

Helicobacte pylori is the human pathogen with the highest infection rate across the world at ~50 % of the entire population. With the stomach as its unique site of infection, it harbours specific biophysical and genome composition for colonization, pathogenesis and persistence survival (19). *H. pylori* encodes unique proteins such as vacuolating cytotoxin A (VacA) whose sequence displays little homology to those from known organisms and common proteins such as flagellin proteins which can be abundantly found in Gram negative bacteria.

TlyA belongs to the latter type of proteins with the presence of homologs across major kingdoms of life (Figure 6.1). *tly*A gene sytheny analysis showed that it belongs in the group of proteins which function primarily in metabolic and regulatory pathways(Figure 6.11). Such syntheny suggests that TlyA could be involved with intracellular biological processes rather than bacterial virulence. Evolutionary relationship between TlyA homologs investigated by phylogenetic analysis reveals that *tly*A genes from 18 species showed that *H. pylori tly*A gene is closely related to those of *Camphylobacter* and *Mycobacterium*, an observation which is supported by high bootstrap values (Figure 6.10). The close phylogenetic association between *H. pylori* TlyA and its homologs in pathogenic bacteria (*Mycobacterium tuberculosis* and *Listeria monocytogenes*) and reported activities such as hemolysis and cytotoxicity put a spot light on putative role of TlyA as a bacterial virulence factor.

TlyA is produced as a 27-kDa protein lacking a typical signal sequence for secretion into extracellular space. Sub-cellular localization prediction by different algorithms suggests it is a cytoplasmic protein (Table 6.1). However, it should be noted that TlyA homologs were reported to be secreted into extracellular space although the putative non-classical secretion system is yet to be identified. From gene syntheny analysis, a conserved putative signal peptide does exist upstream of *tly*A gene assembly (Figure 6.11) and deserves further investigation into its relation and/or interaction with TlyA.

When expressed in *E. coli* as recombinant protein, TlyA is produced mainly as a soluble protein at temperatures lower than 37°C where it was expressed mostly as insoluble aggregates at high temperatures (Figure 5.8). TlyA expression is stable for at least 6 hours after IPTG induction as can be seen in Figure 5.7. It should be noted that TlyA is produced predominately as soluble form when expressed as

Copyright by Mahidol University

FLAG tagged protein but failed to display similar level of expressed protein in soluble fraction when expressed as His tagged protein (Figure 5.6). Protein expression levels are unaffected when expressed either as FLAG-tagged or His-tagged TlyA (Figures 5.5 and 5.7). Analysis of restriction mapping followed by sequencing analysis revealed no mutations in the *tly*A gene suggesting the variation of the soluble protein expression results from intrinsic property of the amino terminal tag (Figures 5.1 and 5.4). A plasmid map of His/TlyA235 or FLAG/TlyA235 can be seen in Figure 5.1 and 5.4. Since antibodies against TlyA from *H. pylori* are not available, anti-FLAG antibody was used for Western blot analysis where it showed a positive signal which further confirmed the presence of FLAG tag and provides a platform for detection of recombinant TlyA for further assays (Figure 5.14).

Analysis of the TlyA amino acid sequence for theoretical isoelectric point revealed pI of ~9.27 which is relatively high when compared to other *E. coli* proteins. Therefore, cation exchange chromatography was employed for biochemical purification of soluble TlyA. To purify proteins based on intrinsic properties such as pI requires the maintenance of charge on that molecule and therefore HEPES buffer at pH 8.2 was used to maintain the net positive charge of TlyA. Purification profile and subsequent analysis by SDS-PAGE analysis revealed the presence of TlyA in fractions with NaCl concentrations higher than 0.5 M suggesting the predicted pI is accurate (Figure 5.9 and 5.10). It should be noted that at physiological pH of ~7.4, several bound proteins were co-eluted with TlyA (Figure 5.11), which pinpoints the importance of pH in selective TlyA binding to the cation exchange resin. TlyA was purified to near homogeneity as can be seen in Figure 5.12. Dialysis against HEPES buffer for removal of salts neither affects TlyA integrity nor solubility (Figure 5.13).

H. pylori TlyA was reported to possess hemolysis activity *in vitro* against animal erythrocytes. Cell lysis could result from formation of membrane pores in lipid bilayer membrane leading to osmotic lysis. However, the structural basis and underlying mechanism for TlyA-mediated cell lysis is not known. Furthermore, the extent of TlyA binding to lipid membranes nor the putative residues critical for TlyA structural assembly is also not reported. In this study, binding and membrane-perturbing activity of TlyA was evaluated using sulforhodamine B dye-engulfed liposomes. Under physiological conditions at 25°C, TlyA displayed-concentration

Copyright by Mahidol University

dependent membrane perturbation activity against liposomes (Figure 5.15). The effect was visible within 10-15 minutes after TlyA addition to the liposomes suggesting the possibility of pre-pore oligomer formation.

A complication toward the understanding of TlyA mechanism and structure-function relationship is the lack of a crystal structure of TlyA. Structural information is also critical to deduce the biological functions based on the sequence-to-structure-to-function paradigm as well. Therefore, a tertiary structural model for TlyA was constructed by *in silico* analysis. Prior to 3-D structure building, secondary structure composition was first predicted by comparative template-based fragment assembly simulations and remote homology detection methods (103,105). As seen in Figure 6.2, TlyA contains anti-parallel β-strands making up a continuous pleated β-sheet surrounded with α-helices. Presence of putative hairpin formation between anti-parallel β-strands near amino terminal region is also observed.

Tertiary structure of the TlyA was constructed by structure and sequence homology-based pairwise multiple alignments. Comparative protein structure modelling approach was employed to maximize the accuracy of the predicted structure. Steps include fold assignment, target-template alignment, model building, and model evaluation (128). The predicted models displayed an overall backbone helical fold with β-sheets stacking on top of each other in parallel and anti-parallel orientations resembling a Rossmann fold (αβα) (Figure 6.4). Accuracy of the predicted model was validated by calculation of phi/psi angles (ϕ, ψ) *via* Ramachandran plot analysis (107). Analysis revealed that most of the residues (95.7 %, 220/235) are located in favoured regions and only 0.9% (2/235) in non-allowed regions (Figure 6.5), implying the model is in line with empirical distribution of data points observed in protein structures. Further analysis of the sequence and model revealed the presence of 4 Cys residues (Cys^{104}, Cys^{124}, Cys^{128}, Cys^{144}) within TlyA. However, distances between Cys residues as predicted by PYMOL program indicated that the Cys residues within monomeric TlyA are too far-off to form intra-molecular disulfide bonds (Figure 6.4). The closest distance between nearest Cys residues (Cys^{104} and Cys^{128}) is 6.7 Å between their thiol groups, exceeding the typical length of a disulfide bond ~2 Å (127) and therefore no intra-molecular disulfide bonds were present according to the constructed model.

Copyright by Mahidol University

However, previously reported studies indicated that disulfide bridges can be present within individual molecules as intra-molecular bonds or between each molecule as inter-molecular bonds (140, 141). And the latter type of disulfide bridges can influence on biological function of the given molecule upon secretion into periplasmic and extracellular space where the oxidizing conditions would allow the bond formation between adjacent thiol groups leading to structural rearrangements and playing a different role as it was as in monomeric form. Inter-molecular disulfide bonds are also known as redox sensing switches where a particular function of a protein is directly modulated by locking and unlocking of the functionally critical residues/regions or indirectly modulated by induced conformational changes which affects the distantly located functionally critical residues/regions (142).

Therefore, modelled TlyA molecule in monomeric form was evaluated for quaternary structure formation *via* disulfide bridges by combining sequence and structure information and physical chemistry principles such as molecular distributions and statistical thermodynamics (143). Selected model of TlyA dimerization showed the putative formation of inter-molecular disulfide bond formation *via* Cys^{124} and Cys^{128} from two neighboring TlyA monomers (Figure 6.6). The calculated distance between thiol groups of these two residues was ~3.6 Å, which still exceeds the typical distance of ~2 Å, however the calculated distance is based on the constructed model and not on the actual crystallographic structure. Further prediction of dimeric interface among TlyA monomers suggested the potential involvement of salt bridges, disulfide bonds and hydrogen bonds in homo-oligomeric assembly (Figure 6.7). The detailed description of atom-atom interaction can be seen in appendix B.

We therefore hypothesized that the putative formation of disulfide bonds might be visible on polyacrylamide gel electrophoresis if analyzed under semi-native conditions (no SDS, no DTT, not heated). And such observation of protein oligomeric assembly under semi-native conditions is reported elsewhere before (144). As expected, purified TlyA showed presence of higher ordered forms when analyzed under semi-native conditions as can be seen in Figure 5.17. Western blot analysis confirms the identities of these quaternary forms as TlyA (Figure 5.17, right panel). The quaternary assemblies represent ~38 and 48-kDa bands on semi-native PAGE which do not correspond precisely to the molecular weight of dimeric or trimeric

Copyright by Mahidol University

oligomers of TlyA (monomeric TlyA is observed ~ 27-kDa band on SDS-PAGE). However, it is possible that dimeric or trimeric as oligomeric forms of TlyA display anomalous migration in SDS-PAGE under the conditions used. TlyA oligomers displayed an interaction mainly dependent on reducing/oxidizing environment as oligomers can be also detected on SDS-PAGE under reducing conditions, suggesting a disulfide bond-dependent nature of observed oligomers (Figure 5.18).

Previous observation led to the assumption that the reducing conditions which effect structural assembly of TlyA could also affect the biological activity of TlyA *in vitro*. Previous assays using liposomes showed that TlyA at certain concentrations leads to nearly ~100% membrane perturbing of dye-entrapped liposomes. However, at similar conditions and TlyA concentration, in the presence of DTT, TlyA mediated liposome membrane- perturbating activity was significantly reduced (Figure 5.16). DTT added to the liposomes displayed slight increase in background dye leakage which would further signifies the observed effect of TlyA in the presence of DTT. Consistent to membrane perturbing activity, TlyA binding to liposomes was also diminished under reducing conditions in liposome pull down assay of TlyA (Figure 5.19) which suggests the efficient binding to lipid bilayers is dependent on formation of disulfide-mediated oligomeric assembly. Efforts to identify the spectrum shift of TlyA under reducing/non-reducing conditions showed very little difference between two states as TlyA amino acid sequence lacks Trp residues which would otherwise indicate different structural conformation, reduced and non-reduced TlyA molecules (Figure 5.23). Previously, the formation of functionally relevant protein dimerization *via* disulfide bridges is reported in other proteins before (145-147). Furthermore, this data would support the concept that dissociation of the TlyA oligomeric assemblies is caused by the breakdown of intermolecular disulfide bonds, a prediction which is substantiated by the structural model and experimental observations.

However, protein dimers are rarely depicted as fully functional oligomers terms of pore formation in membrane environments as dimeric proteins usually lack the central tunnel to allow formation of transmembrane pores (148). Therefore, pore forming proteins are often assembled as trimeric or tetrameric forms for fully functional transmembrane pore formation (148). Protein tetramerization reduces

Copyright by Mahidol University

dynamics within the dimeric unit thereby stabilizing the oligomeric assembly whilst maintaining its desired function (145). Therefore, the putative transmembrane pore forming region of TlyA is analyzed and modelled for putative oligomer assembly which would allow the formation of transmembrane pore long enough to span the lipid bilayer. Analysis of TlyA tertiary structure reveals β-strands intertwined by several α-helices, however only helix 7 (Lys^{190}–Lys^{207}) is long enough to span the lipid bilayer (~2.7 Å) (Figure 6.15). A tetrameric model of TlyA was constructed as described before. The modelled tetramer also displays helix 7 as pore lining region (Figure 6.15). Previously, TlyA dimeric model was predicted to be associated mainly *via* disulfide bonds. Such dimeric TlyA could exist as protomer whilst monomeric TlyA would have to assemble into dimeric form prior to pore formation.

Since TlyA is produced from *H. pylori* which is a gastric pathogen and previous observation of membrane-perturbing activities, the putative activity of TlyA as cytotoxic molecule against human gastric epithelial cells was evaluated by cell viability assay. Viability was evaluated as the amount of resazurin molecules uptake and converted to a red-fluorescent dye by reducing environment of the cytoplasm in living cells (98). TlyA displayed concentration dependent cytotoxicity against AGS cells when incubated for 24 hours as can be seen in Figure 5.20. The observed cytotoxic effect is not evident when incubated for 12 hours where only TlyA binding to the plasma membrane is observed without internalization (Figure 5.21d-f).

Virulence factors from bacteria are often involved in manipulation of host immune response to promote persistent infection in a given environment. In case of *H. pylori*, it has been known to trigger production of cytokines from human gastric cells. Cytokines such as IL-1β, IL-8, TNF-α, IL-6, IL-10 and IL-13 were reported to be overexpressed in response to *H. pylori* infection (149). Most of these cytokines are pro-inflammatory, suggesting that *H. pylori* infection would lead to inflammation and subsequent immune response by the host cells. However, as discussed in literature review. *H. pylori* possesses several molecules which are capable of inducing anti-inflammatory cytokines as well. The strategy of *H. pylori* could be to suppress the local inflammation until certain period of time or certain growth is achieved, and then followed by continuous production of pro-inflammatory cytokines for aggressive growth and invasion of the host (78). Although most of the cytokines and respective

Copyright by Mahidol University

inducers were reported for *H. pylori*, for certain cytokines like IL-8, the inducer molecules are still unclear. It was reported that IL-8 is the single most up-regulated gene in whole genome profiling of *H. pylori* exposed gastric epithelial cells (150) and IL-8 receptors IL-8RA (CXCR1) and IL-8RB (CXCR2) are also reported to be significantly up-regulated in *H. pylori*-infected human gastric biopsy samples (151). Therefore, IL-8 overexpression by *H. pylori* is proposed to play a major role in gastric cancer development and targeting of IL-8 is suggested to be a promising strategy for gastric cancer treatment (74). From the virulence factors produced from *H. pylori*, only CagA is reported to induce IL-8 secretion (152) although CagA-isogenic mutant *H. pylori* strains also displayed increased IL-8 production in several cell lines (153), suggesting that another factor could be responsible for *H. pylori* mediated IL-8 overexpression.

Therefore, it was hypothesized that as a less-known virulence factor from *H. pylori*, TlyA could play a role in inducing cytokine expression from gastric cells. Human gastric adenocarcinoma cells were incubated with TlyA and cytokines in the supernatant were measured by ELISA. Among the cytokines tested (IL-1α, IL-1β, IL-2, IL-4, IL-6, IL-8, IL-10, IL-12, IL-17A, IFN-γ, TNF-α, and GM-CSF), incubation with TlyA down regulates the expression of all but one cytokine, IL-8. When compared to untreated cells, TlyA induces a 5-fold increase in IL-8 production by AGS cells (Figure 5.22). Another interesting observation is that when AGS cells were pre-incubated with TlyA, the production of VacA mediated pro-inflammatory cytokines (IL-1β, IL-2 or IL-4) is reduced. However, the underlying mechanism for this cytokine-balancing ability by TlyA is unclear and deservers further investigations in the future. IL-8 is reported to function as chemoattractant for neutrophils and induce production of angiogenic growth factors for migration and survival of endothelial cells to the target site. Homologs of *H. pylori* TlyA includes those from *M. tuberculosis* which induces hemolysis of human erythrocytes. And *H. pylori* TlyA is reported to possess similar hemolytic activity *in vitro* albeit the underlying mechanism and *in vivo* significance of such activity is never described. Based on the result of previous experiment (Figure 5.22), it is plausible that TlyA-mediated IL-8 overexpression leads to migration of endothelial cells to site of infection followed by angiogenesis and the newly formed blood vessels provides erythrocytes which contains iron and nutrients

Copyright by Mahidol University

which are proved to be critical for *H. pylori* growth and expression of virulence factors such as VacA (92).

Based on the amino acid alignments, TlyA homologs could function as either cytolysins or methyltransferase enzymes (Figure 6.1). Experimental observations in this study suggest a function of TlyA as cytolysin. To identify TlyA as a multi-functional protein, it needs to possess different, but functionally relevant activities. Therefore, putative functions of *H. pylori* TlyA are predicted by conserved domain analysis and it was revealed that TlyA contains two conserved domains, a carboxy terminal nucleic acid binding domain and amino terminal enzymatic domains (Figure 6.8a). The nucleic acid binding domain displays sequence similarity to that of s4 RNA binding domain responsible for initiation of rRNA assembly and structural stability (129,130). For the enzymatic domain, it is similar to that of methyltransferase enzymes which methylate 23 S rRNA at position U2552 of the ribosome of *E. coli* (131). The conserved active site consisting of two Lys residues and the negatively charged Asp residue (132) is also be found in TlyA (Figure 6.8).

The methyltransferase enzymes can be classified based on the structural feature and according to such classification, *H. pylori* TlyA belongs to class I methyltransferases which contains a Rossmann fold (αβα) topology with S-adenosyl methionine (SAM) as a co-substrate (133). To evaluate the presence of a SAM-binding site in TlyA, interaction between two molecules were analyzed by *in silico* docking algorithm which calculates the values of the torsion angles for the rotatable bonds in both ligand and receptor molecules using quasi-Newton optimization method (118). Docking results revealed the model for TlyA-SAM complex and resides involved in protein-ligand interaction. TlyA contains conserved residues for SAM binding (GlyxGlyxGly) at the end of first β-strand and acidic residue at the end of second β-strand (Figure 6.9). Gly^{84}AlaSerLysGly residues represent conserved SAM binding motif and Asp^{106} which is situated at the end of second beta strand represent the conserved acidic residue involved in forming a hydrogen bond to hydroxyl group of SAM (Figure 6.9c-d). Although these residues are identified as conserved motif important for SAM binding, their conservation status within TlyA was still not evaluated. Therefore, the evolutionary conservation rate for each amino acid in TlyA was calculated by evolutionary trace analysis (Figure 6.12).

Copyright by Mahidol University

As in line with the SAM binding motif predicted in Figure 6.9, residues Gly^{84}, Gly^{88}, Gly^{89} and Asp^{106} are among the most conserved residues in *H. pylori* TlyA suggesting the functionally relevant conserved nature of these residues.

TlyA functions as cytolysin *in vitro* as per experimental observation and as nucleic acid binding methyltransferase enzymes as per *in silico* analysis. To validate previous findings, TlyA protein sequence was evaluated for *in vivo* function by sequence and structure-based protein-protein interaction pathways analysis method (123). Analysis of the predicted *in vivo* function includes cyclic compound binding to methyltransferase activity (Figure 6.13, Table 6.2). It should be noted that neither prediction of *in vivo* function nor conserved domain analysis suggested TlyA as a hemolysin or cytolysin. Instead, it was predicted as a protein involved in regulation of nucleic acid metabolism as can be seen from various analysis algorithms. Gene syntheny analysis also support the notion that TlyA gene locus is composed of several genes responsible for DNA replication, signal transduction and transcription regulation rather than virulence. This suggests that the cytolytic property could be a newly acquired function to promote *H. pylori* pathogenesis and if this were true, TlyA could be one of the moonlighting proteins which originally possessed a single function but through evolution, acquired additional functions (154).

Ligand binding to receptor molecules represent specific interactions among two molecules involved, however, structural homologs of either molecules could also possess similar binding sites on the same target molecules. The putative ligands which could bind to TlyA from *H. pylori* were evaluated by multiple sequence alignment and clustering algorithm (123). Putative ligands which could bind to TlyA include methionine, SAM and sinefungin (SFG) (Figure 6.14). Among them, SAM and SFG displayed similar binding region/residues on TlyA (Figure 6.14b). SFG, an analog of SAM, is isolated from *Streptomyces* species and is known to display potent antifungal, antiviral and antiparasitic activities by inhibition of methyltransferase activities by competitive inhibition with SAM (155-157). Sinefungin is also known to inhibit *Pseudomonas* acyl homoserine-lactone quorum-sensing signal generation by interfering with acyl-homoserine-lactone synthase mediated autoinducer synthesis (158). And it was reported that sinefungin binds 8 times stronger to receptor molecules than SAM (159). Altogether, roles of sinefungin in these studies and

Copyright by Mahidol University

docking analysis in current thesis indicates that SFG could be utilized to inhibit the TlyA *in vivo* function which would result in destabilization of *H. pylori* metabolic pathway. Recent guidelines for *H. pylori* treatment for eradication therapies uses combined therapy of β-lactam antibiotics and macrolide antibiotics coupled with proton pump inhibitors for suppression of acid production (160). However, the incidence of *H. pylori* isolates resistant to clarithromycin is steadily increasing (161). Therefore, sinefungin, as a natural analog to SAM, could provide alternative approach to *H. pylori* treatment although it's *in vivo* efficacy and pharmacological kinetics needs to be evaluated in details prior to any trials.

Observations in this study and earlier reports in literature suggested that *H. pylori* virulence proteins could play a role in bacterial persistence infection by evolving to undertake multi-function faceted roles. These proteins are in a class of moonlighting proteins which by evolution gained the abilities to perform secondary functions. TlyA could be a new member of virulence factors produced by *H. pylori* whose function depends on the cellular environment. The primary role of TlyA in *H. pylori* could be as a metabolic regulator by functioning as a ribosomal RNA methyltransferase whereas it could exert the secondary function as virulence factor by promoting cytotoxicity to increase iron and nutrient availability for bacterial growth and by modulation of the host immune response by synchronous interaction with other virulence factors such as VacA for efficient and persistent colonization in the human stomach.

Copyright by Mahidol University

CHAPTER VIII
CONCLUSION

In this study, TlyA protein from *Helicobacter pylori* was over-expressed as a FLAG-tagged protein in *Escherichia coli* and the conditions necessary for soluble protein expression were described. Conditions necessary for efficient TlyA binding to cation exchange resin was also reported. The expressed TlyA confer membrane perturbating activity to liposomes. The liposome membrane damaging activity was concentration-dependent and negatively influenced by reducing conditions. In line with the influence of reducing condition on TlyA activity, the structural assembly also suggests the presence of oligomeric TlyA in the absence of reducing agents. Homology modelling of TlyA structure suggests dimeric assembly mediated by Cys^{124} and Cys^{128} TlyA also displays cytotoxic activity towards human gastric cell line (AGS, ATCC) in vitro. Immunocytochemistry analysis showed that TlyA binds to the AGS cell membrane and putative toxin internalization was also observed. Cytokine array analysis showed that TlyA induce increased production of interleukin-8 from AGS cells highlighting the role of TlyA in H. pylori pathogenesis. In silico modeling and analysis suggested the putative binding between TlyA and s-adenosyl methionine, which could be inhibited by sinefungin, a natural nucleoside analog from *Streptomyces griseolus.* Further structural analysis reveals helix 7 as the membrane insertion region within tetrameric TlyA assembly. Overall, this study identified critical residues responsible for TlyA structural assembly and biological activity and furthermore, identified IL-8 as a major cytokine which is upregulated in response to TlyA.

Copyright by Mahidol University

REFERENCES

1 Bouvard V, Baan R, Straif K, Grosse Y, Secretan B, El Ghissassi F, et al. A review of human carcinogens--Part B: biological agents. Lancet Oncol. 2009;10(4):321-2.

2 Correa P, Piazuelo MB. Natural history of *Helicobacter pylori* infection. Dig Liver Dis. 2008; 40(7):490-6.

3 Kusters JG, van Vliet AH, Kuipers EJ. Pathogenesis of *Helicobacter pylori* infection. Clin Microbiol Rev. 2006; 19(3):449-90.

4 Wen S, Moss SF. *Helicobacter pylori* virulence factors in gastric carcinogenesis. Cancer Lett. 2009; 282(1):1-8.

5 Roesler BM, Rabelo-Goncalves EM, Zeitune JM. Virulence factors of *Helicobacter pylori*: a review. Clin Med Insights Gastroenterol. 2014; 7:9-17.

6 Ansorg R, Rein R, Spies A, von Recklinghausen G. Cell-associated haemolytic activity of *Helicobacter pylori*. Eur J Clin Microbiol Infect Dis. 1993; 12(2):98-104.

7 Martino MC, Stabler RA, Zhang ZW, Farthing MJ, Wren BW, Dorrell N. *Helicobacter pylori* pore-forming cytolysin orthologue TlyA possesses *in vitro* hemolytic activity and has a role in colonization of the gastric mucosa. Infect Immun. 2001; 69(3):1697-703.

8 von Recklinghausen U, von Recklinghausen G, Ansorg R. Haemolytic activity of *Helicobacter pylori* against human and animal erythrocytes. Zentralbl Bakteriol. 1998; 288(2):207-15.

9 Wetherall BL, Johnson AM. Haemolytic activity of *Campylobacter pylori*. Eur J Clin Microbiol Infect Dis. 1989; 8(8):706-10.

10 Javadi MB, Katzenmeier G. The forgotten virulence factor: the 'non-conventional' hemolysin TlyA and its role in *Helicobacter pylori* Infection. Curr Microbiol. 2016; 73(6):930-7.

Copyright by Mahidol University

11 Wetherall BL, McDonald PJ, Johnson AM. Partial characterization of a cell-free hemolytic factor produced by *Helicobacter pylori*. FEMS Microbiol Immunol. 1992; 4(3):123-8.

12 Drazek ES, Dubois A, Holmes RK, Kersulyte D, Akopyants NS, Berg DE, et al. Cloning and characterization of hemolytic genes from *Helicobacter pylori*. Infect Immun. 1995; 63(11):4345-9.

13 Lata K, Chattopadhyay K. *Helicobacter pylori* TlyA agglutinates liposomes and induces fusion and permeabilization of the liposome membranes. Biochemistry. 2014; 53(22):3553-63.

14 Rahman MA, Sobia P, Dwivedi VP, Bhawsar A, Singh DK, Sharma P, et al. *Mycobacterium tuberculosis* TlyA protein negatively regulates T helper (Th)1 and Th17 differentiation and promotes tuberculosis pathogenesis. J Biol Chem. 2015; 290(23):14407-17.

15 Maus CE, Plikaytis BB, Shinnick TM. Mutation of tlyA confers capreomycin resistance in *Mycobacterium tuberculosis*. Antimicrob Agents Chemother. 2005;49(2):571-7.

16 Kumar S, Mittal E, Deore S, Kumar A, Rahman A, Krishnasastry MV. Mycobacterial tlyA gene product is localized to the cell-wall without signal sequence. Front Cell Infect Microbiol. 2015; 5(60):1-13.

17 Lata K, Paul K, Chattopadhyay K. Functional characterization of *Helicobacter pylori* TlyA: pore-forming hemolytic activity and cytotoxic property of the protein. Biochem Biophys Res Commun. 2014; 444(2):153-7.

18 Lata K, Chattopadhyay K. *Helicobacter pylori* TlyA forms amyloid-like aggregates with potent cytotoxic activity. Biochemistry. 2015; 54(23):3649-59.

19 Mobley HLT, Mendz GL, Hazell SL. Overview. In: Mobley HLT, Mendz GL, Hazell SL, editors. *Helicobacter pylori*: physiology and genetics. 1st ed. Washington (DC): ASM Press; 2001.

20 Swanston T, Haakensen M, Deneer H, Walker EG. The characterization of *Helicobacter pylori* DNA associated with ancient human remains recovered from a Canadian glacier. PloS One 2011; 6(2):e16864.

21 Warren JR, Marshall B. Unidentified curved bacilli on gastric epithelium in active chronic gastritis. Lancet. 1983; 1(8336):1273-5.

Copyright by Mahidol University

22. Kasich AM. William Prout and the discovery of hydrochloric acid in the gastric juice. Bull Hist Med. 1946; 20(2):340-58.

23 Hooi JKY, Lai WY, Ng WK, Suen MMY, Underwood FE, Tanyingoh D, et al. Global Prevalence of *Helicobacter pylori* Infection: systematic review and meta-analysis. Gastroenterology. 2017; 153(2):420-9.

24 Blaser MJ, Atherton JC. *Helicobacter pylori* persistence: biology and disease. J Clin Invest. 2004; 113(3):321-33.

25 Schistosomes, liver flukes and *Helicobacter pylori*. IARC Working Group on the Evaluation of Carcinogenic Risks to Humans. 61 vols. 1st ed. Lyon: International Agency for Research on Cancer; 1994.

26 Namavar F, Roosendaal R, Kuipers EJ, de Groot P, van der Bijl MW, Pena AS, et al. Presence of *Helicobacter pylori* in the oral cavity, oesophagus, stomach and faeces of patients with gastritis. Eur J Clin Microbiol Infect Dis. 1995; 14(3):234-7.

27 Fox JG. Non-human reservoirs of *Helicobacter pylori*. Aliment Pharmacol Ther. 1995; 9 Suppl 2:93-103.

28 Brown LM. *Helicobacter pylori*: epidemiology and routes of transmission. Epidemiol Rev. 2000; 22(2):283-97.

29 Poms RE, Tatini SR. Survival of *Helicobacter pylori* in ready-to-eat foods at 4 degrees C. Int J Food Microbiol. 2001; 63(3):281-6.

30 Jiang X, Doyle MP. Optimizing enrichment culture conditions for detecting *Helicobacter pylori* in foods. J Food Prot. 2002; 65(12):1949-54.

31 Ng CG, Loke MF, Goh KL, Vadivelu J, Ho B. Biofilm formation enhances *Helicobacter pylori* survivability in vegetables. Food Microbiol. 2017; 62: 68-76.

32 Stevenson TH, Bauer N, Lucia LM, Acuff GR. Attempts to isolate *Helicobacter* from cattle and survival of *Helicobacter pylori* in beef products. J Food Prot. 2000; 63(2):174-8.

33 Brenner H, Bode G, Boeing H. *Helicobacter pylori* infection among offspring of patients with stomach cancer. Gastroenterology 2000; 118(1):31-5.

Copyright by Mahidol University

34 Drumm B, Perez-Perez GI, Blaser MJ, Sherman PM. Intrafamilial clustering of *Helicobacter pylori* infection. N Engl J Med. 1990; 322(6):359-63.

35 Mitchell HM, Bohane T, Hawkes RA, Lee A. *Helicobacter pylori* infection within families. Zentralbl Bakteriol. 1993; 280(1-2):128-36.

36 Pounder RE, Ng D. The prevalence of *Helicobacter pylori* infection in different countries. Aliment Pharmacol Ther. 1995; 9 Suppl 2:33-9.

37 Wang KJ, Wang RT. [Meta-analysis on the epidemiology of *Helicobacter pylori* infection in China]. Zhonghua Liu Xing Bing Xue Za Zhi. 2003; 24(6):443-6.

38 Poddar U, Yachha SK. *Helicobacter pylori* in children: an Indian perspective. Indian Pediatr. 2007; 44(10):761-70.

39 Fujisawa T, Kumagai T, Akamatsu T, Kiyosawa K, Matsunaga Y. Changes in seroepidemiological pattern of *Helicobacter pylori* and hepatitis A virus over the last 20 years in Japan. Am J Gastroenterol. 1999; 94(8):2094-9.

40 Yim JY, Kim N, Choi SH, Kim YS, Cho KR, Kim SS, et al. Seroprevalence of *Helicobacter pylori* in South Korea. Helicobacter. 2007; 12(4):333-40.

41 Deankanob W, Chomvarin C, Hahnvajanawong C, Intapan PM, Wongwajana S, Mairiang P, et al. Enzyme-linked immunosorbent assay for serodiagnosis of *Helicobacter pylori* in dyspeptic patients and volunteer blood donors. Southeast Asian J Trop Med Public Health. 2006; 37(5):958-65.

42 Dooley CP, Cohen H, Fitzgibbons PL, Bauer M, Appleman MD, Perez-Perez GI, et al. Prevalence of *Helicobacter pylori* infection and histologic gastritis in asymptomatic persons. N Engl J Med. 1989; 321(23):1562-6.

43 Megraud F, Brassens-Rabbe MP, Denis F, Belbouri A, Hoa DQ. Seroepidemiology of *Campylobacter pylori* infection in various populations. J Clin Microbiol. 1989; 27(8):1870-3.

44 Ahmad MM, Rahman M, Rumi AK, Islam S, Huq F, Chowdhury MF, et al. Prevalence of *Helicobacter pylori* in asymptomatic population-a pilot serological study in Bangladesh. J Epidemiol. 1997; 7(4):251-4.

45 World Health Organization. Global priority list of antibiotic-resistant bacteria to guide research,discovery, and development of new antibiotics. 2017.

46 Tomb JF, White O, Kerlavage AR, Clayton RA, Sutton GG, Fleischmann RD, et al. The complete genome sequence of the gastric pathogen *Helicobacter pylori*. Nature 1997; 388(6642):539-47.

Copyright by Mahidol University

47 Oh JD, Kling-Backhed H, Giannakis M, Xu J, Fulton RS, Fulton LA, et al. The complete genome sequence of a chronic atrophic gastritis *Helicobacter pylori* strain: evolution during disease progression. Proc Natl Acad Sci USA. 2006 ;103(26):9999-10004.

48 Alm RA, Ling LS, Moir DT, King BL, Brown ED, Doig PC, et al. Genomic-sequence comparison of two unrelated isolates of the human gastric pathogen *Helicobacter pylori*. Nature 1999 ;397(6715):176-80.

49 Bridge DR, Merrell DS. Polymorphism in the *Helicobacter pylori* CagA and VacA toxins and disease. Gut Microbes. 2013 ;4(2):101-17.

50 Weeks DL, Eskandari S, Scott DR, Sachs G. A H^+-gated urea channel: the link between *Helicobacter pylori* urease and gastric colonization. Science 2000; 287(5452):482-5.

51 Mobley HL. The role of *Helicobacter pylori* urease in the pathogenesis of gastritis and peptic ulceration. Aliment Pharmacol Ther. 1996; 10 Suppl 1:57-64.

52 Montecucco C, Rappuoli R. Living dangerously: how *Helicobacter pylori* survives in the human stomach. Nat Rev Mol Cell Biol. 2001; 2(6):457-66.

53 Censini S, Lange C, Xiang Z, Crabtree JE, Ghiara P, Borodovsky M, et al. Cag, pathogenicity island of *Helicobacter pylori*, encodes type I-specific and disease-associated virulence factors. Proc Natl Acad Sci USA. 1996; 93(25):14648-53.

54 Cadamuro AC, Rossi AF, Maniezzo NM, Silva AE. *Helicobacter pylori* infection: host immune response, implications on gene expression and microRNAs. World J Gastroenterol. 2014; 20(6):1424-37.

55 Leunk RD, Johnson PT, David BC, Kraft WG, Morgan DR. Cytotoxic activity in broth-culture filtrates of *Campylobacter pylori*. J Med Microbiol. 1988; 26(2):93-9.

56 Necchi V, Sommi P, Vanoli A, Fiocca R, Ricci V, Solcia E. Natural history of *Helicobacter pylori* VacA toxin in human gastric epithelium *in vivo*: vacuoles and beyond. Sci Rep. 2017; 7(1):14526.

57 de Bernard M, Arico B, Papini E, Rizzuto R, Grandi G, Rappuoli R, et al. *Helicobacter pylori* toxin VacA induces vacuole formation by acting in the cell cytosol. Mol Microbiol. 1997; 26(4):665-74.

Copyright by Mahidol University

58 Cho SJ, Kang NS, Park SY, Kim BO, Rhee DK, Pyo S. Induction of apoptosis and expression of apoptosis related genes in human epithelial carcinoma cells by *Helicobacter pylori* VacA toxin. Toxicon. 2003; 42(6):601-11.

59 Mobley HL, Hu LT, Foxal PA. *Helicobacter pylori* urease: properties and role in pathogenesis. Scand J Gastroenterol Suppl. 1991; 187:39-46.

60 Rosadini CV, Kagan JC. Early innate immune responses to bacterial LPS. Curr Opin Immunol. 2017; 44:14-9.

61 Cullen TW, Giles DK, Wolf LN, Ecobichon C, Boneca IG, Trent MS. *Helicobacter pylori versus* the host: remodeling of the bacterial outer membrane is required for survival in the gastric mucosa. PLoS Pathog. 2011; 7(12):e1002454.

62 Gewirtz AT, Yu Y, Krishna US, Israel DA, Lyons SL, Peek RM, Jr. *Helicobacter pylori* flagellin evades toll-like receptor 5-mediated innate immunity. J Infect Dis. 2004; 189(10):1914-20.

63 Otani K, Tanigawa T, Watanabe T, Nadatani Y, Sogawa M, Yamagami H, et al. Toll-like receptor 9 signaling has anti-inflammatory effects on the early phase of *Helicobacter pylori*-induced gastritis. Biochem Biophys Res Commun. 2012; 426(3):342-9.

64 Gringhuis SI, den Dunnen J, Litjens M, van der Vlist M, Geijtenbeek TB. Carbohydrate-specific signaling through the DC-SIGN signalosome tailors immunity to *Mycobacterium tuberculosis*, HIV-1 and *Helicobacter pylori*. Nat Immunol. 2009; 10(10):1081-8.

65 van Kooyk Y. C-type lectins on dendritic cells: key modulators for the induction of immune responses. Biochem Soc Trans. 2008; 36(Pt 6):1478-81.

66 Boncristiano M, Paccani SR, Barone S, Ulivieri C, Patrussi L, Ilver D, et al. The *Helicobacter pylori* vacuolating toxin inhibits T cell activation by two independent mechanisms. J Exp Med. 2003; 198(12):1887-97.

67 Gerhard M, Schmees C, Voland P, Endres N, Sander M, Reindl W, et al. A secreted low-molecular-weight protein from *Helicobacter pylori* induces cell-cycle arrest of T cells. Gastroenterology 2005; 128(5):1327-39.

Copyright by Mahidol University

68 Schmees C, Prinz C, Treptau T, Rad R, Hengst L, Voland P, et al. Inhibition of T-cell proliferation by *Helicobacter pylori* gamma-glutamyl transpeptidase. Gastroenterology. 2007; 132(5):1820-33.

69 Lanzavecchia A, Sallusto F. Regulation of T cell immunity by dendritic cells. Cell. 2001 ;106(3):263-6.

70 Kao JY, Zhang M, Miller MJ, Mills JC, Wang B, Liu M, et al. *Helicobacter pylori* immune escape is mediated by dendritic cell-induced Treg skewing and Th17 suppression in mice. Gastroenterology 2010; 138(3):1046-54.

71 Harris PR, Wright SW, Serrano C, Riera F, Duarte I, Torres J, et al. *Helicobacter pylori* gastritis in children is associated with a regulatory T-cell response. Gastroenterology 2008; 134(2):491-9.

72 Lundgren A, Stromberg E, Sjoling A, Lindholm C, Enarsson K, Edebo A, et al. Mucosal FOXP3-expressing $CD4^{+}$ CD^{25} high regulatory T cells in *Helicobacter pylori*-infected patients. Infect Immun. 2005; 73(1):523-31.

73 Enarsson K, Lundgren A, Kindlund B, Hermansson M, Roncador G, Banham AH, et al. Function and recruitment of mucosal regulatory T cells in human chronic *Helicobacter pylori* infection and gastric adenocarcinoma. Clin Immunol. 2006; 121(3):358-68.

74 Lee KE, Khoi PN, Xia Y, Park JS, Joo YE, Kim KK, et al. *Helicobacter pylori* and interleukin-8 in gastric cancer. World J Gastroenterol. 2013; 19(45):8192-202.

75 Futagami S, Hiratsuka T, Tatsuguchi A, Suzuki K, Kusunoki M, Shinji Y, et al. Monocyte chemoattractant protein 1 (MCP-1) released from *Helicobacter pylori* stimulated gastric epithelial cells induces cyclooxygenase 2 expression and activation in T cells. Gut 2003; 52(9):1257-64.

76 Watanabe N, Shimada T, Ohtsuka Y, Hiraishi H, Terano A. Proinflammatory cytokines and *Helicobacter pylori* stimulate CC-chemokine expression in gastric epithelial cells. J Physiol Pharmacol. 1997; 48(3):405-13.

77 Kitadai Y, Sasaki A, Ito M, Tanaka S, Oue N, Yasui W, et al. *Helicobacter pylori* infection influences expression of genes related to angiogenesis and invasion in human gastric carcinoma cells. Biochem Biophys Res Commun. 2003; 311(4):809-14.

Copyright by Mahidol University

78 Salama NR, Hartung ML, Muller A. Life in the human stomach: persistence strategies of the bacterial pathogen *Helicobacter pylori*. Nat Rev Microbiol. 2013; 11(6):385-99.

79 Mucito-Varela E, Castillo-Rojas G, Cevallos MA, Lozano L, Merino E, Lopez-Leal G, et al. Complete genome sequence of *Helicobacter pylori* strain 7C isolated from a Mexican patient with chronic gastritis. Genome Announc. 2016; 4(1):e01503-15.

80 Draper JL, Hansen LM, Bernick DL, Abedrabbo S, Underwood JG, Kong N, et al. Fallacy of the unique genome: sequence diversity within single *Helicobacter pylori* strains. MBio. 2017; 8(1):e02321-16.

81 Satou K, Shiroma A, Teruya K, Shimoji M, Nakano K, Juan A, et al. Complete genome sequences of eight *Helicobacter pylori* strains with different virulence factor genotypes and methylation profiles, isolated from patients with diverse gastrointestinal diseases on Okinawa island, Japan, determined using PacBio single-molecule real-time technology. Genome Announc. 2014; 2(2):e0026-14.

82 Momynaliev K, Chelysheva V, Selezneva O, Akopian T, Alexeev D, Govorun V. Complete genome sequences of *Helicobacter pylori* rifampin-resistant Genome Announc. 2013; 1(4):e00446-13.

83 Thiberge JM, Boursaux-Eude C, Lehours P, Dillies MA, Creno S, Coppee JY, et al. From array-based hybridization of *Helicobacter pylori* isolates to the complete genome sequence of an isolate associated with MALT lymphoma. BMC Genomics. 2010; 11:368.

84 Binh TT, Suzuki R, Kwon DH, Yamaoka Y. Complete genome sequence of a metronidazole-resistant *Helicobacter pylori* strain. Genome Announc. 2015;3 (2).

85 Farnbacher M, Jahns T, Willrodt D, Daniel R, Haas R, Goesmann A, et al. Sequencing, annotation, and comparative genome analysis of the gerbil-adapted *Helicobacter pylori* strain B8. BMC Genomics. 2010; 11:335.

Copyright by Mahidol University

86 Arenas NE, Salazar LM, Soto CY, Vizcaino C, Patarroyo ME, Patarroyo MA, et al. Molecular modeling and *in silico* characterization of *Mycobacterium tuberculosis* TlyA: possible misannotation of this tubercle bacilli-hemolysin. BMC Struct Biol. 2011; 11:16.

87 Casadevall A, Pirofski LA. Virulence factors and their mechanisms of action: the view from a damage-response framework. J Water Health. 2009; 7 Suppl 1:S2-S18.

88 Rahman A, Srivastava SS, Sneh A, Ahmed N, Krishnasastry MV. Molecular characterization of tlyA gene product, Rv1694 of *Mycobacterium tuberculosis*: a non-conventional hemolysin and a ribosomal RNA methyl transferase. BMC Biochem. 2010; 11:35.

89 Witek MA, Kuiper EG, Minten E, Crispell EK, Conn GL. A novel motif for S-Adenosyl-l-methionine binding by the ribosomal RNA methyltransferase TlyA from *Mycobacterium tuberculosis*. J Biol Chem. 2017; 292(5):1977-87.

90 Hyatt DR, ter Huurne AA, van der Zeijst BA, Joens LA. Reduced virulence of Serpulina hyodysenteriae hemolysin-negative mutants in pigs and their potential to protect pigs against challenge with a virulent strain. Infect Immun. 1994; 62(6):2244-8.

91 Salamaszynska-Guz A, Godlewski MM, Klimuszko D. Influence of mutation in cj0183 and cj0588 genes for colonization abilities of *Campylobacter jejuni* in Caco-2 cells using confocal laser scanning microscope. Pol J Vet Sci. 2013; 16(2):387-9.

92 Keenan JI, Allardyce RA. Iron influences the expression of *Helicobacter pylori* outer membrane vesicle-associated virulence factors. Eur J Gastroenterol Hepatol. 2000; 12(12):1267-73.

93 Bini EJ. *Helicobacter pylori* and iron deficiency anemia: guilty as charged? Am J Med. 2001; 111(6):495-7.

94 Razuka-Ebela D, Giupponi B, Franceschi F. *Helicobacter pylori* and extragastric diseases. Helicobacter 2018; 23(1):e12520.

Copyright by Mahidol University

95.Birnboim HC, Doly J. A rapid alkaline extraction procedure for screening recombinant plasmid DNA. Nucleic Acids Res. 1979; 7(6):1513-23.

96 Bergmans HE, van Die IM, Hoekstra WP. Transformation in *Escherichia coli*: stages in the process. J Bacteriol. 1981; 146(2):564-70.

97 Bradford MM. A rapid and sensitive method for the quantitation of microgram quantities of protein utilizing the principle of protein-dye binding. Anal Biochem.1976; 72:248-54.

98 Bueno C, Villegas ML, Bertolotti SG, Previtali CM, Neumann MG, Encinas MV. The excited-state interaction of resazurin and resorufin with amines in aqueous solutions. Photophysics and photochemical reactions. Photochem Photobiol. 2002; 76(4):385-90.

99 Tapani E, Taavitsainen M, Lindros K, Vehmas T, Lehtonen E. Toxicity of ethanol in low concentrations. Experimental evaluation in cell culture. Acta Radiol. 1996; 37(6):923-6.

100 Soding J. Protein homology detection by HMM-HMM comparison. Bioinformatics. 2005; 21(7):951-60.

101 Smith TF, Waterman MS. Identification of common molecular subsequences. J Mol Biol. 1981; 147(1):195-7.

102 Waterhouse AM, Procter JB, Martin DM, Clamp M, Barton GJ. Jalview Version 2--a multiple sequence alignment editor and analysis workbench. Bioinformatics 2009; 25(9):1189-91.

103 Yang J, Yan R, Roy A, Xu D, Poisson J, Zhang Y. The I-TASSER Suite: protein structure and function prediction. Nat Methods. 2015; 12(1):7-8.

104 Laskowski RA, Jablonska J, Pravda L, Varekova RS, Thornton JM. PDBsum: Structural summaries of PDB entries. Protein Sci. 2018; 27(1):129-34.

105 Kelley LA, Mezulis S, Yates CM, Wass MN, Sternberg MJ. The Phyre2 web portal for protein modeling, prediction and analysis. Nat Protoc. 2015; 10(6):845-58.

106 Sali A, Potterton L, Yuan F, van Vlijmen H, Karplus M. Evaluation of comparative protein modeling by MODELLER. Proteins 1995; 23(3): 318-26.

107 Williams CJ, Headd JJ, Moriarty NW, Prisant MG, Videau LL, Deis LN, et al. MolProbity: more and better reference data for improved all-atom structure validation. Protein Sci. 2018; 27(1):293-315.

Copyright by Mahidol University

108 Lovell SC, Davis IW, Arendall WB, 3rd, de Bakker PI, Word JM, Prisant MG, et al. Structure validation by Calpha geometry: phi,psi and Cbeta deviation. Proteins 2003; 50(3):437-50.

109 Pymol.org [Internet]. The PyMOL molecular graphics system 2002; c2019 [update 2019 Feb 11; cited 2019 Feb 15]. Available from: http://www.pymol.org.

110 Kraulis P. MOLSCRIPT: a program to produce both detailed and schematic plots of protein structures. J Appl Crystallogr. 1991; 24(5):946-50.

111 Ko J, Park H, Heo L, Seok C. GalaxyWEB server for protein structure prediction and refinement. Nucleic Acids Res. 2012; 4:W294-7.

112 El-Gebali S, Mistry J, Bateman A, Eddy SR, Luciani A, Potter SC, et al. The Pfam protein families database in 2019. Nucleic Acids Res. 2019; 47(D1): D427-D32.

113 Goldberg T, Hecht M, Hamp T, Karl T, Yachdav G, Ahmed N, et al. LocTree3 prediction of localization. Nucleic Acids Res. 2014; 42:W350-5.

114 Yu CS, Lin CJ, Hwang JK. Predicting subcellular localization of proteins for Gram-negative bacteria by support vector machines based on n-peptide compositions. Protein Sci. 2004; 13(5):1402-6.

115 Juncker AS, Willenbrock H, Von Heijne G, Brunak S, Nielsen H, Krogh A. Prediction of lipoprotein signal peptides in Gram-negative bacteria. Protein Sci. 2003; 12(8):1652-62.

116 Bhasin M, Garg A, Raghava GP. PSLpred: prediction of subcellular localization of bacterial proteins. Bioinformatics 2005; 21(10):2522-4.

117 Matsuda S, Vert JP, Saigo H, Ueda N, Toh H, Akutsu T. A novel representation of protein sequences for prediction of subcellular location using support vector machines. Protein Sci. 2005;14(11):2804-13.

118 Trott O, Olson AJ. AutoDock Vina: improving the speed and accuracy of docking with a new scoring function, efficient optimization, and multithreading. J Comput Chem. 2010; 31(2):455-61.

119 Kumar S, Stecher G, Li M, Knyaz C, Tamura K. MEGA X: Molecular evolutionary genetics analysis across computing platforms. Mol Biol Evol. 2018; 35(6):1547-9.

Copyright by Mahidol University

120 Dereeper A, Audic S, Claverie JM, Blanc G. BLAST-EXPLORER helps you building datasets for phylogenetic analysis. BMC Evol Biol. 2010; 10:8.

121.Oberto J. SyntTax: a web server linking synteny to prokaryotic taxonomy. BMC Bioinformatics. 2013; 14:4.

122 Mihalek I, Res I, Lichtarge O. A family of evolution-entropy hybrid methods for ranking protein residues by importance. J Mol Biol. 2004; 336(5):1265-82.

123 Zhang C, Freddolino PL, Zhang Y. COFACTOR: improved protein function prediction by combining structure, sequence and protein-protein interaction information. Nucleic Acids Res. 2017; 45(W1):W291-W9.

124 Sievers F, Wilm A, Dineen D, Gibson TJ, Karplus K, Li W, et al. Fast, scalable generation of high-quality protein multiple sequence alignments using Clustal Omega. Mol Syst Biol. 2011; 7:539.

125 Righetti PG. Isoelectric focusing: theory, methodology and appliations. Laboratory Techniques in Biochemistry and Molecular Biology. 1987: 175-80.

126 Kozlowski LP. IPC - isoelectric point calculator. Biol Direct. 2016; 11(1):55.

127 Richardson JS. The anatomy and taxonomy of protein structure. Adv Protein Chem. 1981; 34:167-339.

128 Webb B, Sali A. Comparative protein structure modeling using MODELLER. Curr Protoc Bioinformatics. 2016; 54:561. doi: 10.1002/0471250953.bi0506s15

129 Chandra Sanyal S, Liljas A. The end of the beginning: structural studies of ribosomal proteins. Curr Opin Struct Biol. 2000; 10(6):633-6.

130 Aravind L, Koonin EV. Novel predicted RNA-binding domains associated with the translation machinery. J Mol Evol. 1999; 48(3):291-302.

131 Tan J, Jakob U, Bardwell JC. Overexpression of two different GTPases rescues a null mutation in a heat-induced rRNA methyltransferase. J Bacteriol. 2002; 184(10):2692-8.

132 Bugl H, Fauman EB, Staker BL, Zheng F, Kushner SR, Saper MA, et al. RNA methylation under heat shock control. Mol Cell. 2000; 6(2):349-60.

133 Schubert HL, Blumenthal RM, Cheng X. Many paths to methyltransfer: a chronicle of convergence. Trends Biochem Sci. 2003; 28(6):329-35.

Copyright by Mahidol University

134 Berg JM, Tymoczko JL, Gatto GJ, Stryer L. Biochemistry.1 vol. 8th ed. New York: W.H. Freeman & Company, a Macmillan Education Imprint; 2015.

135 Mel SF, Mekalanos JJ. Modulation of horizontal gene transfer in pathogenic bacteria by in vivo signals. Cell. 1996; 87(5):795-8.

136 Saiki RK, Gelfand DH, Stoffel S, Scharf SJ, Higuchi R, Horn GT, et al. Primer-directed enzymatic amplification of DNA with a thermostable DNA polymerase. Science. 1988; 239(4839):487-91.

137 Jordan IK, Rogozin IB, Wolf YI, Koonin EV. Essential genes are more evolutionarily conserved than are nonessential genes in bacteria. Genome Res. 2002; 12(6):962-8.

138 Boriack-Sjodin PA, Swinger KK. Protein methyltransferases: a distinct, diverse, and dynamic family of enzymes. Biochemistry 2016; 55(11):1557-69.

139 Kirschner K, Bisswanger H. Multifunctional proteins. Annu Rev Biochem. 1976; 45:143-66.

140 Henriksen U, Fog JU, Litman T, Gether U. Identification of intra- and intermolecular disulfide bridges in the multidrug resistance transporter ABCG2. J Biol Chem. 2005; 280(44):36926-34.

141 Li T, Yamane H, Arakawa T, Narhi LO, Philo J. Effect of the intermolecular disulfide bond on the conformation and stability of glial cell line-derived neurotrophic factor. Protein Eng. 2002; 15(1):59-64.

142 Nagahara N. Intermolecular disulfide bond to modulate protein function as a redox-sensing switch. Amino Acids 2011;41(1):59-72.

143 Baek M, Park T, Heo L, Park C, Seok C. GalaxyHomomer: a web server for protein homo-oligomer structure prediction from a monomer sequence or structure. Nucleic Acids Res. 2017;45(W1):W320-W4.

144 Sriwimol W, Aroonkesorn A, Sakdee S, Kanchanawarin C, Uchihashi T, Ando T, et al. Potential Prepore Trimer Formation by the *Bacillus thuringiensis* mosquito-specific toxin: molecular insights into a critical prerequisite of membrane-bound monomers. J Biol Chem. 2015; 290(34):20793-803.

Copyright by Mahidol University

145 Burgess BR, Dobson RC, Bailey MF, Atkinson SC, Griffin MD, Jameson GB, et al. Structure and evolution of a novel dimeric enzyme from a clinically important bacterial pathogen. J Biol Chem. 2008; 283(41):27598-603.

146 Jang TH, Park JH, Park HH. Novel disulfide bond-mediated dimerization of the CARD domain was revealed by the crystal structure of CARMA1 CARD. PLoS One 2013; 8(11):e79778.

147 Renatus M, Stennicke HR, Scott FL, Liddington RC, Salvesen GS. Dimer formation drives the activation of the cell death protease caspase 9. Proc Natl Acad Sci USA. 2001; 98(25):14250-5.

148 Ros U, Garcia-Saez AJ. More than a pore: the interplay of pore-forming proteins and lipid membranes. J Membr Biol. 2015; 248(3):545-61.

149 Robinson K, Argent RH, Atherton JC. The inflammatory and immune response to *Helicobacter pylori* infection. Best Pract Res Clin Gastroenterol. 2007; 21(2):237-59.

150 Eftang LL, Esbensen Y, Tannaes TM, Bukholm IR, Bukholm G. Interleukin-8 is the single most up-regulated gene in whole genome profiling of *H. pylori* exposed gastric epithelial cells. BMC Microbiol. 2012 ;12:9.

151 Backhed F, Torstensson E, Seguin D, Richter-Dahlfors A, Rokbi B. *Helicobacter pylori* infection induces interleukin-8 receptor expression in the human gastric epithelium. Infect Immun. 2003; 71(6):3357-60.

152 Fazeli Z, Alebouyeh M, Rezaei Tavirani M, Azimirad M, Yadegar A. *Helicobacter pylori* CagA induced interleukin-8 secretion in gastric epithelial cells. Gastroenterol Hepatol Bed Bench. 2016; 9(Suppl1): S42-S6.

153 Crabtree JE, Xiang Z, Lindley IJ, Tompkins DS, Rappuoli R, Covacci A. Induction of interleukin-8 secretion from gastric epithelial cells by a cagA negative isogenic mutant of *Helicobacter pylori*. J Clin Pathol. 1995; 48(10):967-9.

154 Jeffery CJ. Moonlighting proteins: old proteins learning new tricks. Trends Genet. 2003; 19(8):415-7.

Copyright by Mahidol University

155 Barbes C, Sanchez J, Yebra MJ, Robert-Gero M, Hardisson C. Effects of sinefungin and S-adenosylhomocysteine on DNA and protein methyltransferases from Streptomyces and other bacteria. FEMS Microbiol Lett. 1990; 57(3):239-43.

156 Zheng S, Hausmann S, Liu Q, Ghosh A, Schwer B, Lima CD, et al. Mutational analysis of *Encephalitozoon cuniculi* mRNA cap (guanine-N7) methyltransferase, structure of the enzyme bound to sinefungin, and evidence that cap methyltransferase is the target of sinefungin's antifungal activity. J Biol Chem. 2006; 281(47):35904-13.

157 Trager W, Tershakovec M, Chiang PK, Cantoni GL. Plasmodium falciparum: antimalarial activity in culture of sinefungin and other methylation inhibitors. Exp Parasitol. 1980; 50(1):83-9.

158 Parsek MR, Val DL, Hanzelka BL, Cronan JE, Jr., Greenberg EP. Acyl homoserine-lactone quorum-sensing signal generation. Proc Natl Acad Sci USA. 1999; 96(8):4360-5.

159 Schluckebier G, Kozak M, Bleimling N, Weinhold E, Saenger W. Differential binding of S-adenosylmethionine S-adenosylhomocysteine and Sinefungin to the adenine-specific DNA methyltransferase M.TaqI. J Mol Biol. 1997; 265(1):56-67.

160 O'Morain NR, Dore MP, O'Connor AJP, Gisbert JP, O'Morain CA. Treatment of *Helicobacter pylori* infection in 2018. Helicobacter. 2018; 23 Suppl 1:e12519.161 Shiota S, Reddy R, Alsarraj A, El-Serag HB, Graham DY. Antibiotic resistance of *Helicobacter pylori* among male United States Veterans. Clin Gastroenterol Hepatol. 2015;13(9):1616-24.

Copyright by Mahidol University

APPENDICES

Copyright by Mahidol University

APPENDIX A
BUFFERS AND SOLUTIONS

1. Plasmid extraction solutions

1.1 Solution I (100 ml)

- 50 mM Glucose (180.156 g/mol) 0.9 g
- 10 mM EDTA (292.24 g/mol) 0.29 g
- 25 mM Tris-HCl (121.14 g/mol) 0.3 g

The solution was adjusted pH to 8.0 with 5N NaOH, adjusted volume to 100 ml with distilled water; and then autoclaved at 121°C, for 20 min.

1.2 10 mg/ml RNase A (1.0 ml)

- RNase A 10 mg
- Distilled water 1.0 ml

The solution was sterilized by passing through 0.2 µm filter and aliquoted into 100 µl/micro-centrifuge tube and kept at -20°C.

1.3 Solution II (100ml)

- 0.2 M NaOH (40 g/mol) 0.8 g
- 1% SDS 1 g

The solution was adjusted 100 ml with distilled water; and then kept at room temperature.

1.4 Solution III (100 ml)

- 3 M Potassium acetate (98.15 g/mol) 29.44 g

Copyright by Mahidol University

The solution was adjusted 100 ml with distilled water; and then kept at room temperature.

1.5 10 mg/ml Lysozyme

- Lysozyme 0.01 g
- Distilled water 1 ml

1.6 1 M NaCl (100 ml)

- NaCl (M.W 58.44) 5.84 g

The solution was adjusted to 100 ml with distilled water; and then autoclaved at 121°C, for 20 min.

2. DNA gel electrophoresis solutions

2.1 50 ng/µl λ-*Hin*dIII DNA marker (100 µl)

- λ-*Hin*dIII DNA marker (500 ng/µl) 10 µl
- 4× loading buffer 25 µl
- Distilled water 65 µl

2.2 6× gel loading buffer (5 ml)

- Bromophenol blue 0. 5 g
- Glycerol 30 % (v/v) 1.5 ml

Distilled water was added to make up the volume to 5 ml and kept at -4°C.

3. Competent cell preparation solutions

3.1 0.1 M $CaCl_2$ (100 ml)

- $CaCl_2 \cdot 2H_2O$ (MW 147.02) 1.47 g

Distilled water making final volume to 100 ml. The solution was autoclaved at 121°C, for 20 min.

Copyright by Mahidol University

4. Protein expression solutions

4.1 1 M IPTG (10 ml)

- IPTG (283.32 g/mol) 2.83 g
- Distilled water 10 ml

The solution was passed through 0.2 µm filter and aliquoted into 1 ml/micro-centrifuge tubes and kept at -20°C.

4.2 100 mg/ml Ampicillin (10 ml)

- Ampicillin 1 g
- Distilled water 10 ml

The solution was passed through 0.2 µm filter and aliquoted into 1 ml/ micro-centrifuge tubes and kept at -20°C.

5. Solutions for protein purification and solubilization

5.1 50 mM HEPES, pH 8 (1 L)

- HEPES (238.30 g/mol) 11.92 g

The solution was adjusted pH to 8.0 with 5N NaOH, adjusted volume to 1000 ml with distilled water; and then autoclaved at 121°C, for 20 minutes.

5.2 50 mM HEPES, 1 M NaCl pH 8 (1 L)

- HEPES (238.30 g/mol) 11.92 g
- NaCl (58.44 g/mol) 58.44 g

The solution was adjusted to pH 8.0 with 5N NaOH, adjusted volume to 1000 ml with distilled water, and then autoclaved at 121°C, for 20 minutes.

Copyright by Mahidol University

6. Solutions for SDS-PAGE analysis, gel staining solutions

6.1 10× Running buffer (1 L)

- Tris-base (MW 121.1) 30.0 g
- Glycine 144.13 g
- SDS 10.0 g

Distilled water to final volume of 1 L

6.2 10% SDS (10 ml)

- SDS (288.38 g/mol) 10 g

Distilled water to final volume of 100 ml

6.3 1.5 M Tris-HCl, pH 8.8 (100 ml)

- Tris-base 18.17 g

The solution was adjusted to pH 8.8 with HCl and distilled water was added to final volume of 100 ml.

6.4 0.5 M Tris-HCl, pH 6.8 (100 ml)

- Tris-base 6.07 g

The solution was adjusted to pH 6.8 with HCl and distilled water was added to final volume of 100 ml.

6.5 10% Ammonium persulfate (10 ml)

- Ammonium persulfate 1 g
- Distilled water 10 ml

The solution was passed through 0.2 µm filter and aliquoted into 1 ml/micro-centrifuge tubes and kept at -20°C.

Copyright by Mahidol University

6.6 1M DTT (10 ml)

- DTT (154.253 g/mol) 1.54 g
- Distilled water 10 ml

The solution was passed through 0.2 µm filter and aliquoted into 1 ml/micro-centrifuge tubes and kept at -20°C.

6.7 4× sample buffer (100 ml)

- SDS (8%) 8.0 g
- Glycerol (40%) 40.0 ml
- Tris-HCl(MW 121.1) 2.42 g
- Bromophenol blue (0.4%) 0.4 g

Distilled water making final volume to 100 ml 1 M DTT was added to obtain 100 mM final concentration.

6.8 Staining solution for SDS- gel (1 L)

- Coomassie brilliant blue R-250 (0.1 %) 1 g
- Ethanol 500 ml
- Acetic acid 100 ml

Distilled water making final volume to 1 L

6.9 Destaining solution for acrylamide gel (1 L)

- Ethanol 100 ml
- Acetic acid 100 ml

Distilled water making final volume to 1L

Copyright by Mahidol University

7. Bacterial culture mediums

7.1 LB broth medium (1 L)

- NaCl (1 % w/v) 10 g
- Peptone (1 % w/v) 10 g
- Yeast extract (0.5 % w/v) 5 g

The solution was autoclaved at 121°C, for 20 min and kept at 4°C.

7.2 1.5% LB agar (plate) (100 ml)

- Agar (1.5 % w/v) 1.5 g
- NaCl (1 % w/v) 10 g
- Peptone (1 % w/v) 10 g
- Yeast extract (0.5 % w/v) 5 g

The solution was autoclaved at 121°C, for 20 minutes. and then kept at room temperature and poured onto plates before harden.

Copyright by Mahidol University

APPENDIX B
LIST OF ATOM-ATOM INTERACTIONS ACROSS PROTEIN-PROTEIN INTERFACE

TlyA Chains A }{ B

Hydrogen bonds

	<----- A T O M 1 ----->					<----- A T O M 2 ----->					
	Atom no.	Atom name	Res name	Res no.	Chain		Atom no.	Atom name	Res name	Res no.	Chain	Distance
1.	958	O	LYS	100	A	<-->	1299	NZ	LYS	134	B	2.97
2.	1116	NZ	LYS	117	A	<-->	1229	OE1	GLU	127	B	2.72
3.	1129	NE2	GLN	118	A	<-->	1246	OD2	ASP	129	B	3.09
4.	1192	N	CYS	124	A	<-->	1237	SG	CYS	128	B	3.04
5.	1196	SG	CYS	124	A	<-->	1237	SG	CYS	128	B	3.25
6.	1207	OH	TYR	125	A	<-->	1230	OE2	GLU	127	B	2.76
7.	1229	OE1	GLU	127	A	<-->	1116	NZ	LYS	117	B	2.84
8.	1230	OE2	GLU	127	A	<-->	1207	OH	TYR	125	B	2.82
9.	1237	SG	CYS	128	A	<-->	1192	N	CYS	124	B	3.23
10.	1299	NZ	LYS	134	A	<-->	958	O	LYS	100	B	3.20

Copyright by Mahidol University

APPENDIX C

TlyA HOMOLOG

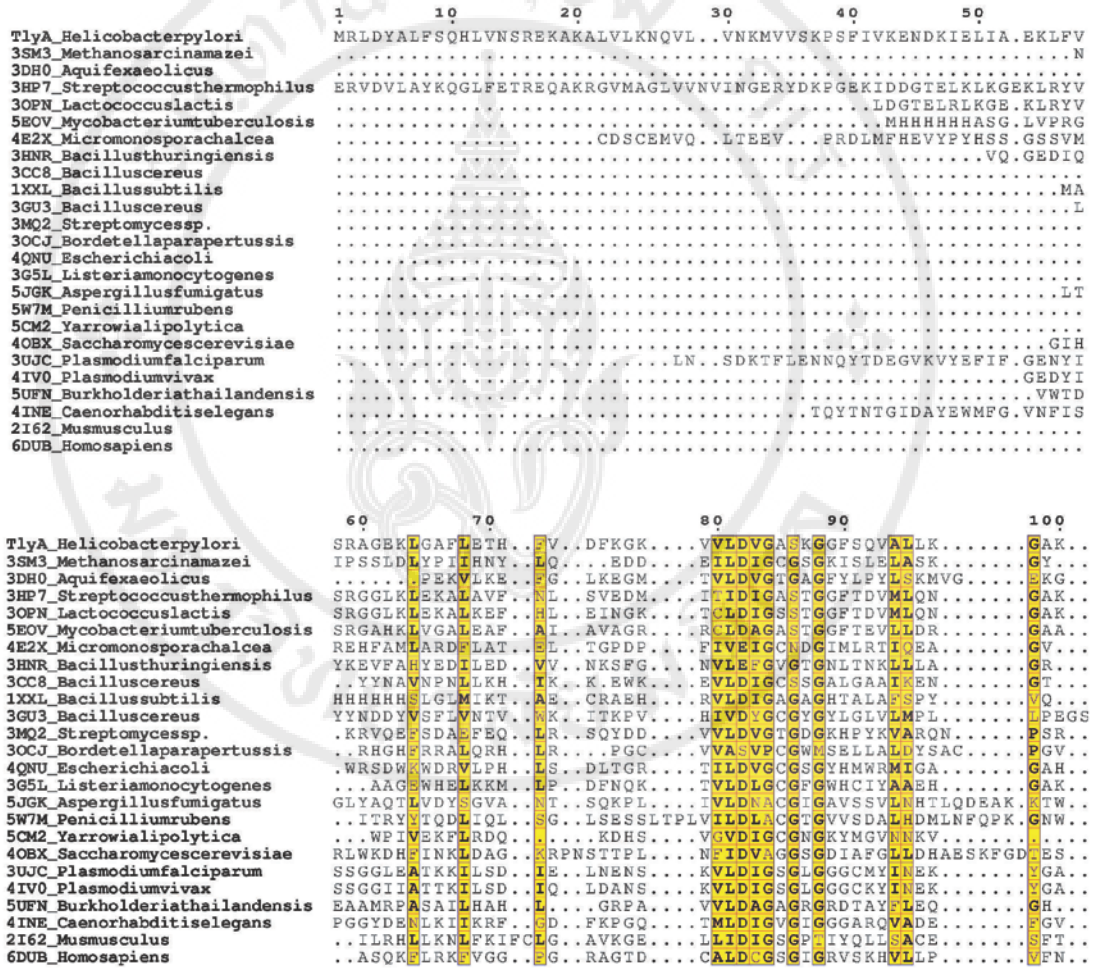

Copyright by Mahidol University

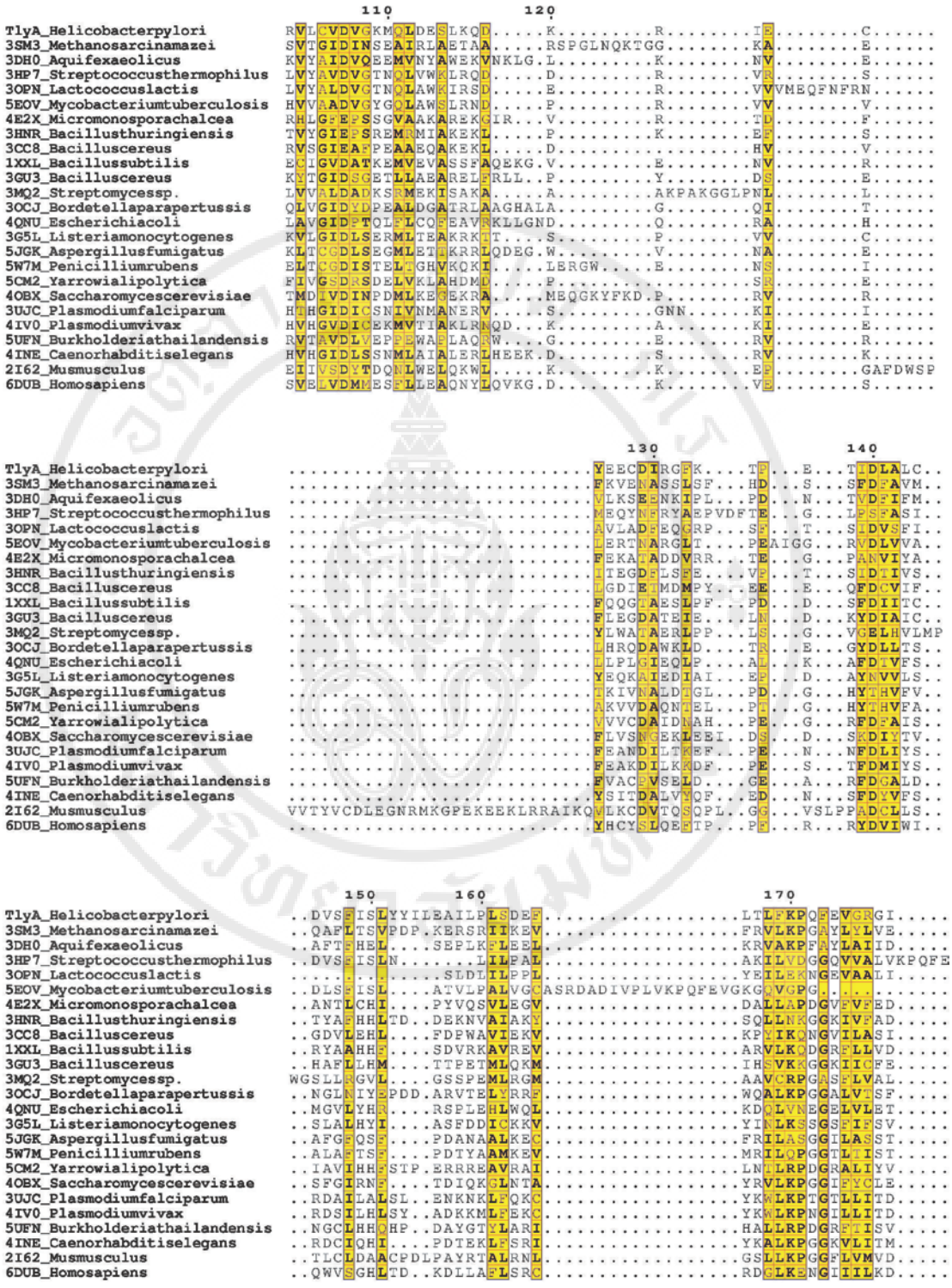

Copyright by Mahidol University

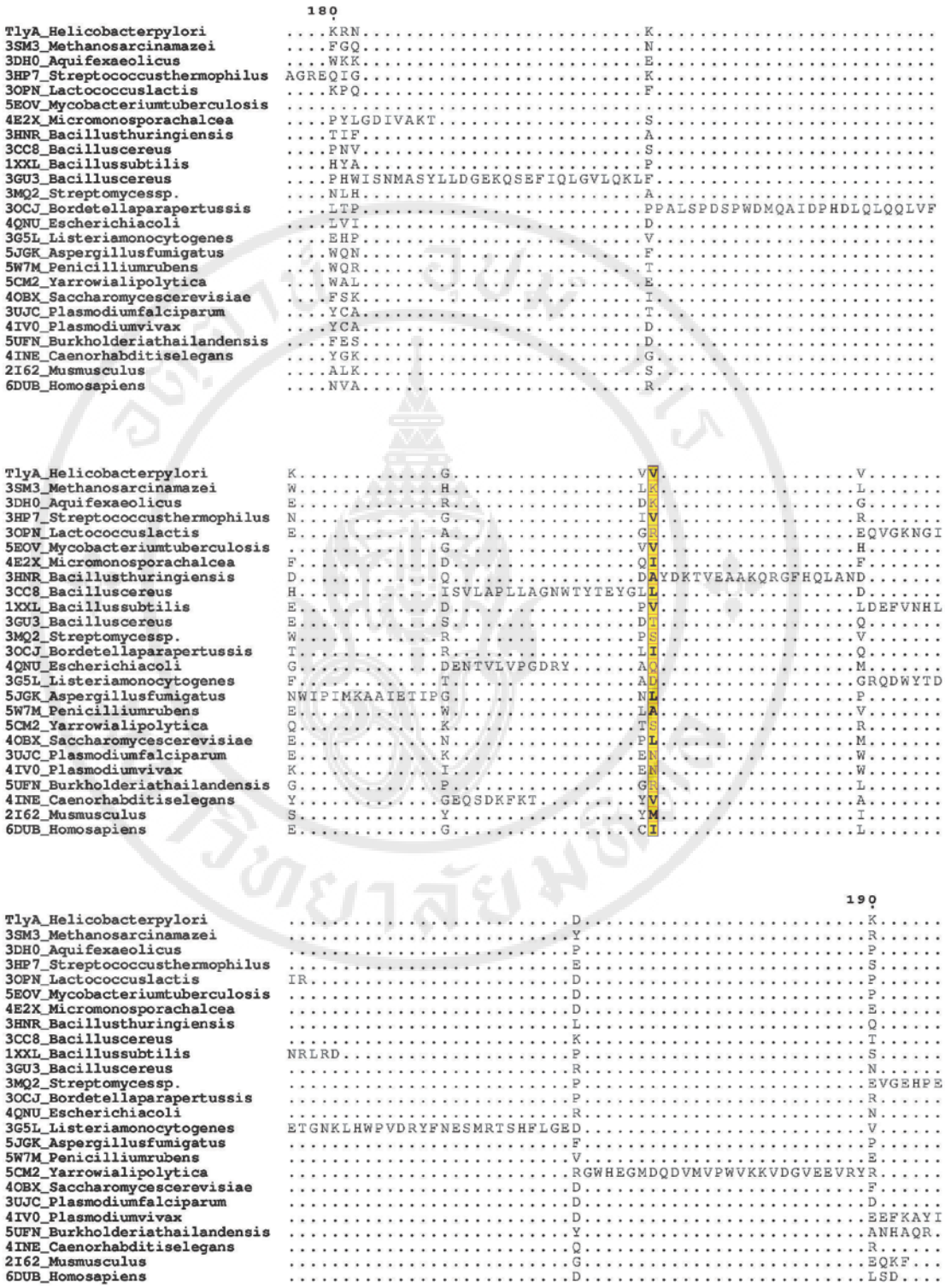

Copyright by Mahidol University

Copyright by Mahidol University

BIOGRAPHY

NAME	Miss Nitchakan Samainukul
DATE OF BIRTH	9 December 1990
PLACE OF BIRTH	Bangkok, Thailand
INSTITUTIONS ATTENDED	Mahidol University, 2008-2012 Bachelor of Science (Biotechnology) Mahidol University, 2012-2015 Master of Science (Molecular Genetics and Genetic Engineering) Mahidol University, 2015-2019 Doctor of Philosophy (Immunology)
RESEARCH GRANTS	Support in part by the Thesis Grant, Faculty of Graduate Studies, Mahidol University
HOME ADDRESS	243/271 Lamchabang Green view 3 village, Moo 4, Sriracha-Sukhumvit 27 Road, Thung Sukla, Sriracha, Chonburi 20230, Thailand. E-mail: samainukul@gmail.com
PUBLICATION / PRESENTATION	Linn AK, **Samainukul N**, Sakdee S, Aungsythanasombat C Katzenmeier G. A *Helicobacter pylori* vacuolation cytotoxin A: mouse DHFR fusion protein triggers dye release from liposome. Curr Microbiol. 2018;75(2): 223-230.

Copyright by Mahidol University